# 5. PLUME OR JET MODELS IN HGSYSTEM

## CONTENTS

# 5. PLUME OR JET MODELS IN HGSYSTEM

The HGSYSTEM package contains two models to describe the dispersion of a jet release from a pressurised vessel. AEROPLUME can be applied to non-reactive, multi-compound two-phase jets and HFPLUME describes jet dispersion using the full hydrogen fluoride (HF) chemistry and thermodynamics. The two thermodynamic models used, are discussed in detail in Chapter 2. Chapter 2.A. describes the thermodynamics as used in AEROPLUME and Chapter 2.B. describes the hydrogen fluoride thermodynamic model as used in HFPLUME.

AEROPLUME and HFPLUME both have a similar discharge model to estimate release (discharge) rates from a given pressurised vessel.

In the new HGSYSTEM version 3.0, AEROPLUME replaces the PLUME model which was available in the first public release, HGSYSTEM version 1.0 (also called NOV90 version). PLUME could only deal with ideal gas releases.

In Chapter 5.A, the *AEROPLUME implementation* in HGSYSTEM version 3.0 is discussed in more detail.

AEROPLUME, HFPLUME and the old PLUME model, all share the same basic *plume development description*. This basic plume model is discussed in Chapter 5.B. In this chapter also validation studies for the HGSYSTEM plume models are discussed.

The main difference between AEROPLUME and HFPLUME (and PLUME) is the thermodynamic description of the released fluid. The way in which the thermodynamic relations are solved is also different in AEROPLUME and HFPLUME. This is discussed in Chapter 5.A., paragraph 5.A.7.

As HFPLUME is very similar to AEROPLUME, apart from the thermodynamics, there is no separate discussion of HFPLUME in this Technical Reference Manual.

# 5.A. THE AEROPLUME MODEL

## 5.A.1. Introduction

The module in HGSYSTEM version 1.0 (or NOV90 version) describing steady-state pressurised releases of a non-reactive pollutant, PLUME, has been updated considerably for use in HGSYSTEM version 3.0, resulting in the newly named AEROPLUME model.

This chapter provides details about the implementation of the AEROPLUME (version 1.4) module of HGSYSTEM version 3.0. AEROPLUME can be used to simulate the jet (plume) development of a release, from a pressurised vessel or from a stack, of a mixture of several non-reacting compounds, which can form one or more single or multi-compound aerosols.

AEROPLUME is in fact the result of combining the multi-compound, two-phase thermo-dynamic model described in Chapter 2.A. with a PLUME (HFPLUME) jet description.

After a general introduction into the AEROPLUME code, the aerosol algorithms will be summarised, then the reservoir and the post-flash calculations will be reviewed and finally a summary of the equations describing the jet development will be given.

In Chapter 5B, the general plume or jet description developed for the old PLUME model, is given. This chapter gives more details on the plume relations as discussed in paragraph 5.A.7 of the current Chapter 5.A.

Detailed information on AEROPLUME input parameters can be found in the AEROPLUME chapter of the HGSYSTEM 3.0 User's Manual.

Please note that the HFPLUME model in HGSYSTEM is simply an HF-specific version of the AEROPLUME model. The basic discharge model and jet description are very similar to the one described in the current chapter. For this reason, HFPLUME will not be described separately in this Technical Reference Manual. HFPLUME input parameters are described in the HGSYSTEM 3.0 User's Manual.

## 5.A.2. The AEROPLUME code

Within the AEROPLUME code several main program blocks can be distinguished.

First there are the *specific thermodynamic routines* which contain the multi-compound aerosol model. These routines calculate the plume thermodynamic variables, the reservoir state and the post-flash or stack conditions. The structure is completely modular in the sense that the

thermodynamic routines are completely separated from the routines calculating the plume development. The only communication is via the parameter lists.

The second main block consists of the routines to calculate the *jet (plume) development*. These are basically the same routines as used in the old PLUME model (HGSYSTEM version 1.0) and in HFPLUME. They contain, among other things, the entrainment models, the geometry model and the plume integration routines which describe the position and composition (air and pollutant) of the plume as it travels onward from its release point.
The original jet development description as used for the old PLUME model can be found in Chapter 5B.
In the current chapter the specific AEROPLUME implementation is discussed.

Two of the solved variables are the plume enthalpy H and the total mass flow rate (pollutant plus mixed-in air) $\dot{m}$ (see paragraph 5.A.7). Together with the pollutant mass flow rate (or discharge rate), which is a constant, these variables are communicated to the thermodynamic routine in which the complete thermodynamic state of the plume at the current position is then calculated. The plume density and temperature and the pollutant concentration are output from the thermodynamic routine. Only the plume density is actually being used by the plume integration routines as will be discussed in more detail in paragraph 5.A.7.

A third main block contains the routines describing the *thermodynamic state of the ambient atmosphere* as a function of height, given the stability class and a set of reference values.

A last block that can be distinguished contains the *input and output* routines.

Because the thermodynamics is now built in a systematic, modular way, it should be a straightforward task to replace the current thermodynamics model by another one if required.

Finally it should be noted that it is still possible to run AEROPLUME in the vapour-only mode (i.e. the old PLUME model), but condensation of ambient water is now fully taken into account.

### 5.A.3. Summary of the aerosol algorithm

A more detailed exposure of the HGSYSTEM multi-compound, two-phase aerosol model can be found in Chapter 2. The formulation as given in this chapter is as used in HEGADAS and HEGABOX. AEROPLUME uses a slightly different formulation as will be discussed below.

Consider a mixture of *N* chemical compounds which in principle can form *M* aerosols. Aerosol $\beta$ ($\beta$ = 1, 2,..., *M*), when actually formed, will contain the compounds $\alpha$ where $\alpha = n^{\beta-1}+1,..., n^{\beta}$ ($0 = n^0 < n^1 < ... < n^M = N$). See Chapter 2 for more details.

Thus any combination of single compound and multi-compound aerosols is possible.

A slightly modified version of the *general* solution algorithm for the aerosol equations as given in Chapter 2.A.

The set of equations, occurring in the innermost iteration loop of the aerosol algorithm, from which the mole fraction liquid $L^{\beta}$ of each aerosol $\beta$ that forms is calculated, is solved using the non-linear algebraic equation solver NAESOL [1]. The solver proves to be very robust: the solutions for the $L^{\beta}$'s are found without any convergence problems.

The modification made to the algorithm as proposed in Chapter 2, concerns the handling of the singular point at T = 0° C (273.15 K) where a phase change of liquid water to ice takes place, if any water is present in the mixture.

To prevent a discontinuity occurring in the enthalpy H at 0° C, because of the ice formation term, a *melting range* $[T_1,T_2]$ has been introduced, where $T_1 < 0°$ C and $T_2 > 0°$ C. Within this melting range the enthalpy changes *linearly* from its value at $T_1$ to its value at $T_2$ and thus effectively the sharp jump has been removed. This was necessary because during the jet development calculations the former discontinuity gave rise to convergence problems of the solver of the differential equations involved. In the present implementation $T_1$ = - 0.15° C and $T_2$ = + 0.15° C .

When calculating the overall aerosol mixture density, in the original formulation (Chapter 2.A.), the volume of the liquid phase is neglected. Within a pressurised release context however, this is no longer a valid simplification as liquid mole fractions can be high. Therefore the overall mixture density $\rho$ in AEROPLUME is calculated as follows:

$$\rho = \frac{M}{\left\{ \sum_{\alpha=1}^{N} \frac{M_\alpha \cdot y_{\alpha\ell}}{\rho_{\alpha\ell}} + (1-L) \cdot \frac{R_0 \cdot T}{P} \right\}} \qquad (1)$$

where M is the mixture molar mass, $M_\alpha$ the molar mass of compound $\alpha$, $y_{\alpha\ell}$ the molar fraction within the mixture of the liquid phase of compound $\alpha$, $\rho_{\alpha\ell}$ is the liquid density of compound $\alpha$, L is the overall liquid mole fraction of the mixture, $R_0$ the universal gas constant, T the mixture temperature and P the mixture (vapour phase) pressure.

Of course the first term within the curly brackets is associated with the *liquid volume* and the second term with the *vapour volume*, assuming ideal gas behaviour.
The mixture molar mass M is found from

$$M = \sum_{\alpha=1}^{N} y_\alpha \cdot M_\alpha \qquad (2)$$

where $y_\alpha$ is the mixture mole fraction of compound $\alpha$.

**5.A.4. The reservoir state calculation**

Within the context of two-phase fluid storage and discharge, it is important to emphasise that the reservoir conditions being used should be representative of the fluid conditions in the immediate neighbourhood of the discharge orifice. The aerosol model in fact uses a *pseudo-one-phase* approach: liquid and vapour are assumed to be *homogeneously* distributed in terms of the vapour-liquid ratios. Single liquid droplets can *not* be distinguished and a droplet size distribution is *not* used.

For a given situation the user should realise that the location of the orifice can strongly influence the liquid-vapour ratio of the discharged fluid. E.g. if in a reservoir filled with propane half of the volume is occupied by liquid propane and the other half by propane vapour, depending on the location of the discharge orifice either a pure liquid release or a pure vapour release would occur. It is the user's responsibility to supply the correct reservoir conditions. The code will give details on the reservoir state and on the post-flash state to enable the user to check if the correct case is being simulated.

From the user-supplied reservoir conditions (temperature and pressure) and from the user-supplied mixture composition (compound names and mole fractions) the equilibrium reservoir state can be calculated using a simplified version of the aerosol algorithm as mentioned above. The simplification lies in the fact that the temperature T is now given. Instead of a double iteration loop to calculate T and the $L^\beta$'s, a single loop for the $L^\beta$'s only, is being used.
Again, the algorithm proves to be very robust.

When using the aerosol thermodynamics model, the user has the option *not* to specify the reservoir pressure. In this case the AEROPLUME program will calculate the reservoir mixture *saturation pressure* at the (user-supplied) reservoir temperature $T_{res}$ using Raoult's law as follows

$$P_{sat,mix} = \sum_{\alpha=1}^{N} y_\alpha \cdot P_{sat,\alpha}(T_{res}) \qquad (3)$$

where $y_\alpha$ is the mixture mole fraction of compound $\alpha$ and $P_{sat,\alpha}(T)$ is the saturated vapour pressure of compound $\alpha$. It is assumed in (3) that the sum of the molar fractions $y_\alpha$ is 1.
The reservoir pressure is then set to this saturation pressure.
It is thus assumed that all compounds $\alpha$ are in the *liquid-only* state. If this assumption is reasonable, then relation (3) will give a reasonable reservoir pressure.

**5.A.5. Calculation of post-flash conditions**

To initiate the actual jet development calculations, the initial post-flash jet properties are calculated from the reservoir state and the user-supplied orifice diameter and discharge mass flow rate. These properties are: $U_{flash}$, $H_{flash}$ and $D_{flash}$, which are velocity, enthalpy and diameter of the jet respectively.
From these the thermodynamic (aerosol) model gives values for the temperature $T_{flash}$ and density $\rho_{flash}$.

The pollutant concentration is taken to be 100 % as air entrainment is assumed to be negligible during this initial flashing process.

The calculation consists of two parts. First an adiabatic and frictionless acceleration of the (stagnant) reservoir fluid to a point just outside the orifice is assumed. Vapour and liquid velocities are assumed equal. There is no inter-phase heat exchange.

The maximum possible mass flow rate is calculated using choked flow relations and some vapour is assumed to be present in all cases, because for a liquid only mixture (L = 1) there is no limitation to the mass flow rate (frictionless flow). The vapour phase is assumed to behave as an ideal gas.

It is also assumed that the mixture liquid-vapour composition does not change during this (rapid) acceleration phase (frozen equilibrium). The fluid velocity and enthalpy just outside the orifice or *stack* are denoted by $U_{stk}$ and $H_{stk}$ respectively and the local fluid pressure there is $P_{stk}$.

The second part of the calculation is called the 'flashing' of the mixture: the new thermodynamic state of the mixture is calculated using the full aerosol algorithm, assuming that the pressure decreases from $P_{stk}$ to the ambient atmospheric pressure $P_{atm}$. At this stage the liquid-vapour composition does change and the post-flash fluid properties as mentioned above are then calculated.

More details about the actual relations being used will now be given below.
To describe the adiabatic and frictionless acceleration from the reservoir to the orifice two basic equations are used. Momentum conservation gives

$$dP/\rho + d(U^2/2) = 0 \tag{4}$$

and energy conservation gives

$$H_{res} = H + U^2/2 \tag{5}$$

These relations are valid at every point between the reservoir and the orifice.

During the acceleration process the vapour phase of the mixture, assumed to be an ideal gas, will experience adiabatic expansion and thus

$$P \cdot \rho_g^{-\gamma} = Cst \tag{6}$$

where $\gamma$ is the ratio of the specific heats of the vapour, i.e. $\gamma = c_p/c_v$ and $\rho_g$ is the vapour density.

The liquid density is *not* affected by the change in pressure.

Integrating (4) and using (1) and (6), $U^2/2$ at any point between reservoir and stack is found to be equal to

$$\frac{U^2}{2} = \frac{\sum_{\alpha=1}^{N} \frac{M_\alpha \cdot y_{\alpha\ell}}{\rho_{\alpha\ell}}}{M} \cdot (P_{res} - P) + \frac{1-L}{1-1/\gamma} \cdot \left( \frac{1}{a_{g,res}} - \frac{1}{a_g} \right) \tag{7}$$

where the auxiliary variables $a_g$ and $a_{g,res}$ are given by

$$a_g = \frac{M}{R_0 \cdot T} \tag{8a}$$

$$a_{g,res} = \frac{M}{R_0 \cdot T_{res}} \tag{8b}$$

To find the maximum mass discharge rate, it can be seen that this is equivalent to finding the maximum of $\rho \cdot u$ (discharge area is constant) or (equivalently) the maximum of $\rho^2 \cdot u^2$, all as function of $\rho$. Thus the equation to be solved is

$$\frac{d}{d\rho}\left(\rho^2 \cdot U^2\right) = 0 \qquad (9)$$

When working out this constraint by using (7), it is found that for the maximum discharge rate occurring at the choke pressure P and choke velocity U the condition

$$\frac{(1-L)\cdot R_0 \cdot T}{M} \cdot \frac{1}{\gamma} \cdot \left(\frac{\rho \cdot U}{P}\right)^2 = 1 \qquad (10)$$

holds, which is valid together with relation (7).

Note that for L = 1 (liquid-only mixture) this relation (10) *no longer* holds: for a frictionless flow the liquid-only mass flow rate is *not* limited.

Using the NAESOL package[1], the set of equations (7) and (10) can be solved for P and U when using the adiabatic expansion relation for an ideal gas to calculate T

$$\frac{T}{T_{res}} = \left(\frac{P}{P_{res}}\right)^{1-1/\gamma} \qquad (11)$$

It is the vapour phase of the mixture which can limit the mass flow rate to the choked flow value, and equation (11) is used to take a temperature drop during expansion of *the vapour* into account because this will significantly influence the value of the maximum (choked) mass flow rate. Using (11), the heat *exchange* between the two phases (liquid and vapour) in the mixture is being neglected.

Once U is found, the maximum mass flow (discharge) rate, $\dot{m}_{max}$, dictated by choked flow, is equal to $\dot{m}_{max} = A_{stk} \cdot U \cdot \rho$, where $A_{stk}$ is the orifice surface area ($= \pi \cdot D_{stk}^2/4$).

It is interesting to consider the alternative approach which *replaces* the condition of maximum mass flow rate (9) by the condition that the maximum mass flow rate occurs when

$$U = C \qquad (12)$$

where C is the local speed of sound in the two-phase mixture. An expression for C given by Wallis ([2], equation 2.51) is used

$$\frac{1}{C^2} = \left(v \cdot \rho_g + (1-v) \cdot \rho_\ell\right) \cdot \left( \frac{v}{\rho_g \cdot C_g^2} + \frac{1-v}{\rho_\ell \cdot C_\ell^2} \right) \tag{13}$$

where $v$ is the volumetric void fraction (volume fraction vapour in the mixture) and $C_g$ and $C_\ell$ the speeds of sound in the gas and liquid phase respectively and $\rho_g$ and $\rho_\ell$ the respective densities.

Now substitute for the speed of sound in the vapour phase, $C_g$, the well-known expression valid for ideal gases

$$C_g^2 = \gamma \cdot \frac{P}{\rho_g} \tag{14}$$

To express $v$ in mass fractions some auxiliary relations are needed, it can be seen after some manipulation that

$$v = \frac{\rho_\ell \cdot (1-X)}{\rho_\ell \cdot (1-X) + \rho_g \cdot X} \tag{15a}$$

where X is the *mass* fraction liquid in the mixture.
X can be expressed in terms of L by the relations

$$\frac{X}{\rho_\ell} = \frac{\sum_{\alpha=1}^{N} \frac{M_\alpha \cdot y_{\alpha\ell}}{\rho_{\alpha\ell}}}{M} \tag{15b}$$

and

$$\frac{1-X}{\rho_g} = (1-L) \cdot \frac{R_0 \cdot T}{M \cdot P} \tag{15c}$$

At this point (and not earlier!) the limit for $C_\ell$ going to infinity is

$$U^2 = C^2 = \frac{\gamma \cdot P^2 \cdot M}{(1-L) \cdot R_0 \cdot T \cdot \rho^2} \tag{16}$$

which is identical to (10).

Thus the *maximum mass flow rate constriction is equivalent to the constriction U = C*, which is a well-known result for ideal gases but is shown here to hold for two-phase flow also.

However, given the fact that the whole concept of *speed of sound* for two-phase fluids is unclear, this result should be considered to be merely a (nice) coincidence. The only correct, unambiguous, way to derive equation (10) is to use the maximum mass flow rate argument, i.e. start from equation (9).

For the special case of a vapour only mixture (L = 0, X = 0 and $v$ = 1) the following relations are valid

$$P = P_{res} \cdot \left( \frac{2}{1+\gamma} \right)^{\gamma/\gamma-1} \qquad (17a)$$

and

$$\frac{U^2}{2} = \frac{\gamma}{1+\gamma} \cdot \frac{P_{res}}{\rho_{res}} \qquad (17b)$$

Thus for this case an *analytical solution* for the set of equations (7) and (10) is available and the numerical code NAESOL is not needed to find U and P.

If the choke pressure turns out to be less than the ambient pressure $P_{atm}$, then the maximum mass flow rate is calculated based on the assumption that $P = P_{atm}$. In fact *unchoked flow* occurs in this case.

The AEROPLUME code checks if the user-specified mass flow rate is admissible (i.e. less than the maximum mass flow rate as calculated above) and if it is, then the *stack conditions* $U_{stk}$, $P_{stk}$, $\rho_{stk}$ and $D_{stk}$ are calculated by solving the mass conservation equation

$$A_{stk} \cdot \rho_{stk} \cdot U_{stk} = \dot{m} \qquad (18)$$

and equation (7) simultaneously.

In general $\dot{m}$ is the plume mass flow rate, but before the actual plume calculations have started $\dot{m}$ is equal to the pollutant release rate (in kg/s) because no ambient air has been entrained into the plume yet.

If $P_{stk}$ is less than the ambient pressure then the AEROPLUME code halts with an error message and the user should modify either $\dot{m}$ or the reservoir conditions.

The enthalpy $H_{stk}$ is calculated using (5)

$$H_{stk} = H_{res} - \frac{U_{stk}^2}{2} \qquad (19)$$

From (19) it can be seen that for high orifice velocities $H_{stk}$ can become large negative. It even can occur that $H_{stk}$ falls below a physically acceptable minimum value (dictated by T > 0 K). The code calculates the minimum value of H for the current mixture composition and halts execution if $H_{stk}$ is less than this minimum value.

If $H_{stk}$ is acceptable then the actual flash calculation is started: the new thermodynamic state of the mixture, when the pressure has dropped from $P_{stk}$ (always ≥ $P_{atm}$) to $P_{atm}$, is calculated. In general, the liquid-vapour ratio will change during flashing.

The velocity after depressurisation is calculated to be

$$U_{flash} = U_{stk} + \frac{P_{stk} - P_{atm}}{\rho_{stk} \cdot U_{stk}} \qquad (20)$$

which follows from a control volume analysis, valid for (assumed) one-dimensional flow and considering momentum-*flux*. It is *not* assumed that the cross-sectional area remains constant during depressurisation.
The enthalpy of the post-flash mixture is then simply

$$H_{flash} = H_{res} - \frac{U_{flash}^2}{2} \qquad (21)$$

Again the code checks whether $H_{flash}$ exceeds the minimum value.

The value of the enthalpy $H_{flash}$ together with the fact that the jet is assumed to be pure pollutant (no entrained air yet) completely determine the thermodynamic state of the post-

flash jet and this state is calculated using the standard aerosol thermodynamic routines. Density, temperature and liquid mole fraction are thus calculated.

The diameter of the post-flash jet is calculated by

$$D_{flash}^2 = \frac{4 \cdot \dot{m}}{\pi \cdot \rho_{flash} \cdot U_{flash}} \qquad (22a)$$

This completes the post-flash jet state calculation.

Please note that instead of the release from a reservoir scenario, the user has the option of simulating a *vent stack* problem using AEROPLUME (see information on input parameters in Appendix A). In this case the reservoir and post-flash calculations, as discussed in paragraph 5.A.3 and 5.A.4, are skipped and the post-flash velocity $U_{flash}$ is calculated directly from the pollutant mass flow rate $\dot{m}$, stack release temperature $T_{stk}$ and the stack diameter $D_{stk}$ (all three user-specified), by simply using

$$U_{flash} = \frac{4 \cdot \dot{m}}{\pi \cdot \rho_{stk} \cdot D_{stk}^2} \qquad (22b)$$

The density of the stack release, $\rho_{stk}$, is calculated by AEROPLUME using the full thermodynamic model and assuming that the stack release mixture has the user-specified temperature $T_{stk}$ and is at the ambient atmospheric pressure $P_{atm}$. This also gives the value of the pollutant stagnation enthalpy at the stack and $H_{flash}$ is found from relation (21) with $H_{res}$ being replaced by the stack stagnation enthalpy.

This option was introduced to simplify the use of AEROPLUME for stack simulations where the concept of a reservoir is not applicable (i.e. the old PLUME scenario).

**5.A.6. Discharge rate specification**

From the discussion above (paragraph 5.A.4), it follows that the user can specify any pollutant discharge rate (mass flow rate) that does not exceed the maximum possible discharge rate as dictated by the AEROPLUME discharge model.

However, it is not always easy to predict the discharge rate for given reservoir conditions and orifice dimensions. Therefore the user of AEROPLUME has the option *not* to specify the pollutant mass flow rate and in this case the code will use a literature correlation to fix its value. Again it is noted that at the start of the plume calculation, the plume mass flow rate $\dot{m}$ is equal to the pollutant mass flow rate, as no ambient air has been entrained yet.

A value of $\dot{m}$ that follows from AEROPLUME's own discharge model is also printed out to give the user more information on the possible range of values and enable him to make a reasonable choice for the actual value of $\dot{m}$ to be used in the simulations.

For a *gas-only* release the discharge rate used by the program is simply the (maximum) discharge rate found for an ideal gas (either choked or unchoked) which the AEROPLUME discharge model will calculate.

For choked vapour only flow, using relations given above, the discharge rate is

$$\dot{m} = C_D^g \cdot A_{stk} \cdot \left(\frac{2}{1+\gamma}\right)^{1/(\gamma-1)} \cdot \left(\frac{\gamma}{1+\gamma}\right) \cdot \sqrt{2 \cdot \rho_{res} \cdot P_{res}} \qquad (23a)$$

and for unchoked vapour only flow, using ideal gas relations

$$\dot{m} = C_D^g \cdot A_{stk} \cdot \sqrt{\frac{\gamma}{\gamma-1}} \cdot \sqrt{2 \cdot \rho_{res} \cdot P_{res} \cdot \left\{ \left(\frac{P_{atm}}{P_{res}}\right)^{\frac{2}{\gamma}} - \left(\frac{P_{atm}}{P_{res}}\right)^{\frac{\gamma+1}{\gamma}} \right\}} \qquad (23b)$$

The vapour discharge coefficient $C_D^g$ has a default value of 1.0, but the user of the AEROPLUME model can override this value if necessary.

For a *two-phase* release, first the mixture saturation pressure $P_{sat}$ is calculated as

$$P_{sat} = \frac{\sum_{\alpha=1}^{N} y_{\alpha\ell} \cdot P_{sat,\alpha}(T)}{\sum_{\alpha=1}^{N} y_{\alpha\ell}} \qquad (24)$$

where $y_{\alpha\ell}$ is the molar fraction within the total mixture of liquid compound $\alpha$ and $P_{sat,\alpha}(t)$ is the saturation pressure of compound $\alpha$ at temperature T.
This relation is based on Raoult's law and should be compared with relation (3). Note that in (3) the sum of the molar fractions is always 1, but in (24) the sum of the $y_{\alpha\ell}$ is not necessarily equal to 1.

If $P_{sat}$ is less than $P_{atm}$ then the liquid mixture is *subcooled* even at atmospheric conditions and no flashing will occur at the exit.
From Fauske and Epstein [3] a Bernoulli-like expression for the discharge rate is found

$$\dot{m}(t) = -C_D^{\ell} \cdot A \cdot \sqrt{2 \cdot \rho_{\ell}(t) \cdot \left(P(t) - P_{atm}\right)} \tag{25}$$

where $\rho_{\ell}$ is the density of the *liquid* in the reservoir. The liquid discharge coefficient $C_D^{\ell}$ has a default value of 0.61 [3], but again the user can override this value by setting a SPILL input parameter.

When $P_{sat}$ exceeds $P_{atm}$, i.e. the liquid mixture in the reservoir, which is subcooled at reservoir conditions, is *not* subcooled at atmospheric conditions, then a distinction must be made between reservoir conditions that are *near the saturation point* and those that are not.

If $\left|P(t) - P_{sat}\right| > 10 \cdot P_{sat}$ (reservoir conditions far from the saturation point) then following [3]

$$\dot{m}(t) = -C_D^{\ell} \cdot A \cdot \sqrt{2 \cdot \rho_{\ell} \cdot \left|P(t) - P_{sat}\right|} \tag{26}$$

If $\left|P(t) - P_{sat}\right| < 0.1 \cdot P_{sat}$ (reservoir conditions near the saturation point), [3] gives

$$\dot{m}(t) = -C_D^{\ell} \cdot A \cdot \sqrt{\left|\frac{1}{dv / dP}\right|} \tag{27}$$

where $v = 1/\rho$ ($m^3/kg$) is the specific volume of the mixture. The term $\left|\frac{1}{dv/dP}\right|$ is estimated, following [3], by

$$\left|\frac{1}{dv/dP}\right| = \left(\frac{h_{vap}}{\Delta v_{vap}}\right)^2 / (T \cdot C_{p,\ell}) \tag{28}$$

where $h_{vap}$ (J/kg) is the heat of vaporisation, $\Delta v_{vap}$ ($m^3/kg$) the change in specific volume going from the liquid to the vapour state, $C_{p,\ell}$ (J/(kg·K)) is the specific heat of the liquid mixture and T (K) is the reservoir temperature.

For the intermediate stage, $0.1 \cdot P_{sat} \le \left|P(t) - P_{sat}\right| \le 10 \cdot P_{sat}$, *linear interpolation* between the two previous cases is used. Let FACTOR, TERM1 and TERM2 be defined by

$$\text{FACTOR} = \frac{\left|P(t) - P_{sat}\right|}{P_{sat}} \tag{29}$$

$$\text{TERM1} = 2 \cdot \rho_{\ell} \cdot \left|P(t) - P_{sat}\right| \tag{30}$$

$$\text{TERM2} = \left| \frac{1}{dv / dP} \right| \tag{31}$$

Define the variable TERM3 by using linear interpolation between TERM1 and TERM2 using FACTOR, that is

$$\text{TERM3} = \text{TERM2} + (\text{FACTOR} - 0.1) \cdot \frac{\text{TERM1} - \text{TERM2}}{10.0 - 0.1} \tag{32}$$

and the reservoir mass discharge rate when $0.1 \cdot P_{sat} \le \left| P(t) - P_{sat} \right| \le 10 \cdot P_{sat}$, is given by

$$\dot{m}(t) = -C_D^{\ell} \cdot A \cdot \sqrt{\text{TERM3}} \tag{33}$$

This linear interpolation procedure for the case where $0.1 \cdot P_{sat} \le \left| P(t) - P_{sat} \right| \le 10 \cdot P_{sat}$ is found to give more satisfactory results than the recommendation in [3] , the latter being equivalent to taking TERM3 = TERM1 + TERM2.

Please note that the mass discharge literature correlations and the definition of $P_{sat}$ used in SPILL and AEROPLUME are completely identical. The SPILL model is discussed in Chapter 3.

The AEROPLUME code will use the appropriate correlation to specify $\dot{m}$ if the user does not specify $\dot{m}$ himself. However if the discharge rate given by the correlations exceeds the maximum mass flow rate as calculated by the AEROPLUME discharge model, then $\dot{m}$ will be set to the value of this maximum mass flow rate. All relevant calculated mass flow rates are given in the AEROPLUME output messages.

Also note that when following the vent stack scenario (no specification of reservoir conditions but specification of the stack release temperature instead) the user *must* specify a positive value for the mass flow rate to completely prescribe the release conditions. In this case (no reservoir and discharge calculations) *any* mass flow rate is acceptable as there is no choked-flow mass flow rate restriction.

### 5.A.7. Plume development model

The development of the plume as it travels from its release point through the ambient atmosphere, including touchdown with the ground surface, is described by a mathematical model as given in Chapter 5.B.

In the current AEROPLUME code, a set of 4 algebraic and 10 first order ordinary differential equations is used to describe the plume development. This set of equations is different from the one used in the old PLUME model or in HFPLUME, because the thermodynamic equations are no longer solved *coupled* with the plume integration ones, but they have been *separated out* into the specific thermodynamic routines as discussed earlier. See Chapter 5.B. for more details on the general PLUME and HFPLUME jet formulation. Furthermore, the temperature T is no longer being used as a basic variable, but the enthalpy H instead. And finally, as the thermodynamic routine calculates the pollutant concentration, using the total mass flow rate and the pollutant mass flow rate, it is no longer needed to have the pollutant concentration as an explicit variable in the plume integration system, as was the case in PLUME and HFPLUME.

For completeness sake the complete set of equations governing the plume development is given below.

The fourteen basic plume variables used are: enthalpy H, velocity U, diameter D, inclination with respect to the horizontal $\varphi$, ambient velocity $U_{atm}$, ambient pressure $P_{atm}$, ambient temperature $T_{atm}$, total mass flowrate $\dot{m}$, excess energy flux $\dot{E}$, excess horizontal momentum flux $\dot{P}x$, excess vertical momentum flux $\dot{P}z$, horizontal displacement X, plume centroid height Z and finally time t.

All variables are plume-diameter-averaged. This is the 'top-hat' approach as mentioned in Chapter 5B.

The time t is not needed for the actual AEROPLUME calculations, but the total elapsed time (release duration) is communicated to HEGADAS if a link between the two programs is being made.

The fourteen equations are now given; first the four *algebraic constraints*, then the ten *ordinary differential equations*.

*Conservation of mass*

$$\dot{m} = A(D, Z, \varphi) \cdot \rho \cdot U \qquad \text{(I)}$$

where the plume surface area $A(D,Z,\varphi)$ depends on the plume state (airborne, touchdown or slumped) as discussed in Chapter 5B.

Note that the plume density ρ is *not* one of the solved variables, but is calculated within the thermodynamic routine which is called every time the thermodynamic state needs to be updated.

*Conservation of excess horizontal momentum*

$$\dot{P}x = \dot{m} \cdot \left( U \cdot \cos(\varphi) - U_{atm} \right) \qquad \text{(II)}$$

*Conservation of excess vertical momentum*

$$\dot{P}z = \dot{m} \cdot U \cdot \sin(\varphi) \qquad \text{(III)}$$

*Conservation of excess energy*

$$\dot{E} = \dot{m} \cdot \left( H + \frac{U^2}{2} - H_{atm} - \frac{U_{atm}^2}{2} \right) \qquad \text{(IV)}$$

where $H_{atm}$ is given by a standard atmospheric correlation.

Next, three differential equations describe the change in atmospheric state variables as the plume travels along.

$$\frac{dU_{atm}}{ds} = \frac{dU_{atm}}{dZ} \cdot \sin(\varphi) \qquad \text{(V)}$$

$$\frac{dP_{atm}}{ds} = -\rho_{atm} \cdot g \cdot \sin(\varphi) \qquad \text{(VI)}$$

$$\frac{dT_{atm}}{ds} = \frac{dT_{atm}}{dZ} \cdot \sin(\varphi) \qquad \text{(VII)}$$

where $\frac{dU_{atm}}{dZ}$, $\rho_{atm}$ and $\frac{dT_{atm}}{dZ}$ are given by standard atmospheric correlations. The parameter s is the integration parameter along the plume axis. Finally, g is the acceleration of gravity.

Next, the differential equations describing the change of the four conserved physical quantities (mass, horizontal and vertical momentum and energy) are given.

$$\frac{d\dot{m}}{ds} = Entr_{Amb}^{A(s)} \qquad \text{(VIII)}$$

where $Entr_{Amb}^{A(s)}$ is the amount of ambient air entrained by the jet as given by the entrainment model as described in Chapter 5.B.

$$\frac{d\dot{E}}{ds} = -\dot{m} \cdot \left( \frac{dH_{atm}}{dZ} + U_{atm} \cdot \frac{dU_{atm}}{dZ} + g \right) \cdot \sin(\varphi) \qquad \text{(IX)}$$

where $\frac{dH_{atm}}{dZ}$ is again given by a correlation.

$$\frac{d\dot{P}x}{ds} = -\text{Shear} - \text{Drag}_x - \text{Impact}_x \qquad \text{(X)}$$

Shear, Drag and Impact are the forces working on the plume. For details see Chapter 5B.

$$\frac{d\dot{P}x}{ds} = -\text{Buoy} - \text{Foot} - \text{Drag}_z - \text{Impact}_z \qquad \text{(XI)}$$

where again expressions for Buoy and Foot are given in Chapter 5B.

Finally there are three simple differential equations describing displacement, height and time development.

$$\frac{dX}{ds} = \cos(\varphi) \qquad \text{(XII)}$$

$$\frac{dZ}{ds} = \sin(\varphi) \qquad \text{(XIII)}$$

$$\frac{dt}{ds} = \frac{1}{U} \qquad \text{(XIV)}$$

This complete set of fourteen equations is solved using the SPRINT package [4] in the same way as in PLUME and HFPLUME.

### 5.A.8. References

1. Scales, L.E., '*NAESOL - A Software toolkit for the solution of non-linear algebraic equation systems; User Guide - Version 1.5*', Shell Research Limited, Thornton Research Centre, TRCP.3661R, 1994.

2. Wallis, G.B., '*One-dimensional two-phase flow*', McGraw-Hill, New York, 1969.

3. Fauske, H.K., Epstein, M., '*Source term considerations in connection with chemical accidents and vapour cloud modelling*', J. Loss Prev. Process Ind., vol 1, April 1988.

4. Berzins, M., Furzeland, R.M., '*A user's manual for SPRINT - a versatile software package for solving systems of algebraic, ordinary and partial differential equations: Part 1 - Algebraic and ordinary differential equations*', Shell Research Limited, Thornton Research Centre, TNER.85.058, 1985.

**5.A.9. Notation**

| | |
|---|---|
| A | surface area ($m^2$) |
| C | speed of sound (m/s) |
| $C_D$ | discharge coefficient (-) |
| D | diameter (m) |
| $\dot{E}$ | excess energy flux (J/s) |
| g | acceleration of gravity ($m/s^2$) |
| H | enthalpy (J/kg) |
| L | mole fraction liquid in aerosol mixture (-) |
| M | molar mass of mixture (kg/mole) |
| *M* | number of aerosols in mixture |
| $\dot{m}$ | mass flow rate or discharge rate (kg/s) |
| *N* | total number of compounds |
| P | pressure (Pa) |
| $\dot{P}x$ | excess horizontal momentum flux ($kg \cdot m/s^2$) |
| $\dot{P}z$ | excess vertical momentum flux ($kg \cdot m/s^2$) |
| $R_0$ | universal gas constant (8314 J/(kmol·K)) |
| s | distance along plume axis (m) |
| T | temperature (K or °C) |
| t | time (s) |
| U | plume velocity in direction of plume axis (m/s) |
| v | specific volume ($m^3/kg$) |
| X | mass fraction liquid (-) |
| X | horizontal plume displacement (m) |
| y | molar fraction (-) |
| Z | plume centroid height (m) |
| $\gamma$ | ratio of specific heats ($c_p/c_v$) for ideal gas (-) |
| $\varphi$ | plume inclination with respect to horizontal (°) |
| $\rho$ | plume density ($kg/m^3$) |

| | |
|---|---|
| $v$ | volumetric void fraction (-) |

Subscripts and superscripts

| | |
|---|---|
| atm | ambient atmosphere |
| $\alpha$ | compound indicator |
| flash | post-flash |
| g | vapour (gas) phase of a two-phase mixture |
| $\ell$ | liquid phase of a two-phase mixture |
| res | reservoir |
| sat | saturation |
| stk | stack, orifice |

# 5.B. DEVELOPMENT OF PLUME AND JET RELEASE MODELS

## 5.B.8. Introduction

This chapter sets out the basic formulation and structure of the plume models PLUME, AEROPLUME and HFPLUME. The model describes initial jet flow, elevated plume, plume touchdown, and gravity-slumping following a pressurised release of an ideal gas (PLUME) or a two-phase multi-compound mixture (AEROPLUME) or an anhydrous hydrogen fluoride (HFPLUME).
PLUME and HFPLUME are available in version 1.0 of HGSYSTEM (NOV90 version). In version 3.0 of HGSYSTEM, PLUME has been replaced by AEROPLUME.

The HGSYSTEM plume models are comprehensive models of dispersion in the near-field. Prediction of far-field dispersion requires that these plume models be 'matched' (linked) either to a heavy gas dispersion model, such as HEGADAS-S, or else, for neutral or buoyant releases, to a passive dispersion model PGPLUME. See relevant Chapters on these far-field models in the HGSYSTEM documentation.

Previous work (Ooms 1972; Wheatley 1987a, 1987b); Forney and Droescher 1985; Birch and Brown 1988; McFarlane 1988; Raj and Morris 1987) on dense and buoyant plumes, two-phase and pressurised gas jets, reactive and ground-affected jets, supported the view that predictions accurate in context could be obtained by means of an essentially simple, one-dimensional, integral-averaged model.

The plume models have been validated against thermodynamic data for HF/moist-air systems (Schotte 1987, 1988); their entrainment formulations have been checked against observed dispersion of buoyant (Peterson 1987) and dense (Hoot, Meroney and Peterka 1973) (ideal) gases, and against (atmospheric) releases of liquid propane gas (Cowley and Tam 1988, McFarlane 1988).
The two-phase model AEROPLUME has been validated using data of liquid propane releases (Post 1994).

In addition the model combination HFPLUME/HEGADAS-S has been used (Chapter 7.A.) to simulate large-scale experimental releases of anhydrous hydrogen fluoride (Blewitt, Yohn, Koopman and Brown 1987; Blewitt, Yohn and Ermak 1987; Blewitt 1988).

The indications are that the plume models are satisfactory predictors of the early dispersion (plume rise, fall, touchdown, and early slumping) of a dense, neutral, or buoyant release.

### 5.B.9. The Stages of Plume Development

Prior to the development of the HGSYSTEM plume models, specifically for the HFPLUME model, we conducted a literature review in order to determine whether any existing model could be adapted to simulate a jet of anhydrous hydrogen fluoride (HF). The following sub-sections describe the results of that review for a number of models. The discussion is presented for the various zones of importance: external flashing, flow establishment, airborne plume, touchdown plume, slumped plume, and the far field.

From point of release to the far-field a dense plume passes through a series of (phenomenological) stages. These stages form the basis of the computer based models AEROPLUME, PLUME and HFPLUME: the identification, sequence, and characteristics of these stages is therefore of considerable importance. This section should make clear the need for a careful selection of literature available models, and for their extension to cover regions not previously considered.

#### External Flashing

Consider a pressurised release of an evaporating liquid (say HF). Such a release forms at the orifice a narrow zone in which take place pressure relaxation and violent 'flashing'. 'Flashing' is the sudden and disruptive evaporation of superheated liquid in response to a sharp fall in fluid pressure. This results in prompt atomisation of any residual liquid and in the development of a two-phase flow. This stage of plume development is extremely complex.

Fortunately details of 'flashing' flow are not needed: it is sufficient to 'bridge' this zone by means of integral conservation laws and by assuming that air entrainment during flashing is negligible (Wheatley 1987a, Raj and Morris 1987). The flashing zone ends when approximate thermal equilibrium, ambient pressure, and negligible inter-phase slip between vapour and liquid (droplet) phases are established. The velocity profile is roughly uniform; the cross-section may be assumed circular; deflection due to ambient pressure in cross-flow is typically negligible (Figure 5.1).

#### Flow Establishment

Immediately beyond the flashing zone there exists a second zone 'of flow establishment': air entrainment as the result of shear-induced turbulence results in the progressive dilution of the evaporating liquid jet, and in the radial diffusion of air towards the plume centre-line.

The flow is described by an unperturbed 'core' region, which diffusion of air has not reached, and by an axi-symmetric 'outer' region, in which turbulent diffusion has resulted in a near Gaussian distribution of entrained air. This zone ends with the complete 'erosion' of the core

region and with the establishment of approximately self-similar conditions within the flow. The cross-section may be assumed circular (Figure 5.2).

Generally this region is either neglected (Raj and Morris 1987; Hoot, Meroney and Peterka 1973; Forney and Droescher 1985), or else considered in conjunction with such effects as stack 'downwash' (Hanna 1982; Ooms 1972; Havens 1987) and represented by an empirically derived correlation (Keffer and Baines 1963, Kanatani and Greber 1972). The discussion follows an analysis of Albertson Dai, Jensen and Hunter Rouse (1948), and of Abramovich (1963).

**Airborne Plume**

Following flow establishment, plume development is described by the interaction of plume, ambient wind, and buoyancy effects: the influence of the ground, except as a generator of ambient turbulence and of wind-shear is negligible.

This is the simplest of all the stages of plume development: nonetheless it is not without controversy. Arguments exists over the level of description necessary: whether *Gaussian* (Ooms 1972; Ooms and Duijm 1983; Petersen 1986; Schatzmann 1979) or '*top-hat*' (Hoot, Meroney and Peterka 1973; Forney and Droescher 1985; Davidson 1986) models are preferable; whether the effects of gradients within the atmosphere need be considered (Schatzmann and Policastro 1984); and whether or not significant 'drag' forces act upon a plume in cross-wind (Briggs 1984; Ooms 1972; Schatzmann 1979, Hoult, Fay and Forney 1969; Coelho and Hunt 1989).

Several different formulations for the crosswind entrainment have been proposed and checked against experimental data (Peterson 1978, 1987; Schatzmann 1978, Spillane 1983).

Even the basic formulation of the equations of motion has resulted in discussion (Schatzmann 1978, 1979; McFarlane 1988), and in the use of special devices, such as plume 'truncation' and dilute gas thermodynamics (Ooms 1972, Petersen 1978).

The cross-section is generally assumed to be circular; the flow axi-symmetric. However the presence of trailing vortices in cross-flow, and the cumulative effect of differences in vertical and horizontal diffusivity in the undisturbed atmosphere, will result in asymmetry and ultimately in an elliptic cross-section (Bloom 1980; Li, Leijdens and Ooms 1986). The role of dilute plume asymptotics in allowing estimation of certain entrainment coefficients from plume-rise and other data should be emphasised. Such early work as that of Briggs (1975) in

the development of semi-empirical plume-rise correlations based on such analyses should not be neglected. (Figure 5.3).

**Touchdown Plume**

Dense plumes must ultimately drift to ground or at any rate expand as the result of entrainment so as to intersect the ground surface.

The ground interacts with a descending plume in several ways. First it acts as a geometrical constraint resulting in the redistribution of plume material. Second the ground allows the development of pressure forces as the result of pre-existing vertical momentum within the plume. These are impact forces resulting in the conversion of vertical to horizontal momentum. Third the ground permits the development of internal pressure within the plume as the result of gravity-slumping, in which the transverse motion of a gravity current is driven by an internally generated pressure acting at the ground surface. Finally drag forces must act at the ground as the result of differences in horizontal speed between plume and ambient wind.

In this region a transition must be made between a circular cross-section appropriate to an airborne plume, and a semi-elliptical (say) cross-section appropriate to an advected heavy-gas plume resting upon the ground (Figure 5.4). The touchdown region is described by a cross-section in the form of a circular segment. The region ends when a semi-circular cross-section first develops.

This transition region is neglected by Havens (1987, 1988a) following Ooms (1972) and Ooms and Duijm (1984), as well as (inter alia) by Bloom (1980), by Schatzmann (1979) and by Raj and Morris (1987).
No previous model exists which attempts to make a smooth transition from airborne dense to advected slumped plume. Limited experimental evidence does exist in the form of an unpublished study of dense salt water plumes (Karman 1986). In addition photographic evidence collected but not published by Hoot, Meroney and Peterka (1973) may form a useful data set for model validation.

**Slumped Plume**

Following touchdown the plume cross-section may be assumed semi-elliptic. Changes in plume eccentricity (aspect ratio) accommodate gravity slumping and the influence of residual ground-drag and impact pressure-forces. Vertical motions will be small compared to horizontal (Figure 5.5). An asymptotic approach, based on assumed horizontal flow, prescribed air entrainment, and a representation of gravity-spreading, is therefore possible.

Such a model is that proposed by Raj and Morris (1988) for dense plumes released horizontally at or near ground-level. The model incorporates jet entrainment, ground drag, and a formula for dense-gas gravity spreading. This model is (however) not valid for buoyant slumped plumes; neither is an interface for initially vertical releases provided.

Havens (1988) does not attempt to deal rigorously with the transition zone, for which horizontal momentum may be significant, but rather makes a simple transition from first plume/ground contact to heavy-gas advection. It may be questioned whether such a transition is physically appropriate.

**The Far-Field**

Ultimately differences in velocity between (heavy-gas) plume and ambient atmosphere must become negligible, so that the representation of the HGSYSTEM plume models or that of Raj and Morris (1988) must merge into a heavy gas dispersion model such as HEGADAS. This is accomplished (Chapter 7.A, section 7.A.4.2.) by means of *asymptotic matching*.

Alternatively for asymptotically buoyant plumes a transition may be made directly to a passive advection (Gaussian) model such as PGPLUME (Chapter 6, Hanna 1982). It is also possible to incorporate the observed horizontal and vertical diffusion for a passive plume into the near-field formalism (Bloom 1980, Disselhorst 1984). This procedure is computationally costly; its advantage over simple matching unclear.

Curiously for horizontal slumped releases Raj and Morris (1988) are content to use their grounded jet model throughout the heavy-gas advection region, matching ultimately with a passive advection model (Figures 5.6, 5.7). This procedure fails to make use of well-validated models for heavy-gas dispersion.

To summarise: a review of the literature revealed clear gaps in existing models of early plume dispersion. These relate particularly to complex thermodynamics, to plume touchdown, and to the dispersion on the ground of possibly buoyant possibly dense clouds, such as arise for example from the interaction of HF and moist air. There was need of a *consistent* fundamentally-based model capable of describing all of the stages of plume development. No such formalism existed prior to the development of HFPLUME. It is to the development and validation of such a comprehensive model that this Chapter is addressed.

### 5.B.10. Control Volume Analysis: Basic equations of Motion

Consider a steady plume or jet issuing from a pipe break at pressure and at an angle to the horizontal. The atmosphere into which a release takes place is in a state of steady turbulent

flow and has a mean wind-speed which is both horizontal and aligned with the horizontal component of the released jet. This last assumption is inessential, and is introduced to simplify the equations of plume motion.

We shall regard the jet and ambient atmosphere as a single fluid (of variable composition due to entrainment of ambient air) occupying the upper half-plane above a horizontal ground-surface. The jet and ambient atmosphere merge infinitesimally so that no jet 'boundary' exists at finite distance from the jet-axis; entrainment occurs therefore 'at infinity'. No slip occurs amongst the constituent phases of the developing jet; mean-flow within both ambient atmosphere and jet/plume is everywhere steady.

We begin by introducing a set of control-volumes $\tau(s)$, $s > 0$, an analysis of which results in an integral-averaged description of jet development independent of detailed assumptions regarding induced and ambient turbulence.

> *The Control-Volume* $\tau(s)$: First construct a vertical surface at such distance upwind of the release-point that ambient flow is negligibly perturbed. Second, at arbitrary distance $s > 0$ downwind of the release-point, construct a 'cross-section' $A(s)$ through the developing jet. Third link these (semi-infinite) surfaces by skirting the ground and pipe-work surfaces and passing through the jet at the plane of release. Finally construct a fourth bounding surface $A_\infty$ at great (notionally infinite) distance from the jet-axis such as to enclose the (infinite) volume $\tau(s)$. [See Figure 5.1-5.3; Figure 5.8]

By a 'cross-section' $A(s)$ we intend a curved surface locally perpendicular to the (turbulent mean) flow-velocity u. We shall assume that these surfaces form a family parameterized by a distance $s > 0$ measured along a (mean flow) stream-line (the plume-axis) originating at the point of release. Such a cross-section is orthogonal to the plume centre-line and asymptotically vertical at great off-axis distance. It reflects the progressive rotation of the mean plume velocity from centre-line to undisturbed atmospheric values.
We shall assume that the characteristic length-scales for plume development parallel and perpendicular to the mean-flow are asymptotically ordered, at any rate in those regions of the flow for which departures between the plume and undisturbed ambient flows are significant. Specifically we shall take the parallel length-scale to be much greater than the perpendicular: it is in this sense that the jet/plume may be described, following Hinze (1959), as 'thin'. Finally we shall have regard to that part of the ground surface over which there exist significant departures from the undisturbed ambient either in pollutant concentration, in pressure, or in ground-shear. This area, the intersection of plume and ground, we term the plume 'footprint' $F(s)$.

Integration of the basic equations of motion over such a control-volume results, given an assumed 'thin' jet, in the integral forms (Hinze 1959):

**Pollutant mass-flux**

$$\iint_{A(s)} c\mathbf{u}\cdot d\mathbf{A} = (c_0/\rho_0)\, dm/dt_0 \tag{34}$$

**Entrained mass-flux**

$$\iint_{A(S)} (\rho\mathbf{u} - \rho_\infty \mathbf{u}_\infty)\cdot d\mathbf{A} = \mathbf{A}_0\cdot(\rho_0\mathbf{u}_0 - \rho_\infty\mathbf{u}_\infty) - \iint_{A_\infty(s)} \rho\mathbf{u}\cdot d\mathbf{A} \tag{35}$$

**Horizontal excess-momentum flux**

$$\begin{aligned}\iint_{A(s)} \left[\rho\mathbf{u}(u_x - u_\infty) + (p - p_\infty)\mathbf{e}_x\right]\cdot d\mathbf{A} &= (u_{x,0} - u_\infty)dm/dt_0 + A_0\cos\phi_0(p_0 - p_\infty) + \\ -\iiint_{\tau(s)} \rho\mathbf{u}\cdot\nabla u_\infty d\tau - \iint_{F(s)} (\Sigma_{xz} - \Sigma^\infty_{xz})dA\end{aligned} \tag{36}$$

**Vertical momentum flux**

$$\begin{aligned}\iint_{A(s)} [\rho\mathbf{u}u_z + (p - p_\infty)\mathbf{e}_z]\cdot d\mathbf{A} &= u_{z,0}\, dm/dt_0 + A_0\sin\phi_0(p_0 - p_\infty) \\ -\iiint_{\tau(s)} (\rho - \rho_\infty)g\, d\tau + \iint_{F(s)} (p - p_\infty)\, dA\end{aligned} \tag{37}$$

**Total energy flux**

$$\begin{aligned}\iint_{A(s)} [\rho\mathbf{u}(h + \tfrac{1}{2}\mathbf{u}^2 - h_\infty - \tfrac{1}{2}\mathbf{u}_\infty^2)]\cdot d\mathbf{A} &= \iint_{F(s)} (\Phi - \Phi_a)dA + \\ +(h_0 + \tfrac{1}{2}u_0^2 - h_{\infty,0} - \tfrac{1}{2}u_{\infty,0}^2)\, dm/dt_0 - \iiint_{\tau(s)} \rho\mathbf{u}\cdot\nabla(h_\infty + \tfrac{1}{2}u_\infty^2 + gz)\, d\tau\end{aligned} \tag{38}$$

Notation: vectors are given in bold type and the '·' denotes a vector product, $dm/dt_0$, mass flow-rate issuing from the release-point; ($\rho$,c,**u**,p,h), density, pollutant mass-concentration, velocity, absolute pressure, and specific enthalpy of the ensemble-averaged flow. $\phi$ angle to

the horizontal of the plume-axis (co-ordinate stream-line), Φ the surface to air heat-flux, $å_{xz}$ the Reynolds stress as the result (ultimately) of viscous drag at the ground. $\mathbf{e}_x$ and $\mathbf{e}_y$ denote unit vectors in the horizontal (wind aligned) and vertical (upward) directions. The affix '0' identifies conditions at the release-plane; the suffix '¥' conditions within the unperturbed atmosphere.

These equations express in integral form conservation of pollutant (e.g. HF) mass-flux, air entrainment, conservation of the excess above ambient of momentum (both horizontal and vertical), and conservation of energy.

The pollutant continuity equation (**Pollutant mass-flux**) expresses that the released pollutant (for example HF), is merely transported and diluted by the atmosphere.

Total mass continuity (**Entrained mass-flux**) allows the identification of the entrained air mass-flux with the integrated sum of mass-flows induced 'at infinity', that is at great distance from the plume centre-line. The equation is formulated as a difference in mass-flux between the undisturbed atmosphere and the system that exists following a sustained release of a pollutant. This has advantages over conventional (total mass-flux) formulations (Ooms 1972, Petersen 1987) in that it is not necessary to introduce a 'cut-off' point in a Gaussian plume model beyond which conditions revert (discontinuously) to atmosphere values (Schatzmann 1978). This permits *true* Gaussian profiles to be introduced in estimating concentrations and temperatures within the developing plume or jet, with a consequent improvement in the accuracy of predicted centre-line concentrations (Davidson 1986, McFarlane 1988).

The horizontal momentum equation (**Horizontal excess-momentum flux**) states that (in the absence of ground drag and significant vertical wind-shear) the excess-flux of horizontal momentum is conserved. Horizontal momentum excess is therefore a natural variable of the jet/plume system (Hinze 1959, McFarlane 1988). Conventional plume models neglect 'ground-effects' (have zero 'footprint' area) and consider only the weak effect of vertical wind-shear upon horizontal momentum flux. The present model, in dealing consistently with 'jet', buoyant plume, and 'slumped' plume, necessarily incorporates a ground-drag force, acting over the plume 'footprint', the effect of which is (substantially) to decelerate an 'airborne' plume at first ground 'impact'. Note that the drag force is expressed over the 'footprint' area F(s), and in terms of the *difference* between the ground-level stresses $\Sigma_{xz}$ and $\Sigma_{xz}^{\infty}$ in the presence or absence of released material. Clearly drag forces exist even in the undisturbed atmosphere: these, however, are balanced in steady atmosphere flow by (weak) horizontal gradients in the ambient pressure field, and are therefore absent from the difference formulation adopted here.

The vertical momentum equation (**Vertical momentum-flux**) expresses the variation in the flux of vertical momentum in terms of forces arising from either buoyancy or pressures developed at the ground surface at 'touchdown' and beyond. Conventional descriptions model either buoyancy forces alone, or else buoyancy together with 'airborne' plume drag, that is the pressure force that arises over the cross-section A(s) as the result of small local differences between undisturbed ambient and plume pressure (Frick 1984).
'Airborne' drag is a controversial element (Briggs 1984), being found necessary by some (Ooms 1972, Petersen 1978, Schatzmann 1979) but not by others (Petersen 1987; Forney and Droescher 1985; Hoot, Meroney and Peterka 1973). The present model necessarily includes pressure forces developed over the plume 'footprint' in response to velocity changes implied by air entrainment, buoyancy, ground-drag, and the geometrical constraint of an impermeable (level) ground. Pressure forces at the ground develop in response to the interaction of 'top' entrainment and 'gravity slumping', and hence are plausibly expressed in terms of the spreading velocity and buoyancy force in a manner consistent with the gravity current spreading (van Ulden 1984, Raj and Morris 1987).

Finally consider the energy equation (**Total energy flux**), which expresses the near constancy of the excess flux above ambient values of the plume total energy (essentially enthalpy). This flux is altered by small vertical gradients in atmospheric enthalpy and wind-speed, and by the potential energy changes associated with vertical motion under terrestrial gravity The 'airborne' plume is assumed to exert negligible influence on the heat transfer from ground to atmosphere. In addition for a touchdown plume whose temperature differs substantially from that of the ground the heat flux at the ground surface may become important. The heat-flux from the ground is mediated via a heat transfer coefficient the magnitude of which is related to the vertical turbulent transport of heat from ground surface into the overlying plume. For the unperturbed atmosphere such fluxes are also present but are balanced by vertical temperature gradients and by (typically small) systematic variation in temperature downwind. This unperturbed heat flux is therefore absent from the difference model here developed, except inasmuch as it determines the Monin-Obukhov length, wind-speed and temperature profiles within the undisturbed atmosphere (Plate 1982, Colenbrander 1985). No provision has been made for this enhanced ground/plume heat transfer in the current model formulation. Such provision is however encoded within the heavy-gas advection module HEGADAS.
Inasmuch as the HGSYSTEM plume models are intended as a 'front-end' to a heavy-gas advection model such as HEGADAS, the neglect of heat transfer from the ground at touchdown and beyond was judged insignificant.

### 5.B.11. External flashing; Flow Establishment; Gaussian profiles

This section 'bridges' the external flash (depressurisation) and flow-establishment zones prior to the development within a released plume/jet of (approximately) self-similar conditions. The discussion of flow establishment relates particularly to the prediction of *point-local* from *sectionally averaged* concentrations within the early jet, and to the prediction of the zone length. This analysis is *not* incorporated within the (integral averaged) HGSYSTEM plume models. Such detailed formulation (as it affects air entrainment) requires careful experimental validation and exerts a modest influence upon predictions in the range of greatest interest, perhaps 10 to 500 m downwind of release; it has, however, clear implications for a purely Gaussian plume model.

**External Flashing**

Having set up the basic equations of motion in integral form, we specialise in order to 'bridge' the external flashing zone, or for a gas-jet the depressurisation zone, that occurs immediately beyond the breakpoint in choked flow. In the absence of choked flow this transitional region may still be present. For example, for a purely liquid release, pressure at the orifice may be an appreciable fraction of the storage (reservoir) pressure; this pressure, however, rapidly relaxes within the vena contracta to an essentially ambient value. During flashing radial and axial velocities within the developing jet are of co-magnitude so that the 'thin jet' approximation is invalid. In addition interphase slip and thermal disequilibrium are likely to occur.

Nonetheless depressurisation occurs so quickly, within a few (perhaps 5) diameters of the release plane, that 'thin jet', equilibrated conditions may be presumed to exist everywhere except within a narrow transition zone adjacent to the release point. We shall assume further, in view of the strongly expanding flow of a flashing jet, or the very large density differences between jet and ambient of a liquid jet, that negligible air entrainment occurs within this depressurisation zone. The length of the zone will in the context of evaporating liquid jets or plumes ordinarily be negligible and will hereafter be ignored: the models have initial conditions defined 'immediately post flash' at (axial) displacement zero.

Neglecting further the influence of gravity and of wind-shear upon the integral conservation laws, we deduce, for the conditions 'immediately post flash', the elementary forms (Figure 5.1)

$$u = u_0 + \frac{A_0 (p_0 - p_\infty)}{dm / dt_0}$$

$$c = \rho$$

$$\phi = \phi_0 \qquad (39)$$

$$A\ c\ u = dm / dt_0$$

$$\left[h + \tfrac{1}{2}u^2 - h^0_\infty - \tfrac{1}{2}u^2_{\infty,0}\right] = \left[h_0 + \tfrac{1}{2}u^2_0 - h^0_\infty - \tfrac{1}{2}u^2_{\infty,0}\right]$$

The notation is that $\phi$ is the angle of inclination to the horizontal, and that $A_0$ is the (true) area of the release orifice. The values of velocity u, density $\rho$, and area A are averaged values, that is they assume an essentially uniform velocity or density within the jet as it emerges from the depressurisation zone.

This is approximately valid for a liquid jet, (Albertson, Dai, Jensen, and Hunter Rouse 1948) and is at any rate plausible for a gaseous or two-phase jet. Certainly drag forces at the jet edge and the momentum redistribution associated with the entrainment of air are for consistency necessarily small.

**Flow Establishment**

Beyond the zone of depressurisation there exists a second transitional zone, a zone of 'flow establishment', in which the interaction of jet and ambient result in the progressive turbulent diffusion of air towards, and of jet momentum away from, the jet centre-line. This zone is characterised by a progressive change from a 'top-hat' velocity profile to an essentially Gaussian profile (Hinze 1959, Abramovich 1963) in the asymptotic far-field. Within this zone, neither 'top-hat' nor Gaussian profiles properly describe the cross-sectional variation in jet velocity and pollutant concentration (Figure 5.2).

What is needed is a transitional profile (Albertson, Dai, Jensen, and Hunter Rouse 1948) in which an inner 'core' jet (of uniform velocity and pollutant concentration of 100 %) is 'eroded' by a spreading Gaussian profile coupling inner 'core' and outer ambient flows. An order of magnitude analysis yield that this zone is of typical length $\ell/D = 1/e_{jet}$, in which D is a representative diameter 'immediately post flash', and in which $e_{jet}$ is a (dimensionless) coefficient whose magnitude measures the effectiveness of jet/ambient shear in causing air entrainment.

For gas jets this magnitude is most probably comparable to that seen following the establishment of self-similar flow (Ricou and Spalding 1961), which for a 'top-hat' model yields a value $e_{jet} = 0.08$. This is certainly reduced for a two-phase system (McFarlane 1988), and may be much smaller for a liquid jet for which dynamical break-up, rather than flashing 'atomisation', may dictate the entrainment rate (Wheatley 1987a, Ohnesorge 1936, van de Sande and Smith 1976, McCarthy and Molloy 1973).

We shall assume that all modelled releases result in prompt atomisation rather than gradual break-up, as is consistent with the earlier assumptions of negligible interphase slip and thermodynamic equilibrium. This results in a zone of flow establishment whose length is perhaps 20 orifice diameters. This zone is therefore also of a negligible length compared with downwind displacements of orders ten or hundred metres.
More complex models are possible and have been suggested (Jones 1988, Ianello and Rothe 1988): they require further and uncertain details regarding jet and droplet break-up and evaporation.

This zone ends with the diffusion of air to the jet centre-line, the elimination o the undisturbed 'core' zone, and the establishment of simple Gaussian profiles for jet velocity and pollutant concentration. Given estimates of the fluxes of mass, momentum, and energy, we may locate the zone boundary at least to moderate precision simply by requiring that these principal fluxes be invariable whatever self-similar 'profiles' are assumed to describe the cross-sectional variation in velocity and pollutant concentration.

The zone boundary is then located at that displacement s > 0 for which the centre-line concentration first differs from 100 % pollutant. Let therefore the profiles of jet velocity and pollutant mass concentration be described by the Gaussian forms:

$$
\begin{aligned}
c / c_* &= \phi_c(r / D_*; \gamma^2) \\
\frac{u - u_\infty}{u_* - u_\infty} &= \phi_u(r / D_*) \\
\phi_u(r / D_*) &= \exp\left(-\frac{4r^2}{D_*^2}\right) \\
\phi_c(r / D_*; \gamma^2) &= \exp\left(-\frac{4r^2}{\gamma^2 D_*^2}\right)
\end{aligned}
\qquad (40)
$$

where r is the off-axis displacement, $\gamma^2$ the turbulent Schmidt number (Hinze 1959), $u_*(s)$ the centre-line velocity and $c_*(s)$ the centre-line concentration. $D_*(t)$ is an effective jet 'diameter'.
Invariance of the principal fluxes results in a set of (non-linear) integral equations for the parameters $u_*$,$c_*$ and $D_*$, namely (Figure 5.2),

$$\iint_{A(s)} cu \, dA = dm / dt_0$$

$$\iint_{A(s)} (\rho u - \rho_\infty u_\infty)\, dA = dm/dt$$

$$\iint_{A(s)} \rho u (u - u_\infty)\, dA = dP_x/dt - u_\infty dm/dt$$

where $dm/dt_0$ is the pollutant mass flux coming from the orifice and dm/dt is the total plume mass flux at any location (pollutant plus entrained air).

The above non-linear system has a solution space which properly contains the set of physically admissible 'self-similar' profiles. Additionally *a-physical* solutions exist for which $c_* > \rho_*$, that is for which the pollutant mass-concentration exceeds the total mixture density; for which $u_* > u_{post\ flash}$, that is for which the centre-line velocity is greater than the velocity immediately post flash; and finally for which $c_* > c_{post\ flash}$, that is for which the centre-line concentration, consistent with an assumed Gaussian profile, actually exceeds that found at the jet-axis immediately following jet depressurisation.

The correct diagnosis from these symptoms is that the set of principal fluxes ($dm/dt_0$, dm/dt, $dP_x/dt$) and the atmosphere properties ($\rho_\infty$, $u_\infty$) correspond not to Gaussian self-similarity, but rather to a cross-section located within the zone of flow development. The zone boundary is therefore defined by the simultaneous solution of the above integral equations, together with the 'boundary equation', $c_* = c_{post\ flash}$

**5.B.12. The Airborne Plume: geometry and shear entrainment**

We consider in this section the representation of the 'airborne' plume, that is the plume from a point 'immediately post flashing' to the point of first plume 'touchdown'. We have chosen to represent the plume development in terms of a simple, integral-averaged, or 'top-hat' model in which is tracked the plume 'centre-line'. The plume consists of a set of circular cross-sections, each of defined diameter, mean density, temperature, and mass concentration of pollutant. Within each cross-section the velocity is assumed uniform; outside conditions are those of the undisturbed atmosphere.

We seek to introduce a (global) co-ordinate system the level surfaces of which are everywhere orthogonal to the turbulent-mean flow. Such co-ordinates, however, cannot be found without detailed knowledge of the turbulent flow in the presence of a dense-gas plume. In the circumstances we must be content with an approximate co-ordinate description valid in the neighbourhood of the plume-axis. We begin by introducing a local ('canonical') co-ordinate

system (s,r,θ) defined in the neighbourhood of the plume centre-line (Figures 5.8, 5.9, Schatzmann 1978):

$$r = (x, y, z) = r_0 + (\int_0^s \cos\phi \, ds, 0, \int_0^s \sin\phi \, ds) + r(-\sin\phi \sin\theta, \cos\theta, \cos\phi \sin\theta) \qquad (41)$$

with $r_0 = (x_0, y_0, z_0)$; $(s, r, \theta)$: $0 \le s \le \infty$, $0 \le r \le \infty$, $-\frac{\pi}{2} \le \phi \le \frac{3\pi}{2}$, $0 \le \theta \le 2\pi$

The co-ordinate s marks the distance along the plume centre-line from release point to a general plume cross-section **A**(s). The co-ordinate pair (r,θ) defines a set of plane polar co-ordinates in the cross-section **A**(s). The angle ϕ(s) is the inclination of the plume centre-line at displacement s from the release point (Figure 5.3).

Such co-ordinates are not and cannot be globally defined. Neither do the level surfaces ds = 0 coincide precisely with the surface **A**(s) in the sense of the original control-volumes t(s) of section 5.B.3. In particular the level surface ds = 0 are not asymptotically vertical as are the original surfaces **A**(s). They do nonetheless approximate such cross-sections **A**(s) in the vicinity of the plume centre-line, that is in that region of the plume for which the differences between plume and ambient are most pronounced. This certainly suggests, though it cannot confirm that it is legitimate to cast the equations of plume motion in terms of a 'top-hat' model and its associated, 'canonical', co-ordinate system.

Differentiation of the integral equations of section 5.B.3. then yields, for the canonical co-ordinates (s,r,θ), the basic differential equations;

$$\begin{aligned}
&d/ds(dm/dt) = Entr_{Amb}^{A(s)};\\
&d/ds(dP_x/dt) = -\mathbf{Drag}_{Amb}^{A(s)}.\mathbf{e}_x - Shear_{Amb}^{A(s)}\\
&d/ds(dP_z/dt) = -\mathbf{Drag}_{Amb}^{A(s)}.\mathbf{e}_z - Buoy_{Amb}^{A(s)};\\
&d/ds(dE/dt) = -Ener_{Amb}^{A(s)}\\
&dx/ds = \cos\phi\\
&dz/ds = \sin\phi
\end{aligned} \qquad (42)$$

together with the algebraic constraints

$$A = (p/4)\, D^2$$

$$dm/dt = A\, \rho\, u$$

$$dm/dt_0 = A\, c\, u$$

$$dP_z/dt = dm/dt\, u \sin\phi \qquad (43)$$

$$dP_x/dt = dm/dt\, (u \cos\phi - u_¥)$$

$$dE/dt = dm/dt\, (h + ½u^2 - h_¥ - ½u_¥^2)$$

Notation: A cross-section area, D plume diameter (circle), x horizontal axis-displacement, z axis height above level ground, dm/dt released and entrained mass-flux, ($dP_x/dt$, $dP_z/dt$) excess (horizontal, vertical) momentum flux, dE/dt excess energy flux, $dm/dt_0$ pollutant mass-flux; u mean flow-speed, $\phi$ axis inclination, $\rho$ mean plume-density, c mean pollutant mass-concentration, $h(\rho,c,P_¥)$ specific enthalpy the suffix '¥' denotes ambient conditions at the *centroid* height $z > 0$.

The quantities **Drag,** Shear, Entr, Buoy, and Ener have the formal definitions,

$$\mathbf{Drag}_{Amb}^{A(s)} = (d/ds) \iint_{A(s)} (p - p_¥) d\mathbf{A} \qquad (44)$$

$$Shear_{Amb}^{A(s)} = \iint_{A(s)} \rho \sin\phi\, (du_¥/dz)\, ½\mathbf{J}½/r\, dA \qquad (45)$$

$$Entr_{Amb}^{A(s)} = \iint_{A_\infty} \rho\, \mathbf{u}.d\mathbf{A} \qquad (46)$$

$$Buoy_{Amb}^{A(s)} = \iint_{A(s)} (\rho - \rho_¥)\, g½\mathbf{J}½/r\, dA \qquad (47)$$

$$Ener_{Amb}^{A(s)} = \iint_{A(s)} \rho\, u \sin\phi\, (d/dz)\, (h_¥ + ½u_\infty^2 + gz)\, ½\mathbf{J}½/r\, dA \qquad (48)$$

Notation: s displacement along plume centre-line, z height above ground, f plume centre-line inclination, $\rho$ local (turbulent averaged) density, u flow-speed, p (absolute) pressure, h specific enthalpy, $½\mathbf{J}½ = r\text{-}r^2 \sin\theta\, df/ds$ Jacobian determinant, g acceleration due to gravity, $dA = rdrd\theta$ (scalar) area element.

They represent (respectively) the 'drag' force $\mathbf{Drag}^{A(s)}_{Amb}$ acting on the plume in cross-flow as the result of vortex formation in the plume wake (Ooms 1972, Schatzmann 1979), the shear force $Shear^{A(s)}_{Amb}$ associated with the vertical gradient of wind-speed, the total entrainment rate $Entr^{A(s)}_{Amb}$ per unit axis length, the section-averaged buoyancy force $Buoy^{A(s)}_{Amb}$, and the variation in plume total energy $Ener^{A(s)}_{Amb}$ resulting from vertical gradients of temperature (enthalpy) and wind-speed.

The pressure is that deduced for hydrostatic equilibrium, except insofar as departures result in the (airborne) drag force.

These integrals are in actual practice replaced by empirical formulae chosen for compatibility with existing plume models and literature available data. These formulae express, for example, the contribution to air entrainment within the plume of the difference in velocity between mean cross-sectional velocity and the ambient wind-speed. Model closure is therefore in terms solely of mean cross-sectional and local atmospheric ambient parameters.

The above 'algebraic constraints' can be viewed as definitions of, for example, the total mass-flux within the plume, or the area of a circle. It is algebraically convenient to regard these as algebraic equations forming part of a differential/algebraic system. Such a system is then solved by means of the differential/algebraic package SPRINT (Berzins, Dew, and Furzeland 1983; Berzins and Furzeland 1985). Such a formulation allows the somewhat different descriptions of 'touchdown' and 'slumped' plumes to be incorporated within the same formalism.

### 5.B.13. The Touchdown and Slumped Plume

Consider next the representation of the plume following first 'touchdown'. Touchdown occurs at that axial displacement $s > 0$ for which an assumed circular cross-section just touches the horizontal ground surface $z = 0$.

It is also the point beyond which the plume footprint width first assumes a non-zero value.

The cross-section of a plume following touchdown is modelled not by a *circle* but rather by a *circular segment*. This centroid location will, for a dense plume, continue to fall, so that after some time a *semicircular cross section* is certain to arise. At this point the plume has passed through a transitional region between circular 'airborne' and *semi-elliptic 'slumped' cross-sections*. Further development will, at least initially, be characterised by (transverse) gravity spreading (van Ulden 1974, Raj and Morris 1987), and by air entrainment principally through the 'upper' plume surface.

These elements may be assembled within the framework of a 'top-hat' model as the differential system:

$$d/ds(dm/dt) = Entr_{Amb}^{A(s)}$$

$$d/ds(dP_x/dt) = -\mathbf{Drag}_{Amb}^{A(s)}.\mathbf{e}_x - Shear_{Amb}^{A(s)}$$

$$d/ds(dP_z/dt) = -\mathbf{Drag}_{Amb}^{A(s)}.\mathbf{e}_z - Buoy_{Amb}^{A(s)} + Foot_{Amb}^{F(s)} \qquad (49)$$

$$d/ds(dE/dt) = Ener_{Amb}^{A(s)}$$

$$dx/ds = \cos\phi$$

$$dz/ds = \sin\phi$$

together with the algebraic constraints

**'Touchdown' Plume**

$$A = \frac{D^2}{4}\left[\cos^{-1}(-\eta_c) + \sqrt{1-\eta_c^2}\right]$$

$$dm/dt = A\ \rho\ u$$

$$dm/dt_0 = A\ c\ u$$

$$dP_z/dt = dm/dt\ u \sin\phi$$

$$dP_x/dt = dm/dt\ (u\cos\phi - u_¥) \qquad (50)$$

$$dE/dt = dm/dt\ (h + ½u^2 - h_¥ - ½u_¥^2)$$

$$\eta_c = \eta - \frac{2}{3}\left\{\frac{(1-\eta_c)^{3/2}}{\cos^{-1}(-\eta_c) + \eta_c\sqrt{1-\eta_c^2}}\right\}$$

$$\eta = \frac{2z}{D\,|\cos\phi|}$$

$$\eta_c = \frac{2z_c}{D\,|\cos\phi|}$$

Notation: A cross-section area (circular segment), D circle diameter, x centroid horizontal displacement, z centroid height, $z_C$ centre height; dm/dt total (released plus entrained) mass-flux, ($dP_x/dt$, $dP_z/dt$) excess (horizontal, vertical) momentum flux, dE/dt excess energy flux, $dm/dt_0$ pollutant mass-flux, u mean flow-speed, $\phi$ axis inclination, $\rho$ mean plume density, c mean pollutant mass-concentration, h specific enthalpy; the suffix '¥' denotes ambient conditions at the centroid height. (See Figure 5.4).

Note that the *centroid* is the centre-of-mass of the plume and the *centre* is the centre of the circle of which the plume is a cut-off segment. The maximum width of the plume is D, at ground level it is $D\sqrt{1-\eta_c^2}$. The plume height is given by $D/2\,(1+\eta_c)\cos\phi$.
In the plume calculations $\eta$ will be known and $\eta_c$ has to be calculated using the non-linear equation for $\eta_c$ as given above. This equation can be solved using a simple iterative method.

**'Slumped' Plume**

$$A = (e\ p/8)\ D^2 \quad \text{with } e = (3p/2)\ (z/D)^{½}\cos\phi^{½}$$

$$dm/dt = A\ \rho\ u$$

$$dm/dt_0 = A\ c\ u$$

$$dP_z/dt = dm/dt\ u\ \sin\phi \qquad (51)$$

$$dP_x/dt = dm/dt\ (u\ \cos\phi - u_¥)$$

$$dE/dt = dm/dt\ (h + ½u^2 - h_¥ - ½u_¥^2)$$

Notation: A cross-section area (semi-ellipse), D ellipse major-axis length, e ellipse eccentricity (ratio minor to major ellipse axis), x centroid horizontal displacement, z centroid height; dm/dt total (released plus entrained) mass-flux, ($dP_x/dt$, $dP_z/dt$) excess (horizontal, vertical) momentum flux, dE/dt excess energy flux, $dm/dt_0$ pollutant mass-flux; u mean flow-speed, $\phi$ axis inclination, $\rho$ mean plume density, c mean pollutant mass-concentration, h specific enthalpy; the suffix '¥' denotes ambient conditions at the centroid height. (See Figure 5.5).

For the slumped plume the width is equal to D and the height is given by $\frac{3\pi}{4}z$.

Note that the differential system is modified in that, in addition to any 'airborne' drag forces, we have (generally significant) 'ground' drag associated with the strong shear layer at the ground-surface following plume touchdown. A further (pressure) force $Foot_{Amb}^{F(s)}$ is exerted at the ground surface as the result either of the destruction of vertical momentum impacting the ground, or in response to a pressure build-up associated with the limited (gravity-slumping) rate of transverse plume expansion. These additional forces exist following touchdown and in the slumped plume regime. They have the formal definitions:

$$Foot_{Amb}^{F(s)} = (d/ds) \iint_{F(s)} (p - p_{¥}) dA \tag{52}$$

$$Drag_{Amb}^{F(s)} = (d/ds) \iint_{F(s)} (å_{xz} - å_{xz}^{\infty}) dA \tag{53}$$

and are replaced in the actual plume models by intuitively derived functions which reflect known spreading and impact behaviour.

For the circular cut-off segment the cross-sectional area A and centroid height z are not explicitly related but coupled via a single non-linear equation for the geometric centre $z_C$. In the case of the slumped plume both the area A and centroid height z are related to the eccentricity e of the semi-ellipse; however the eccentricity is given explicitly in terms of known parameters z, $\phi$, and D.

### 5.B.14. Closure Assumptions for the 'Top-Hat' Model

In this section are considered the assumptions, arguments, and simplifications that enable closure of the 'top-hat' model: We shall ask: 'Which expressions and what coefficient values are appropriate for the formulation of impact forces, drag forces, and buoyancy in each of the three plume regions; airborne, touchdown, and slumped plume?'.

**Atmosphere-Gradient Induced Forces: Plume Buoyancy:**

We begin by considering the simplest of these functions, $Shear_{Amb}^{A(s)}$, $Ener_{Amb}^{A(s)}$, and $Buoy_{Amb}^{A(s)}$, and take first of all the buoyancy force $Buoy_{Amb}^{A(s)}$. This has the formal definition,

$$Buoy_{Amb}^{A(s)} = \iint_{A(s)} (\rho - \rho_{¥}) \, g \, ½\mathbf{J}½/r \, dA \tag{54}$$

in which the Jacobian determinant has the value

$$½\mathbf{J}½ = r - r^2 \sin\theta \, d\phi/ds, \; ½\mathbf{J}½ > 0 \tag{55}$$

The buoyancy term is well approximated by the simple expression,

$$\text{Buoy}_{\text{Amb}}^{\text{A(s)}} = A\,(\rho - \rho_{¥})\,g \tag{56}$$

a result which extends for expansion about the plume *centroid* (centre-of-mass) for both touchdown and slumped plume.

Analyses and order of magnitude arguments yield analogous results for the functions $\text{Shear}_{\text{Amb}}^{\text{A(s)}}$, and $\text{Ener}_{\text{Amb}}^{\text{A(s)}}$. It follows that

$$\text{Shear}_{\text{Amb}}^{\text{A(s)}} = dm/dt\,\sin\phi\,du_{¥}/dz \tag{57}$$

$$\text{Ener}_{\text{Amb}}^{\text{A(s)}} = dm/dt\,\sin\phi\,(d/dz)[h_{¥} + ½u_{¥}^{2} + gz] \tag{58}$$

**Airborne Drag**

Consider next the 'drag' function associated with an airborne plume in cross-flow. This function represents the force acting upon the plume as the result of pressure forces created by trailing (wake) vortices. The term 'drag' is by analogy to the drag force exerted upon a *rigid* body immersed in a uniform stream.

There are, however, major differences between the pressure field of a fluid jet and of a (geometrically similar) rigid body. Firstly there is no sharply defined boundary at which the 'no slip' condition may be applied. Secondly the external flow, and hence the boundary integral of pressure, may differ substantially between plume and body.

The analogy is therefore weak, so that not only the coefficient magnitudes but also the functional form appropriate to a rigid body may be questioned when applied to a plume in cross-flow. The form and magnitude of this airborne drag force is therefore particularly uncertain. It is found necessary by some (Ooms 1972, Petersen 1978, Schatzmann 1978), but not by others (Hoot, Meroney and Peterka 1973; Hoult, Fay and Forney 1969; Petersen 1987). A recent study (Coelho and Hunt 1989) of the near-field following release orthogonal to a steady flow found no evidence either experimental or theoretical for a significant 'drag' force. Plume deflection was satisfactorily explained by air entrainment alone.

We assume that

$$\textbf{Drag}_{\text{Amb}}^{\text{A(s)}} = 0 \tag{59}$$

**Plume impact Forces**

Consider next the pressure forces exerted over the plume 'footprint' for a touchdown or slumped plume. These forces arise from two distinct physical mechanisms: the destruction of momentum associated with the impact of a dense plume upon the ground surface; and the pressurisation associated with the gravity-limited rate of lateral plume spreading.

Take first the case of a plume impacting the ground surface (Figure 5.10). The assumption of an elastic collision applied to the plume as a whole requires that the impact pressure force be at right angles to the momentary orientation of the centroid axis. This ensures conservation of kinetic energy for a system without entrainment or other disturbing influences such as gravity. Focus next upon that proportion of the descending plume impinging upon level ground in time $dt > 0$.
If the footprint is of width $\ell$ then the impinging momentum flux is correspondingly,

$$d\mathbf{P} = dA\ \rho\ u(\cos\phi, 0, \sin\phi);\ dA = \ell\ u\tfrac{1}{2}\tan\phi\tfrac{1}{2}dt \qquad (60)$$

in which dA is the sectional area 'absorbed' into the ground surface.
We assume further that the magnitude of the impact force is such as to destroy completely the momentum-flux impinging at any instant upon the ground. The impact pressure force is therefore,

$$\mathbf{Impact}^{F(s)}_{Amb} = \ell\ \rho\ u^2\tfrac{1}{2}\tan\phi\tfrac{1}{2}(\sin\phi, 0, -\cos\phi);\ \sin\phi \geq 0 \qquad (61)$$

This formula differs somewhat from that expected from the control-volume analysis, in that both horizontal and vertical moments undergo continuous change. The pressure force integral implies a change solely in the vertical momentum. Additionally consideration of the destruction of horizontal momentum yields that flows in the negative x-direction are induced for impact angles in excess of 45°.
Certainly, for vertical incidence, the spreading pattern is axi-symmetric about the point of impact except inasmuch as this is modified by the ambient wind. For steeply descending plumes, therefore, upwind spreading, vortex formation, and flow separation make a simple transition described in terms of a continuous mean-flow at least difficult. However, for shallow incidence, such upwind spreading is typically absent, so that a 'top-hat' transition remains entirely feasible.
The form of the impact force $\mathbf{Impact}^{F(s)}_{Amb}$ implies a transition between 'steeply descending' and 'shallow incidence' plumes at an angle of descent $\phi = 45°$. This is precisely the value observed experimentally by Karman (1986). We restrict attention, therefore, to plume touchdown at angles $\phi$ less than 45°. Steeply descending plumes will require either empirical matching of

airborne and slumped plumes (Karman 1986), or else matching to a 'spreading pool' model, possibly analogous to the HGSYSTEM area source slumping model HEXABOX.

In addition, in the absence of air entrainment or drag forces, such as would describe shallow incidence impact of a liquid jet, the above impact force implies that the mean jet/plume speed remains constant throughout the impact process. This is consistent with a direct application of Bernoulli's theorem, gravity and ground drag being negligible, and is consistent with the impact of a liquid jet on a curved vane (Fox 1974). For this case the horizontal impact force evidently arises from pressure components developed along the curved surface of the deflecting vane. For the actual case of ground impact we may 'square the above circle' by regarding the jet/plume as existing above a recirculating flow the common interface of which is the analogue of the physical vane. In the immediate vicinity of first ground impact, therefore, the top-hat model represents not the complete flow but only the non-recirculating portion. Plume impact may then be modelled as a simple (elastic) collision.

**Gravity-Slumping Pressure Forces**

Consider next the pressure force induced over the plume 'footprint' by the interaction of ('top') entrainment and gravity-'slumping'. This pressure arises from the fact that entrainment may increase the cross-sectional mass-flux at a rate incompatible with a prescribed gravity-spreading unless the centre of mass is also raised. Such a raising of the centre of mass against gravity can be accomplished only by means of a pressure force acting over the plume footprint. The absolute magnitude of this pressure is small; its integrated effect significant. Let us begin (refer Figure 5.11) with the gravity-spreading relation (van Ulden 1983, Raj and Morris 1987) for a rectangular, 'slumped' jet

$$\tfrac{1}{2}dD/ds = (k/u)\sqrt{g\,h(1 - \rho_{\infty}/\rho)} \qquad (62)$$

Notation: h plume height, D plume width, g acceleration due to gravity, ($\rho$,u) mean density and flow-speed, $\rho_{¥}$ ambient density, k (0.85-1.20) empirical coefficient, s centre-line displacement.

We seek a formulation for the vertical momentum equation such that this gravity-slumping behaviour is asymptotically recovered for dense, advected plumes. For such a plume the spatial rate of change of vertical momentum is undoubtedly small, that is the sum of vertical forces is approximately zero. We interpret Raj's formula for gravity spreading as a statement of the approximate balance of a buoyancy force, and the reactive pressure force driven by the interaction of slumping and entrainment. Given, therefore, that the buoyancy force has the form,

$$Buoy^{A(s)}_{Amb} = h\ D\ g\ (\rho - \rho_{¥}) \tag{63}$$

we propose a reactive pressure force,

$$Foot^{F(s)}_{Amb} = (1/k^2)\ D\ \rho\ u^2\ [½dD/ds]^2 \tag{64}$$

proportional to the local footprint width, and to the square of the lateral spreading velocity.
In the case of a semi-elliptic cross-section we must reinterpret the lateral spreading velocity, and effective plume height h in terms of the plume width D and centroid height z.
The height h is for a rectangular section exactly twice the centroid height which allows the identification h = 2z. Additionally the rectangular section has area hD equal to that of a semi-ellipse $(3p^2/16)zD$ of centroid z and footprint width D.

This results in the final expression, modified for the semi-elliptic geometry

$$Foot^{F(s)}_{Amb} = (3p^2/32)^3\ (1/k^2)\ \ell\ \rho\ u^2\ [½dD/ds]^2,\ k = 1.15 \tag{65}$$

We follow van Ulden (1983), rather than Raj and Morris (1988) in the choice of the gravity-spreading coefficient. Further work is, however, necessary in order optimally to determine the coefficient value for a semi-elliptic, slumped plume.

This revised formulation will evidently reproduce the gravity spreading behaviour 'hard-wired' by Raj and Morris (1988). It is, moreover, physically meaningful for an asymptotically neutral or buoyant plume/jet for which significant departures from gravity-spreading must be expected. In particular the original spreading formula is not defined for a buoyant plume. Initially dense, subsequently buoyant, plumes occur frequently for the release of pressurised liquid HF or other liquid gases, to ambient atmospheres of moderate humidity (> 50 %) and temperature (perhaps 20 °C).

**Gravity Current Collapse**

Gravity spreading as formulated by van Ulden (1983) and Puttock (1988) assumes the existence of a (relatively) sharp interface between plume and undisturbed air. Recent experiments by Linden and Simpson (1988) indicate that the leading vortex of such a gravity current is not unconditionally stable but may be disrupted by locally enhanced turbulence. Following gravity current collapse the cloud edge is more diffuse; lateral spreading much reduced.

Study of the HTAG ('Heavier than Air Gas') data set (Petersen and Ratcliff 1989), reveals evidence for the existence of such gravity current collapse for uniform ambient turbulence and increasingly weak gravity-head. We propose a collapse criterion and post-collapse spreading rate (essentially) as follows:

$$½dD/ds = (2\ \rho_{¥}\ u_{*}\ h)/(3\ k\ C_D\ u\ D)\ Ri_{*}\ F(Ri_{*}) \tag{66}$$

$$\sqrt{\rho_{\infty}/\rho}\ \frac{D}{h} > \frac{16}{3\kappa}\sqrt{Ri_{*}}\ \Phi(Ri_{*}) \tag{67}$$

$$\Phi(Ri_{*}) = \begin{cases} \dfrac{1}{\sqrt{1-3Ri_{*}/5}} & Ri_{*} < 0 \\ 1 & 0 \le Ri_{*} < \dfrac{189}{80} \\ \max\left(\dfrac{Ri_{*}}{7}, \dfrac{10}{17}\sqrt{1+4Ri_{*}/5}\right) & Ri_{*} \ge \dfrac{189}{80} \end{cases} \tag{68}$$

with $Ri_{*} = g\ h\ (\rho - \rho_{\infty})$ and $h = 2z$.

Notation: h plume height, D plume width, g acceleration due to gravity, (ρ,u) mean density and flow-speed, $\rho_{¥}$ ambient density, κ is the Von Kármán constant, $C_D$ (with value 5.0) empirical (spreading) coefficient, s centre-line displacement, $u_{*}$ friction velocity, $Ri_{*}$ (bulk) Richardson number ; $F(Ri_{*})$ heavy gas entrainment function.

Spreading, 'post collapse', is represented in the HGSYSTEM plume models by the limit of the vertical momentum equation for which the corresponding 'footprint' force is simply

$$Foot^{F(s)}_{Amb} = (3p^2/64)^3\ (3\ k\ C_D/F(Ri_{*}))\ \ell\ \rho\ u\ u_{*}\ (D/z)\ dD/ds \tag{69}$$

$$\sqrt{\frac{\rho_{\infty}}{\rho}}\ \frac{D}{z} > \frac{1024}{9\pi^2}\sqrt{Ri_{*}}\ \Phi(Ri_{*})/\kappa \tag{70}$$

with $C_D = 5.0$ and $Ri_{*} = 2\ g\ z\ (\rho/\rho_{¥} - 1)/u_{*}^2$

The possibility exists that a gravity current may reform following initial turbulent collapse. Intuition suggests that such reformation may occur, but that the collapsed state is 'metastable', that is vortex (re-) formation may be considerably delayed. In the absence of detailed experimental evidence, we may presume gravity current collapse irreversible.

**Ground-surface Drag**

Finally we consider the drag force exerted at the ground surface by an impacting or slumped plume. This force has the formal definition

$$\text{Drag}_{\text{Amb}}^{\text{F(s)}} = (d/ds)\iint_{\text{F(s)}} (\text{å}_{xz} - \text{å}_{xz}^{\infty})\, dA \qquad (71)$$

and results from differences in the mean horizontal and undisturbed wind speeds in the neighbourhood of the ground surface. The surface stress associated with the wind profile is $\rho_{¥} u_{*}^{2}$, in which $u_{*}$ is the friction velocity.

Equivalently $\text{å}_{xz}^{\infty}$ is proportional to the square of the velocity gradient $du_{¥}/dz$ at the roughness height $z_r > 0$.

Profile information regarding the vertical variation in flow-speed within the impacting or slumped plume is therefore necessary in order to estimate the drag force. For an assumed neutrally buoyant plume and a logarithmic velocity profile the friction velocity associated with a plume of velocity at centroid height z is $u/u_{¥}$ times that of the unperturbed wind. This suggests (for a neutral plume) the drag function

$$\text{Drag}_{\text{Amb}}^{\text{F(s)}} = \ell\, \rho_{¥}\, u_{*}^{2}\, [(u/u_{¥})\cos\phi - 1][(u/u_{¥})\cos\phi + 1], \text{ with } u_{¥} > 0 \qquad (72)$$

in which $\ell$ is the footprint width.

For high speed flows we expect the (established) shear profile within a dense gas plume to be governed by surface roughness analogously to that in a neutral boundary layer. The surface stress is simply $\rho u_{*}^{2}$, in which $u_{*}$ is set by the known (mean) jet velocity at the centroid height. Substitution then yields the drag function in the presence of dense gas effects

$$\text{Drag}_{\text{Amb}}^{\text{F(s)}} = \ell\, \rho_{¥}\, u_{*}^{2}[\sqrt{\rho/\rho_{\infty}}\ (u/u_{\infty})\cos\phi - 1][\sqrt{\rho/\rho_{\infty}}\ (u/u_{¥})\cos\phi + 1] \qquad (73)$$

Density stratification damps turbulence and affects both friction velocity and plume drag. The drag force might be presumed proportional to some power of the Richardson number correction $F(Ri_{*})$ proposed by Witlox (1988) in the context of heavy-gas entrainment. Now the suppression of entrainment at a dense gas interface is largely due to gravity-driven 'recapture' of disturbed dense gas rather than to a lowering of turbulent energies within the system as a whole. This suggests that the influence of density stratification upon ground drag is rather small. We presume the effect negligible.

### 5.B.15. The Entrainment Function

We consider in this section the form of the entrainment function appropriate to each of the plume regions; airborne, touchdown, and slumped plume. The entrainment function is taken (barring interactions) to be the sum of contributions arising from different physical mechanisms; jet entrainment, cross-wind entrainment, gravity-slumping entrainment, and airborne or heavy-gas passive entrainment. These mechanisms are present to varying degree in each of the plume regions.

**Jet Entrainment**

For the discharge of (neutrally buoyant) gas jets to quiescent of co-flowing ambient the form and magnitude of the entrainment function is well established (Briggs 1984; Morton, Taylor and Turner 1956). It assumes for the 'top-hat' formulation the symbolic form

$$Entr_{jet} = e_{jet}\, p\, D\, \rho_{¥}½u - u_{¥}½ \text{ with } e_{jet} = 0.08 \tag{74}$$

This form (or related variants) has been found satisfactory in addition for the early release of two-phase propane jets (McFarlane 1988, Cowley and Tam 1988), and for ammonia releases (Wheatley 1987a, 1987b).

For dense two-phase jets in cross-flow, we propose the correlation

$$Entr_{jet} = e_{jet}\, \eta(\rho/\rho_{¥})\, L^{free}_{surface}\, \rho_{¥}\, ½u - u_{¥}\cos\phi½ \tag{75}$$

with $\eta(\rho/\rho_{¥}) = [1 + (4/3)(\rho/\rho_{¥} - 1)]/[1 + (5/3)(\rho/\rho_{¥} - 1)]$

Jet entrainment is thus *proportional to the absolute difference between the jet speed and the aligned component of the ambient wind*.

Entrainment takes place over that part of the plume perimeter exposed to the ambient air. The form, excepting the small density correction, has been found satisfactory by several authors (Petersen 1978; Ooms 1972; Hoot, Meroney and Peterka 1973) in combination with various cross-wind formulations for the description of buoyant and dense gas plumes released orthogonal to an imposed wind.

It, other than the densimetric correction, is used by Raj and Morris (1987) for their gravity-slumping jet. It is closely analogous (asymptotically equivalent) to a 'shear' entrainment formulation based upon Prandtl closure of the turbulent kinetic equation proposed by McFarlane (1988). This formulation showed good agreement with large scale experimental data gathered by Cowley and Tam (1988).

**Cross-wind Entrainment:**

Crosswind entrainment is associated with the formation in the wake of a rising or falling plume of trailing vortices in response to the deflection by the release plume of ambient air. This mechanism is absent for release to a quiescent atmosphere, or for a wind aligned release, and is assumed to be maximum for releases at right angles to the ambient wind. This suggests immediately the functional form,

$$\mathrm{Entr}_{\mathrm{wind}}^{\mathrm{cross}} = e_{\mathrm{wind}}^{\mathrm{cross}}\, L_{\mathrm{surface}}^{\mathrm{free}}\, \rho_{¥}\, u_{¥}½\sin\phi½ \tag{76}$$

(Morton, Taylor and Turner 1956; Hoot, Meroney and Peterka 1973; Hoult, Fay and Forney 1969).

By contrast Ooms (1972), and later Petersen (1978,1987) have found good agreement for Gaussian models with the modified form

$$\mathrm{Entr}_{\mathrm{wind}}^{\mathrm{cross}} = e_{\mathrm{wind}}^{\mathrm{cross}}\, L_{\mathrm{surface}}^{\mathrm{free}}\, \rho_{¥}\, u_{¥}½\cos\phi\, \sin\phi½ \tag{77}$$

when used in conjunction with non-zero airborne drag correlation

$$\mathbf{Drag}_{\mathrm{Amb}}^{\mathrm{A(s)}} = e_{\mathrm{Amb}}^{\mathrm{drag}}\, L_{\mathrm{wind}}^{\mathrm{cross}}\, \rho_{¥}\, u_{¥}^{2}\, \sin^{2}\phi\, (\sin\phi,0,-\cos\phi) \tag{78}$$

This formulation is reported by Li, Leijdens and Ooms (1986), and by Havens (1988) to be a successful predictor not only of buoyant and neutral plumes, but of dense emissions as well. Several other formulations have been tried (Schatzmann 1979, Spillane 1983, Frick 1984) and are reported as satisfactory in predicting plume rise and lateral spread (Schatzmann and Policastro 1984a, 1984b).

We have encoded various cross-wind entrainment terms within the (ideal-gas) plume model PLUME, and find, following Briggs (1984), that the cases of neutral and buoyant plume rise are adequately represented by the ½sinϕ½correlation and a coefficient value $e_{\mathrm{wind}}^{\mathrm{cross}}$ of 0.60.
By contrast, the dense plume data-base of Hoot, Meroney and Peterka is incompatible with *any* uniform choice for the crosswind entrainment coefficient.

Except in the immediate vicinity of the source, plume development is well represented by the Boussinesq approximation (Schatzmann and Policastro 1984b). It follows that rising dense plumes, and descending buoyant plumes should exhibit essentially the same behaviour in response to an imposed cross-wind. This suggests strongly that the same functional form be

chosen to represent both dense and buoyant plumes, and that in the limit of great dilution the simple½sinϕ½ dependence be recovered.

We find that cross-wind entrainment is weakened by high exit velocities and for rising dense plumes by density excess. Analysis of buoyant (Petersen 1978), and dense (Hoot, Meroney and Peterka 1973) gas-plume data suggests the functional form

$$Entr_{wind}^{cross} = Cu_{wind}^{cross}\ \eta(\rho/\rho_{¥},\phi)\ L_{surface}^{free}\ \rho_{¥}\ u_{¥}\ \sqrt{u_{\infty} / u}\ ½\sin\phi½ \qquad (79)$$

with $\eta(\rho/\rho_{¥},\phi)= [1 + C\rho_{wind}^{cross}\ \max(0,(\rho/\rho_{¥} - 1)\ \sin\phi)]^{-1}$ and the coefficients $Cu_{wind}^{cross} = 0.60$, $C\rho_{wind}^{cross} = 7.50$.

The coefficient $C\rho_{wind}^{cross}$ is matched to dense gas maximum rise-height, and the release velocity correction is suggested by an analysis of (early) buoyant plume rise. This expression, when used in conjunction with the above jet entrainment, is a satisfactory predictor of buoyant (Petersen 1978), and of dense plume-rise (both maximum rise-height and its downwind displacement).

Plume 'touchdown' is also satisfactory, though the validation is complicated by differences between the plume width of a 'top-hat' model, and the 'visible edge' data presented by Hoot, Meroney and Peterka (1973). The model adequately reproduces the downward releases of buoyant gas conducted by Li, Leijdens and Ooms (1986), and is of comparable accuracy to the truncated Gaussian model of Ooms and Duijm (1984), and to the similar model proposed by Havens (1988) after Morrow and co-workers (1982).

It should be emphasised that this entrainment term is *empirical*. It is a satisfactory predictor of both dense and buoyant plumes released orthogonal to a laminar cross-wind. Nonetheless it is rather likely that an improved correlation can be developed should plume centre-line touchdown data become available.

**Gravity Slumping Entrainment**

By 'gravity-slumping' entrainment we intend the absorption of ambient air within a 'slumped' plume as the result of lateral expansion in response to density differences between (dense) plume and ambient. This phenomenon was studied by van Ulden (1974) in the context of the initial development of a cylindrical (area) source of dense gas. Van Ulden (1974) proposed the entrainment relation,

$$Entr_{slump}^{grav} = ½e_{slump}^{grav}\ p\ D\ \rho_{¥}\ h\ (dD/dt), \text{ with } e_{slump}^{grav} = 0.05 \qquad (80)$$

Notation: h plume height, D plume diameter, dD/dt slumping rate.

Entrainment is proportional to the spreading velocity (½dD/dt), to the ambient density ($\rho_{¥}$) , and to the area (phD) of the plume 'edge'.
Almost all of the adjacent air is, for such cylindrical slumping, displaced by rather than entrained within the expanding cloud 'edge'. The analogue of van Ulden's entrainment relation for the (steady) state geometry of the slumped plume is

$$Entr^{grav}_{slump} = e^{grav}_{slump}\ \rho_{¥}\ z\ u½cos\phi½(dD/ds) \qquad (81)$$

in which we have assumed an equivalent cloud height which is twice that of the plume centroid.
We have also adopted this formula for the slumped plume.

Puttock (1988), in the model HEGABOX (available in HGSYSTEM version 3.0), proposed an entrainment coefficient $e^{grav}_{slump} = 0.85$, this in accordance with observations on cylindrical collapse conducted at Thorney Island (McQuaid 1984).
The coefficient value, $e^{grav}_{slump} = 0.85$, may reflect a contribution to entrainment associated with turbulence generated in the cylindrical collapse, turbulence which must decay as the plume is advected downwind. This suggests that the entrainment coefficient $e^{grav}_{slump}$ appropriate to a semi-elliptic plume may have a value considerably less than 0.85.

Alternatively some dependence of $e^{grav}_{slump}$ upon such flow parameters as the local (bulk) Richardson number or upon the local versus initial spreading-rate (Eidsvik 1978) might be investigated.

Conventionally (Ooms 1972, Petersen 1987, Schatzmann 1978, Briggs 1984) such lateral entrainment is absent from the airborne plume: indeed its inclusion results for the approximate equations of motion in an *exponential* growth in plume width. The touchdown plume is physically and geometrically intermediate between airborne and slumped plume. In this region forces are first developed whose interaction with buoyancy results in the subsequent (slumped plume) gravity current. Plausibly gravity current entrainment is weak in this intermediate zone. Certainly this is consistent with the observations of Puttock (1988) who found it necessary to 'switch off' gravity-current entrainment for an interval following initial (cylindrical source) release. This delay is required for the formation of a vortex system at the cloud leading 'edge'.
For the touchdown plume, therefore, we propose the interpolated form

$$e^{grav}_{slump} = [1 - 2z_c/D/½cos\phi½]\, e^{grav}_{slump}\, \rho_¥\, z\, u½cos\phi½(dD/ds) \quad (82)$$

in which $z_c$ and D denote centre and diameter of the circular segment cross-section. This formulation is of necessity preliminary, and may require modification of 'tuning' in the light of subsequent validation of analysis.

**Slumped Plume: Heavy Gas Entrainment**

The dilution of a 'severely slumped plume' is dominated by 'top' entrainment of ambient air in response to ambient turbulence when modified by density stratification. The circumstances of such 'severely slumped' plumes are precisely those for which the heavy-gas advection model HEGADAS was designed.

As the HGSYSTEM plume models are required to merge smoothly with the far-field HEGADAS model, it is appropriate to take the 'top' entrainment formulation used by the latter, modified to allow for the different cross-sectional geometry's.

We are led immediately to the entrainment relation,

$$Entr^{heavy}_{gas} = [\Phi(Ri_*)]^{-1}\, L^{free}_{surface}\, \kappa\, \rho_\infty\, u_* \quad (83)$$

$$\text{with } \Phi(Ri_*) = \begin{cases} \dfrac{1}{\sqrt{1-3Ri_*/5}} & Ri_* < 0 \\ 1 & 0 \le Ri_* < \dfrac{189}{80} \\ \max\left(\dfrac{Ri_*}{7}, \dfrac{10}{17}\sqrt{1+4Ri_*/5}\right) & Ri_* \ge \dfrac{189}{80} \end{cases} \quad (50a)$$

and $Ri_* = 2\, g\, z\, (\rho - \rho_\infty)$. Relation (50a) is of course equal to relation (35).

The Richardson number correction to the turbulent entrainment is a modification to the HEGADAS formulation suggested by Witlox (1988) following a critical analysis of McQuaid's wind-tunnel data.

**Airborne Plume: Passive Entrainment**

In addition to 'jet' and 'crosswind' mechanisms, entrainment within the airborne plume is influenced by the state of ambient turbulence. Asymptotically it is this mechanism which is predominant, and which results in the far field in the Pasquill/Gifford correlations for the Gaussian standard deviations (Plate 1982; Stern, Boubel, Turner and Fox 1984) $\sigma_y(x,z)$, and $\sigma_z(x,z)$, as functions of the distance x downwind of release and (Pasquill 1976) of the (effective) plume height z. Additionally the ambient turbulence in the surface layer (Plate

1982; Stern, Boubel, Turner and Fox 1984) is governed (at any rate approximately) by Monin-Obukhov similarity theory, so that the entrainment function should be expressible in terms of the surface roughness, Monin-Obukhov length, and the plume centroid height above the ground surface.

Three approaches seem possible in formulating the passive entrainment function for the airborne plume. First we may attempt direct 'matching' from a plume-rise model in which passive entrainment is neglected to a Gaussian Pasquill-Gifford model for the far-field. Conservation of the fluxes of entrained mass, pollutant mass, horizontal momentum excess, prescribe the location of a virtual point source needed by the Gaussian model. This approach has clear computational advantages; it removes the need for the 'step by step' downwind integration of a set of ordinary differential equations describing plume motion. It takes advantage of well established empirical correlations for the far-field.

Notwithstanding, we may attempt to introduce within the range of plume rise and fall an approximate passive entrainment function, the effect of which will be to correct somewhat the predictions made in the absence of turbulent diffusion. The range of application will be such that the passive entrainment term is at most of co-magnitude with contributions from 'jet' and from 'crosswind'. Reference to the literature reveals essentially two procedures for the determination of the passive entrainment function; procedures based upon 'matching' to the Pasquill/Gifford correlations (Bloom 1980), and methods based upon an analysis of Monin-Obukhov similarity (Ooms 1972). Of these methods the former class may be criticised in that they rely on function forms constructed from far-field data, yet they are used in the near field when effects of buoyancy and release momentum are yet significant. We prefer the latter class, and in particular propose a (previously unpublished) formulation developed by Disselhorst (1987).

$$\mathrm{Entr}_{amb}^{turb} = (1 - \ell/D)\, p\, e_{amb}^{turb}\ \rho_{¥}\, e^{1/3}\, [\ell_y^{4/3} + \ell_z^{4/3}] \tag{84}$$

$$\ell_y = \begin{cases} \min[D/2,\ 0.88(z + z_r)(1 - 7.4\,\kappa z)/(1 - 5\kappa z)], & P/G = \{'A','B','C'\} \\ \min[D/2,\ 0.88(z + z_r)], & P/G = \{'D'\} \\ \min[D/2,\ 0.88(z + z_r)/(1 + 0.1z)] & P/G = \{'E','F'\} \end{cases} \tag{85}$$

$$\ell_z = \begin{cases} \min[D/2,\ 0.88(z + z_r)(1 - 7.4\,\kappa z)/(1 - 5\kappa z)] & P/G = \{'A','B','C'\} \\ \min[D/2,\ 0.88(z + z_r)] & P/G = \{'D'\} \\ \min[D/2,\ 0.88(z + z_r)/(1 + 4z)] & P/G = \{'E','F'\} \end{cases} \tag{86}$$

$$\begin{aligned} e = {} & (1 - 5\,\kappa z)u_*^3/\kappa/(z + z_r) && \text{P/G} = \{\text{'A','B','C'}\} \\ & u_*^3/\kappa/(z + z_r) && \text{P/G} = \{\text{'D'}\} \\ & (1 + 4\kappa)u_*^3/\kappa/(z + z_r) && \text{P/G} = \{\text{'E','F'}\} \end{aligned} \qquad (87)$$

and $e^{turb}_{amb} = 1.0$, $z = (z + z_r)L$, $L = u_*^3/\kappa/(g/T_g)/(u_*T_*)$.

Notation: $z_r$ surface roughness, L Monin/Obukhov length, $u_*$ friction velocity, $\kappa$ Von Kármán constant, $T_g$ ground (absolute) temperature, $u_*T_*$ surface/air heat-flux, e dissipation rate of turbulent kinetic energy, ($\ell_y$, $\ell_z$) turbulent (transverse horizontal, vertical) eddy length-scales; $\ell$ plume 'base'-length, D plume 'diameter', z centroid height; P/G Pasquill/Gifford atmospheric stability class.

This formulation differs from that proposed by Disselhorst in three ways. First the cross-section of an airborne plume is circular and not elliptic: nonetheless the different horizontal and vertical length scales within the atmosphere are represented. Second the atmospheric boundary layer is presumed effectively infinite: this should prove unproblematical for near ground releases of dense gas. Third the entrainment term is in the touchdown region given a linear scaling in 1-$\ell$D in order to vanish identically at (and beyond) the point of first plume slumping.

**Interactions**

Heavy-gas and jet entrainment are *not* independent mechanisms; each modifies the level of turbulence by inducing vertical gradients of velocity. These velocity gradients are (in general) antagonistic; the presence of dense gas requires a positive, of a (strong) jet a negative, gradient at the cloud surface.

We take the combined effect of jet and heavy-gas entrainment as the greater of the two contributions when acting in isolation. Further, pursuing the analogy with HEGADAS, we regard the heavy-gas entrainment as taking place across the plume 'top', with jet entrainment acting over both 'top' and 'side'. This maximum entrainment is (for reasons of continuity) partitioned amongst heavy-gas and jet mechanisms in the same proportion as would have arisen from the addition of the contributions $Entr_{jet}$ and $Entr^{heavy}_{gas}$:

$$Entr^{jet}_{heavy\ gas} = (\ell/L^{free}_{surface})\ \max(Entr_{jet}, Entr^{heavy}_{gas}) + (1 - \ell/L^{free}_{surface})\ Entr_{jet} \qquad (88)$$

$$_{jet}Entr^{jet}_{heavy\ gas} = [Entr_{jet}/(Entr_{jet} + Entr^{heavy}_{gas})]\ Entr^{jet}_{heavy\ gas} \qquad (89)$$

$$^{heavy}_{gas}Entr^{jet}_{heavy\ gas} = [Entr^{heavy}_{gas}/(Entr_{jet} + Entr^{heavy}_{gas})]\ Entr^{jet}_{heavy\ gas} \qquad (90)$$

The concepts of 'top' and 'side' require elucidation: we take the 'top' to have a length equal to the length $\ell$ of intersection between cross-section and level ground; the 'side' we identify with the balance $L^{free}_{surface}$ - $\ell > 0$ of the 'free surface' or perimetric length.

The interaction between passive and gravity-slumping entrainment is treated similarly; interaction arises inasmuch as the contribution of passive entrainment induces lateral expansion which itself induces entrainment represented by gravity slumping. Such 'feedback' of entrainment is clearly a-physical, and results, for an 'airborne' plume, in the exponential increase of plume diameter and dilution. The assumptions are summarised below

$$Entr^{pass}_{grav\ slump} = \max(Entr_{pass}, Entr^{grav}_{slump}) \tag{91}$$

$$_{pass}Entr^{pass}_{grav\ slump} = [Entr_{pass}/(Entr_{pass} + Entr^{grav}_{slump})]\ Entr^{pass}_{grav\ slump} \tag{92}$$

$$_{slump}^{grav}Entr^{pass}_{grav\ slump} = [Entr^{grav}_{slump}/(Entr_{pass} + Entr^{grav}_{slump})]\ Entr^{pass}_{grav\ slump} \tag{93}$$

### 5.B.16. The atmosphere model.

In the HGSYSTEM version 3.0 plume models, the same profiles for ambient wind speed and temperature are used as in the HEGADAS model. See Appendix 7.A.A for a description of these profiles.

### 5.B.17. Plume cross-sectional over-lap: curvature limited entrainment

The co-ordinate system used in formulating the 'top-hat' model of plume development determines and is determined by the physical interaction of the released jet and the ambient wind.

The co-ordinate system is not universal but exists only within a limited distance from the plume axis. Circumstances may arise in which plume curvature, whether in response to strong cross-winds, or to ground impact, results in the predicted 'over-lap' of successive plume cross-sections. Such behaviour is certainly rare for gas (including heavy gas) releases, and is largely absent from the wind-tunnel data sets of Hoot, Meroney and Peterka (1973) (dense gases), and of Petersen (1978) (buoyant plumes). Nevertheless, in view of the higher density and lower velocity to be expected in the near-field following release of pressurised dense jets, it seemed expedient to include provision for such plume 'overlap' within the HGSYSTEM plume models.

This section outlines the method employed by the HGSYSTEM plume models in treating such behaviour: the method adopted is *not* universally effective, but is successful in the clear majority of cases.

We begin by analysing the conditions under which plume overlap occurs in each of the three regions; airborne, touchdown, and slumped plume. Incipient overlap is defined by a geometrical relation in which a representative plume 'width' is compared with the axis curvature dϕ/ds. The results are as follows:

**Airborne Plume**

$$D/2 \, |d\phi/ds| = 1 \tag{94}$$

**Touchdown Plume**

$$-z/|\cos\phi| \, d\phi/ds = 1, \text{ for } d\phi/ds < 0$$

$$[D/2 - (z - z_c)/|\cos\phi|] \, d\phi/ds = 1, \text{ for } d\phi/ds < 0 \tag{95}$$

**Slumped Plume**

$$-z/|\cos\phi| \, d\phi/ds = 1, \text{ for } d\phi/ds < 0$$

$$[\max(1,e) \, D/2 - z/|\cos\phi|] \, d\phi/ds = 1, \text{ for } d\phi/ds<0 \tag{96}$$

$$e = (3p/2) \, (z/D)/|\cos\phi|$$

Notation: D plume (effective) 'diameter', z centroid height, e eccentricity (ratio minor to major axis for semi-ellipse), $z_c$ centre height (circular segment), ϕ axis-inclination, s centre-line displacement, dϕ/ds centre-line curvature.

These conditions define the limits imposed by cross-section geometry upon the integration of the pollutant source and ambient atmosphere implied by the conservation laws, and by the (empirically determined) entrainment function. Should these limits be exceeded we are faced with two alternatives: alter the geometry of the cross-section, or modify the entrainment function itself.

Modification of the sectional geometry is the more complex option: we must *simultaneously* satisfy the original entrainment equation and a consistency relation requiring that plume 'overlap', while incipient, does not actually occur within the zone of high axis-curvature. Introduction of variable geometry (within the three plume regions already recognised) substantially increases the number and complexity of geometrical transitions that must be represented within a computer based model. Such high curvature regions are, in any case, quite rare, or have quite limited geometrical extent, so that the need for such an increase in complexity did not seem, a priori, justified.

As an alternative to the modification of plume geometry, we may alter the entrainment function in regions of high curvature so as to prevent the occurrence of plume overlap. Concretely we replace the entrainment relation, d/ds(dm/dt) = Entr, by whichever of the geometrical constraints for incipient plume overlap is appropriate for the present cross-sectional shape. This revised equation system is of necessity geometrically consistent, and may be matched by continuity arguments to the previously existing plume structure. In addition the entrainment rate implied by the geometrical constraint may be calculated as the derivative d/ds(dm/dt). This parameter is then compared with the entrainment rate that would have occurred for the same plume description in terms of sectional mean velocity, density, and the like, from the empirically determined entrainment function Entr.
The model reverts to this usual description, should the 'curvature limited' entrainment exceed that calculated from the empirical entrainment function. This procedure introduces a minimal change into the basic model consistent with the existence of 'curvature limited' behaviour. The procedure rests upon the idea that excessive plume curvature is the result of too rapid air entrainment, and that the reduction of air entrainment to the maximum value compatible with plume geometry will permit integration to continue through the high curvature zone and to recover the basic model at some greater downwind displacement.

The success of this device of 'curvature limited' entrainment rests on the ability of the curvature limited model to recover normal entrainment rates. However it may occur that the corollary entrainment rate d/ds(dm/dt) inferred from a curvature limited model actually decreases *more rapidly* than does the associated empirically determined entrainment rate (Entr) for the *same* plume description.
Should this occur termination of the curvature limited zone will occur following detection of the a-physical entrainment step d/ds(dm/dt) £ 0. The plume models will terminates with an error message.

### 5.B.18. The HGSYSTEM plume models: algorithmic structure.

In order to solve the set of ordinary differential equations and non-linear algebraic which result from our plume modelling, a numerical solver capable of treating systems of this complexity is required.

SPRINT (Software for PRoblems IN Time) is such a solver: it was developed by Shell Research and by Leeds university (Berzins, Dew, and Furzeland 1983; Berzins and Furzeland 1985). SPRINT is effective for the solution of the differential/algebraic system in each plume region. It employs, for the solution of the algebraic constraints, a technique which is efficient for starting values near to the solution (values as are typically found for successive ODE steps). It may, however, prove inadequate for the determination of the 'initial conditions' needed at the release orifice, post flash, at touchdown, or at first plume slumping. Initial values are needed not only for the variables themselves, but also and equally importantly, for the first derivatives d/ds of all variables. These derivatives are typically discontinuous at the several model region boundaries, boundaries at which the assumed geometrical shape or phase composition of the developing plume change abruptly.

This difficulty with initial conditions is well known (Berzins, Furzeland and Scales 1988) and, for the HFPLUME model, it is made even more difficult due to the severe non-linearity introduced by the complex thermodynamic interaction of hydrogen fluoride and moist air.
The 'starting' problem, and in particular the calculation of initial derivative values 'immediately post transition' may be formulated as a non-linear algebraic problem for which we may employ a 'state of the art' non-linear equation solver. Such a solver, NAESOL (Non-LineAr Equation SOLver), has recently been developed at Thornton Research Centre (Scales 1994). This solver, which incorporates advanced search strategies, and provision for the solution of ill-conditioned or locally singular problems, typically succeeds where SPRINT would fail.

### 5.B.19. Validation studies, entrainment formulae

Several components of the model encoded in the HGSYSTEM plume models have been subject to independent experimental test. This section summaries the results of these validation studies, noting successes and limitations. Suggestions are made for further work in this area. The plume models as available in HGSYSTEM have *not* been tailored to data arising from the Goldfish experiments (Blewitt, Yohn, Koopman and Brown 1987; Blewitt, Yohn and Ermak 1987; Blewitt 1988), or other prototypical data: they have rather been *assembled* of separately validated models for plume entrainment and thermodynamics. Its success , when coupled with HEGADAS, in predicting the Goldfish experiments should be viewed in that light.

**Buoyant plumes: crosswind entrainment and plume-path**

Petersen (1978) carried out an extensive set of wind tunnel tests in which plume-path and concentration decay were examined as a function of distance downwind of a vertical release into a (near uniform) cross-wind. We consider those (19) experiments conducted for 'low' ambient turbulence in the Meteorological (boundary layer) Wind Tunnel at Colorado State University. High temperature air releases were simulated by the (isothermal) release of helium/air mixtures. The plumes were made visible by passing the stack gases over $TiCl_4$ (titanium tetrachloride) prior to release.

We have compared the experimental results obtained by Petersen with model runs in the limit of negligible ambient turbulence and with the entrainment formulation

$$\begin{aligned} \text{Entr} &= (pD)\,[e_{jet}\,\eta_{jet}\,\rho_{¥}\tfrac{1}{2}u - u_{¥}\cos\phi\tfrac{1}{2} + \text{Cue}^{\text{cross}}_{\text{wind}}\,\eta^{\text{cross}}_{\text{wind}}\,\rho_{¥}\,u_{¥}\,\sqrt{u_{\infty}/u}\,\tfrac{1}{2}\sin\phi\tfrac{1}{2}] \\ \eta_{jet}(\rho/\rho_{¥}) &= [1+(4/3)(\rho/\rho_{¥} - 1)]/]1 + (5/3)\,(\rho/\rho_{¥} - 1)] \\ \eta^{\text{cross}}_{\text{wind}}(\rho/\rho_{¥},\phi) &= [1 + C\rho e^{\text{cross}}_{\text{wind}}\,\max\{0,\,\rho/\rho_{¥} - 1)\,\sin\phi\}] \\ \text{with coefficents } e_{jet} &= 0.08,\ \text{Cue}^{\text{cross}}_{\text{wind}} = 0.60,\ C\rho e^{\text{cross}}_{\text{wind}} = 7.5 \end{aligned} \tag{97}$$

We compare the experimental rise-heights $z_k$ with those $z(x_k)$ predicted to occur at the experimental (horizontal) displacement $x_k$ downwind of release. The results are summarised in Figure 5.12. Agreement is satisfactory, with the predicted values almost always within 15% of those observed. The function form, and coefficient values for jet and crosswind entrainment are essentially those (0.08 and 0.60) recommended by Briggs (1984) on the basis of extensive data concerning neutral and buoyant plumes released at right angles to an imposed wind.

**Dense plumes: crosswind entrainment and plume-path**

Hoot, Meroney and Peterka (1973) conducted experiments in the (boundary layer) wind tunnel at Colorado State University the purpose of which was the characterisation of dense plume dispersion. Dense gas was formed by mixing air and Freon 12; releases were directed upwards and at right angles to the ambient wind; plumes were made visible by impinging the premixed (dense gas) jet on the surface of titanium tetrachloride ($TiCl_4$).

We consider a series of releases into a laminar crosswind, for which the velocity profile (Hoot, Meroney and Peterka (1973) Figure 4) is essentially constant above 3 inch from the tunnel floor.

We have compared the experimental results obtained by Hoot, Meroney and Peterka (1973) with predictions obtained in the limit of negligible ambient turbulence. The entrainment formulation are as above.

Comparison is made between observed and predicted maximum (centre-line) rise-height, and between (visible leading edge) touchdown and the impact of 'top-hat' leading-edge, or extrapolated plume centre-line, the tunnel floor. Initial conditions and observed rise heights and touchdown distances are as recorded in HMP (Hoot, Meroney and Peterka (1973)) (Report: Figure 2). In addition, comparison is made with horizontal displacement of maximum plume rise correlated by HMP's formula

$$x/D_0 = (u_¥u_0)/(gD_0)(\rho_0/\rho_¥ - 1) \qquad (98)$$

The results of a comparison between the predictions of the PLUME model and HMP date are presented in Figures 5.13 through 5.16. Generally the agreement is good, with (maximum) rise-height fitted to within perhaps 10%, maximum-rise displacement.

As regards plume 'touchdown' the situation is more complex. HMP measured the horizontal displacement from release of the point of 'visible plume edge' touchdown. This differs significantly from (extrapolated) plume centre-line touchdown, and with the touchdown of the integral averaged plume width. It is well known (Briggs 1984) that the 'momentum' and 'concentration' widths of plume differ significantly. A 'top-hat' model, which represents mass and momentum entrainment with a single plume width, cannot accurately predict concentration width. Neither is it possible to identify the 'visible plume edge' with any fixed proportion of the equivalent Gaussian (concentration) width. The systematic dilution on the plume centre-line must imply that the 'visible edge' is an increasingly small proportion of the Gaussian width. Ultimately, of course, the visible plume must dissipate entirely. In the circumstances we are content to compare 'visible edge' data with predicted centre-line (Figure 5.15) and 'top-hat' edge displacements at 'touchdown' (Figure 5.16). The centre-line displacement is systematically larger, the 'top-hat' edge smaller, than visible edge touchdown observed by HMP.
Considerable scatter is evident: this reflects the sensitivity of plume touchdown to small variations in entrainment taking place in weakly descending (marginally dense) plumes. We consider this comparison satisfactory. Further improvements in the modelled entrainment must await more accurate experimental data on (extrapolated) centre-line touchdown. This latter could be deducible from photographs of visible plume-path taken (but not published) by Hoot, Meroney and Peterka.

In addition a comparison has been made with the small but well instrumented data set of Li, Leijdens and Ooms (1986). These authors measured the detailed vertical profiles that resulted from the downward release of heated air into an essentially uniform air stream. Differences between air and plume density are everywhere small, so that these experiments should be analogous to weakly dense plumes released upwards. The results are presented in Figure 5.17. Agreement is satisfactory, as regards both plume path and width. Accuracy is comparable or better to that achieved by Havens (1988), but is inferior to that of Li, Leijdens and Ooms using their elliptic sectioned Gaussian model. Nevertheless the overall predicative accuracy of the entrainment formulation advanced here is judged sufficient for purpose. Certainly the very large experimental scatter, and range of correlation based predictions should be borne in mind (Petersen 1987).

**AEROPLUME validation**

Post (1994) describes several validation test done with the HGSYSTEM 3.0 plume model AEROPLUME. Comparison with data is favourable including measurements for the distance to Lower Flammability Limit (LFL) for pressurised liquid propane releases.

### 5.B.20. Comparison with models of Wheatley, Raj and Morris, and Havens

It is useful to contrast the models of Morris and Raj (1987) for grounded jet, Wheatley (1986) for a two-phase jet, and Havens and Spicer (1988) for a dense gas plume with that here proposed for the representation of two-phase/dense gas releases (AEROPLUME) or HF releases (HFPLUME). Each of these models have limitations which restrict, more or less severely, the range of applicability. Certainly none will span the range of release conditions encompassed by AEROPLUME/HFPLUME.

**The free jet model of Wheatley**

This model (Wheatley 1987a, 1987b) was developed in order to predict the downwind distribution of concentration and temperature resulting from a pressurised release of liquid ammonia. The model structure is: steady state, no atmosphere gradients, (isobaric) thermal equilibrium, entrainment dominated by jet/ambient shear, negligible gravity slumping.

Though the model (TRAUMA) was originally 'tailored' for liquid ammonia releases, its thermodynamic structure permits the release of several reactive liquids and in particular anhydrous HF. No provision is made for the impact of jet upon the ground, either in respect of induced drag, or of geometrical distortions. Model applicability is thus limited under prototypical conditions to a downwind range of perhaps 10m, and to HF concentrations in excess of some 1% by volume HF.

The model differs from HFPLUME in that complete 'atomisation' of the released liquid is not *assumed*, but is rather *checked* against a criterion first developed by Ohnesorge (1936) for

thermodynamically stable liquid jets. Maximum stable droplet size and gravitational settlement of droplets (Clift, Grace and Weber 1978) are considered in the context of droplet 'rain-out'; a simple (inequality) condition is developed for the absence of droplet rain-out. The analysis takes no account of droplet evaporation. The restricted downwind range of Wheatley's model make it suitable for the near-field prior to plume touchdown. No provision is made for other than horizontal releases. Overall the accuracy and range of validity of this model (comparable to HFPLUME) is, we judge, insufficient for a confident 'matching' to either heavy gas or passive dispersion models in the far field.

**The grounded jet model of Morris and Raj:**

Raj and Morris (1987) proposed a 'top-hat' (sectionally averaged) model for a ground affected (rectangular) jet. The range of validity extends from (plume) touchdown through momentum dominated jet, towards heavy gas dispersion. The model structure takes account of wind shear and atmospheric stability, and incorporates ground drag and gravity slumping effects. The cross-section is vertical. The equation system comprises horizontal momentum, conservation of pollutant mass-flux, a (differential) entrainment relation, and a gravity spreading law. Thermal equilibrium is assumed throughout. The entrainment relation is proportional to the mean difference (over 'top' or 'side') between ambient wind-speed and jet velocity.

Entrainment is further proportional to the ambient density and to a dimensionless entrainment coefficient which on the basis of gas jets has an anticipated magnitude $e \approx 0.08$. This is analogous to the formulations in the HGSYSTEM plume models, except that all parameters are referred in these latter cases to the centroid height. The drag force comprises two parts, a shear force exerted at the 'top' surface, and a 'drag' at the ground. Drag on either surface is assumed proportional to the square of the difference at the bounding surfaces between jet velocity and wind speed. Account is taken of density differences inasmuch as the drag at the jet 'top' is assumed proportional to the *ambient* density, whereas that at the ground is linear in the jet mean density.

This model is strongly empirical, however, in that both ground and atmosphere drag are assigned adjustable coefficients for matching with experimental data. Additional entrainment terms, representing ambient atmosphere entrainment, and lateral spreading entrainment (Puttock 1988) are entirely absent. The several empirically adjustable coefficients are obtained (and the model tuned) by comparison of model predictions against an extremely small data set, the Desert Tortoise 4 Ammonia Release (Ermak, Chapman, Goldwise, Gouveia and Rodean 1987).

In spite of these limitations it seems likely that the model of Raj and Morris represents a significant improvement on that of Wheatley for a free jet. The key difference rests in the explicit representation of gravity slumping in the formula

$$\frac{dD}{ds} = \frac{k}{u}\sqrt{gh(\rho/\rho_{\infty} - 1)}, \text{ with } k = 1.15 \qquad (99)$$

This permits a reasonable description of gravity slumping for a near horizontal release in which horizontal and vertical motions are largely decoupled. Entrainment is dominated by jet/atmosphere shear. The structure is, however, incompatible with existing integral-averaged plume models, and cannot represent the early interaction between impacting plume and ground that accompanies 'touchdown'. Neither can the early (airborne) jet be followed, so that for predictions near the source a 'free' jet model, such as AEROPLUME, HFPLUME or TRAUMA, must be matched to that of Raj and Morris (1988).

The problem, mathematically, is that a gravity slumping formula has replaced the vertical momentum equation in the limit of horizontal jet flow: the solution (section 5.B.7) is to introduce pressure forces, acting at the ground surface, such as allow recovery of gravity slumping and plume descent in the appropriate asymptotic limits. Such a formulation we expect to be of comparable or greater accuracy for horizontal pressurised releases, whilst permitting extrapolation to vertical releases, and releases inclined to the ambient wind. The formulation of the drag forces at upper and lower jet edge is complex, and highly empirical. Formulations based on an analysis of the turbulent averaged equations of motion lead rather directly (section 5.B.7) to a drag force expressed in terms of ambient parameters at the centroid height, the form of which introduces no empiricism beyond that required for heavy gas (ambient) entrainment. The formulation of the HGSYSTEM plume models is therefore consistent throughout the free jet, touchdown, and slumped plume regions, and contains entrainment mechanisms relevant to all. The HGSYSTEM plume models is uniformly valid from point of release to far within the heavy gas advection regime.

**The atmosphere plume model of Havens and Spicer:**

Havens and Spicer (Havens 1988) have proposed that the model of Ooms, Mahieu, and Zelis (1974) be used for the representation of dense gas releases prior to plume touchdown. The model is a variant of the simple integral average models in that a truncated Gaussian ('similarity') profile is imposed upon velocity, density, and concentration within the developing plume. The model also includes an initial zone model, in which are adopted empirical correlations spanning the region prior to the establishment within the plume of (approximately) Gaussian conditions. This initial zone model is uncertain, even in the context

of gaseous releases (Keffer and Baines 1963, Kanotani and Greber 1972); it is doubtful whether this additional complexity is necessary or desirable.

Specific comments may be made regarding such (truncated Gaussian) formulations. The centre-line concentration is artificially heightened by the process of profile 'cut-off' whereby the mass in the Gaussian 'tail' is redistributed toward the plume centre. The use of a cut-off is not necessary for such a self-similarity theory and may be eliminated by a reformulation of the integral equations of motion (Schatzmann 1978, McFarlane 1988).

Li, Leijdens and Ooms (1986) employed a 'drag' force in order to reproduce the observed plume path for a set of 3 buoyant jets released downwards: the use of such a drag force is controversial (Briggs 1984); the data set severely limited. Coefficient values and the functional form of the entrainment function are uncertain (Petersen 1978, Schatzmann 1978); there is considerable scatter in the experimental data (Petersen 1987).

*The benefits of truncated Gaussian over simpler 'top-hat' models seem to us unproved*, even in the context of gas plumes. For reactive, initially two-phase releases, solution of such models requires numerical integration of the energy equation at each downwind advance of the discretized differential system for plume motion; it is not possible to introduce the several simplifications to the system thermodynamics that allow explicit integration of the enthalpy excess over the plume cross-section (Havens 1987). For complex reactive flows, and in particular for pressurised releases of anhydrous HF, the computational cost of a Gaussian model seems prohibitive. Additionally the model requires initial zone information appropriate to pressurised gas or two-phase, or atomised liquid phase releases.

In practical terms what is required is a model prior to plume touchdown passing integral averaged information to a grounded jet model (Raj and Morris 1987), a slumping pool model (Raj and Morris 1987), or (perhaps) a heavy gas advection model (Colenbrander and Puttock 1988). Details of concentration behaviour off-axis cannot readily be passed from model to model; nor is this information likely to be accurate. *A sectionally-averaged or 'top-hat' model seems to be a reasonable compromise between computational complexity and predicative accuracy*. Development of the energy equation for such a model presents no difficulty (Davidson 1986); neither are problems found with the inclusion of reaction chemistry (Forney and Droescher 1985).

> The touchdown model of Havens and Spicer has the merit of simplicity:
> 'The Ooms model' .. ' is terminated when the lower edge of the plume impinges the ground. The resulting downwind distance, plume centre line concentration and

temperature, and plume radius ($b_j Ö2$) are used as input to DEGADIS. The ground level gas source input to DEGADIS is a circular area source with radius ($b_j Ö2$) and concentration and temperature equal to the centre-line values output from Ooms model.' (Havens 1988a, 1988b)

Insufficient detail is given to permit full consideration of the touchdown assumptions. We presume however that the DEGADIS circular source has an 'evaporation rate' such as to conserve mass- and excess-enthalpy flux at the plane of transition. No account is taken of the momentum excess in either horizontal or vertical direction developed in the course of plume rise and fall. Substantial vertical velocities must imply enhanced (impact) spreading; differences in horizontal velocity between plume and wind imply transition to a grounded jet model, or to some intermediate touchdown model. It seems essential to take some account of these velocity (momentum) differences in the vicinity of plume touchdown. We suggest transition to a spreading pool model (fed from above) or to a slumped plume model in the manner of the HGSYSTEM plume models. Alternatively some empirical correlation between plume and heavy-gas advection might be developed.

For releases which result in much delayed plume touchdown, (> 1 km, say) we agree with Havens that the use of Ooms model is compromised by the much earlier touchdown of the leading plume edge. A possible solution is to include an 'image' plume as a model of the (horizontal) ground. However dilution is likely to be such that plume behaviour more closely approximates passive dispersion than that appropriate to heavy-gas advection models such as DEGADIS or HEGADAS. We suggest that for these cases transition should be made to a Gaussian far-field dispersion model (Hanna 1982) based upon asymptotic matching of plume and Pasquill/Gifford standard deviations $s_y$ and $s_z$. Discussion of 'image' plume dynamics illustrates the additional complexity imported with Gaussian rather than 'top-hat' models in plume touchdown.

**5.B.21. References**

Abramovich G N: The Theory of Turbulent Jets, MIT Press, Cambridge, Massachusetts, 1963; §1.7 Heat Transfer in a Submerged Jet, pp 17-22; §1.8 Diffusion of Constituents in a Submerged Jet, pp 23-25.

Albertson M L, Dai Y B, Jensen R A, and Hunter Rouse M: Diffusion of Submerged Jets, Transactions American Society of Civil Engineers, Paper No. 2409, Proceedings December 1948, pp 639-665.

Berzins M, Dew P M, and Furzeland R M: Software for Time Dependent Problems; PDE Software: Modules, Interfaces and Systems. Given at The IFIP TC Working Conference, Soderkoping, Sweden, 22nd-26th August 1983. Proceedings (Enquist and Smedsaas ed.s) published by North Holland, Amsterdam, The Netherlands, 1983.

Berzins M and Furzeland R M: A user's manual for SPRINT - a versatile software package for solving systems of algebraic, ordinary, and partial differential equations: Part 1 - algebraic and ordinary differential equations, Shell Research Limited, Thornton Research Centre, 1985, TNER.85.058, Non-Confidential.

Berzins M, Furzeland R M and Scales L E: A User's Manual for SPRINT, a Versatile Software Package for solving Systems of Algebraic Ordinary and Partial Differential Equations: Part 3 - Advanced Use of SPRINT; Shell Research Limited, Thornton Research Centre, 1988, TNER.88.034, Non-Confidential.

Birch A D and Brown D R: The Use of Integral Models for predicting Jet Flows, in Mathematics in Major Accident Risk Assessment, Cox R A (editor), Proceedings of the IMA Conference on Mathematics in Major Accident Risk Assessment, Oxford, England July 1986. Published Oxford at the Clarendon Press, 1989.

Blewitt D N, Yohn J F, and Ermak D L: An Evaluation of SLAB and DEGADIS Heavy Gas Dispersion Models Using the HF Spill Test Data; AIChE International Conference on Vapour Cloud Modelling; Cambridge, Massachusetts, November 2nd-4th 1987; Center of Chemical Process Safety; AIChE 1987.

Blewitt D N, Yohn J F, Koopman R P and Brown T C: Conduct of Anhydrous Hydrofluoric acid Spill Experiments; AIChE International Conference on Vapour Cloud Modelling; Cambridge, Massachusetts, November 2nd-4th 1987; Center of Chemical Process Safety; AIChE 1987.

Blewitt D N: Preliminary Draft Data Analysis Report for the HF Spill Test Experiments, Draft for Internal Review, Amoco Corporation, undated 1988.

Bloom S: A mathematical model for reactive, negatively buoyant atmospheric plumes; Heavy Gas ND Risk Assessment Conference; Frankfurt am Main, West Germany 1980; Proceedings, Hartig S editor.

Botterill J A, Williams I, and Woodhead T J: The Transient Release of Pressurized LPG from a Small-Diameter Pipe, in The Protection of Exothermic Reactors and Pressurised Storage Vessels, Proceedings of the Institution of Chemical Engineers Symposium, Chester, England, April 1984, Published by Pergamon Press, 1984, pp 265-278.

Briggs G A: Plume Rise Predictions, in Lectures on Air Pollution and Environmental Impact Analyses, Workshop Proceedings, Boston Massachusetts, 29th September - 3rd October 1975; Published American Meteorological Society, Boston, pp 59-111.

Briggs G A: Plume Rise and Buoyancy Effects, Chapter 9, pp 327-366 of Randerson D (ed.) Atmospheric Science and Power Production, Technical Information Centre, Office of Scientific and Technical Information, US Department of Energy, DOE/TIC-27601(DE84005177), 1984.
Coelho L V and Hunt J C R: The dynamics of the near field of strong jets in crossflows; J Fluid Mech **200** (1989), 95-120.

Clift R, Grace J R, and Weber M E: Bubbles, Drops, and Particles; Academic Press, London, 1978.

Clough P N, Grist D R and Wheatley C J: Thermodynamics of Mixing and Final State of a Mixture formed by the Dilution of anhydrous Hydrogen Fluoride with Moist Air; Safety and Reliability directorate (SRD), United Kingdom Atomic Energy Authority (UKAEA), Wigshaw Lane, Culcheth, Warrington, Cheshire, England, WA3 4NE, SRD R 396, 1987.

Colenbrander GW: A Mathematical Model for the Transient Behaviour of Dense Vapour Clouds; 3rd International Symposium on Loss Prevention and Safety Promotion in the Process Industries; Basil, Switzerland; September 1980.

Colenbrander G W: Atmospheric dispersion of heavy gases emitted at, or near, ground level **1.** Formulation of dispersion in the vertical direction in the HEGADAS model; Shell Internationale Research Maatschappij B V, KSLA, Amsterdam AMGR.84.059, December 1985, Figure 8, Private Communication**.**

Colenbrander G W and Puttock J S: Dispersion of Releases of Dense Gas: development of the HEGADAS model; HEGADAS Public Release Documentation; US Environmental Protection Agency. Distributed by the National Technical Information Centre (NTIS); 1988.

Cowley L T and Tam V H Y: Consequences of Pressurized LPG Releases: The Isle of Grain Full Scale Experiments, 13th Int. Conf. LNG/LPG Conference and Exhibition, Kuala Lumpur, Malaysia, October 18-21, 1988.

Davidson G A: Gaussian versus Top-Hat Profile Assumptions in Integral Plume Models, Atmospheric Environment **20**(1986), 471-478.

Disselhorst J H M: The Incorporation of Atmospheric Turbulence in the KSLA Plume Path Program; Shell Internationale Research Maatschappij B V, The Hague, AMGR.84.059, September 1984. Private Communication**.**

Du Pont: Hydrofluoric Acid, Anhydrous-Technical, Properties, Uses, Storage and Handling; undated Bulletin; E I du pont de Nemours & Co. )Inc.), Wilmington, Delaware 19898; received 1988.

Eidsvik K J: Dispersion of heavy gas clouds in the atmosphere, Report No 32/78, (ref. 25077), Norwegian Institute for Air Research, 1978.

Ermak D L, Chapman R, Goldwire H C, Gouveia F J, and Rodean H C: Heavy Gas Dispersion Test Summary Report; Air Force Engineering and Services Laboratory, Summary Report, Draft, 1987.

Forney L J and Droescher F M: Reactive Plume Model: Effect of Stack Exit Conditions on Gas Phase Precursors and Sulphate Formulation; Atmospheric Environment **19** (1985), 879-891.

Fox J A: An Introduction to Engineering Fluid Mechanics; The MacMillan Press Ltd., London 1974. §4.9.2, pp 135-138.

Frick W E: Non-Empirical Closure of the Plume Equations; Atmospheric Environment **18**(1984), 653-662.

Gray R: HFMIT - Program to Calculate Heat and Mass Balance for HF/Water/Air Streams; version 1: March 1987; Applied Thermodynamics Group, Chemical Engineering Technology Division, Exxon Engineering, Florham Park, New Jersey USA. Private Communication**.**

Hanna S R: Turbulent Diffusion: Chimneys and Cooling Towers, in Plate E J: Engineering meteorology, Elsevier Scientific Publishing Company, Amsterdam, 1982; Chapter 10, pp 429-451, especially §10.2.3, pp 438-439.

Havens J: Modelling Trajectory and Dispersion of Relief Valve Gas Discharges; US Environmental Protection Agency, Office of Air Quality Planning and Standards, Research Triangle Park, North Carolina, (Draft) EPA Purchase Order 6D1678NASA, February 1987.

Havens J: A Dispersion Model for Elevated Dense Gas Jet Chemical Releases - Volume 1, US Environmental Protection Agency, Research Triangle Park, North Carolina, PB88-20238, April 1988.

Havens J: A Dispersion Model for Elevated Dense Gas Jet Chemical Releases Volume 2. User's Guide, US Environmental Protection Agency, Research Triangle Park, North Carolina, PB88-20239, April 1988.

Hinze J O: Turbulence An Introduction to its Mechanisms and Theory, McGraw-Hill Book Company, London, 1959, Chapter 6, §6.7: pp 404-447.

Hoot T G, Meroney R N, and Peterka J A: Wind Tunnel Tests of Negatively Buoyant Plumes; Fluid Dynamics and Diffusion Laboratory, Colorado State University; distributed by National Technical Information Service, US Department of Commerce, Report PB-231-590, October 1973.

Hoult D P, Fay J A, and Forney L J: A theory of plume rise compared with field observations, J. Air. Poll. Ass. **19**(1969), 585-.

Iannello V and Rotha P H: May Project Report for Liquid Release Project; letter to Blewitt D, Amoco Corporation, 27th June 1988; Creare Incorporated, Engineering Research and Development, Computer Systems and Software, Etna Road, PO Box 71, Hanover, New Hampshire 03755; Private Communication**.**

Irwin J S: A theoretical variation of the wind profile power-law exponent as a function of surface roughness; Atmospheric Environment **13**(1979) 191-194.

Johnson G W and Thompson D S: Liquified Gaseous Fuels Spill Test Facility Description; Lawrence Livermore National Laboratory, UCID-20291, December 1984.

Jones A: Mass Transfer - Characterization of Initial HF Release for Dispersion Calculations; letter to Shepard R W, CONOCO Houston, Texas, dated 15th July 1988; E I du Pont de Nemours & Co. (Inc.), C & P Department, La Porte, WR 398761; Private Communication**.**

Kanotani Y and Greber I: Experiments on a Turbulent Jet in a Cross-Wind; AIAA Journal **10** 1425-1429, November 1972.

Karman J G: Touch-Down of a Heavy Plume, Laboratorium voor Aero- en Hydrodynamica, Techische Hogeschool, Rotterdamseweg 145, DELFT, The Netherlands; Report No. MEAH 56: Private Communication, 1986.

Keffer J F and Baines W D: The Round Turbulent Jet in a Cross-Wind; J. Fluid Mech. **15**(1963), 481-496.

Koopman R P: A Facility for Large-Scale Hazardous Gas Testing including Recent Test Results; Lawrence Livermore National Laboratory; Preprint intended publication: The Hazardous Materials Management Conference and Exhibition, Longbeach, California, 3rd-5th December 1985.

Li X-Y, Leijdens H, and Ooms G: An Experimental Verification of a Theoretical Model for the Dispersion of a Stack Plume Heavier than Air; Atmospheric Environment **20**(1986).

Linden P F and Simpson J E: Development of Density Discontinuity in a Turbulent Fluid; in Stably Stratified Flow and Dense Gas Dispersion, Puttock J E (ed.), Oxford, Clarendon Press, 1988.

List E J: Turbulent Jets and Plumes, Ann. Rev. Fluid Mech. **14**(1982), 189-212.

McCarthy M J and Molloy N A: Review of Stability of Liquid Jets and the Influence of Nozzle Design; The Chemical Engineering Journal **7**(1973), 1-20.

McFarlane K: Development of Models for Flashing Two-Phase Releases from Pressurised Containment; ECMI Conference on The Application of Mathematics in Industry; Strathclyde University, Glasgow, Scotland, 28th-31st August 1988; Accepted Proceedings April 1988.

McQuaid J: Some Experiments on the Structure of Stably Stratified Shear Flows; Safety in Mines Research Establishment, Sheffield, England; Technical Paper P21, 1976.

McQuaid J (ed.): Heavy Gas Dispersion Trials at Thorney Island; Proceedings of a Symposium held at the University of Sheffield, Sheffield, England, 3rd-5th April 1984, Elsevier, Amsterdam, 1984.

Morrow T et alia: Analytical and Experimental Study to Improve Computer Models for Mixing and Dilution of Soluble Hazardous Chemicals; Final Report; Contract No. DOT-CG-920622-A with South west Research Institute; US Coast Guard; August 1982.

Morton B R, Taylor G I, and Turner J S: Turbulent Gravitational Convection from Maintained and Instantaneous Sources, Procs. Roy,. Soc. Series A, **234**(1956), 1-23.

Ohnesorge W van: Die Bildung von Tropen an Düsen und die Auflösung flüssiger Strahlen; (Drop Formation at Nozzles and the Decomposition of Liquid Jets) Ztschr. f. angew. Math. und Mech. **16**(1936) 355-358.

Ooms G: A New Method for the Calculation of the Plume Path of Gases emitted by a Stack, Atmospheric Environment **6**(1972), 899-909.

Ooms G and Duijm N J: Dispersion of a Stack Plume Heavier than Air; International Union of Theoretical and Applied Mechanics; 'Atmospheric Dispersion of Heavy Gases and Small Particles'; Symposium, Delft, The Netherlands, 29th August - 2nd September 1983; Published Springer-Verlag, Berlin, 1984.

Ooms G, Mahieu A P, and Zelis F: The Plume Path of Vent Gases Heavier than Air; First International Symposium on Loss Prevention and Safety Promotion in the Process Industries (Buschmann C H ed.); Elsevier Press, 1974.

Pasquill F: Atmospheric Dispersion Parameters in Gaussian Plume Modelling Part 2. Possible Requirements for Change in the Turner Workbook Values; US Environmental Protection Agency, Office of Research and Development, Environmental Sciences Research Laboratory, Research Triangle Park, North Caroline 27711. EPA-600/4-76-030b, June 1976.

Petersen R L: Plume Rise and Dispersion for varying ambient turbulence, thermal stratification, and stack exit conditions, PhD thesis, Colorado State University, Fall, 1978. Published by University Microfilms International, London, WC1R 4EJ, 1986.

Petersen R L: Performance Evaluation of Integral and Analytical Plume Rise Algorithms, JAPCA **37**(1987), 1314-1319.

Petersen R L and Ratcliff M A: Effect of Homogeneous and Heterogeneous Surface Roughness on Heavier than Air Gas Dispersion; Cermak, Peterka, and Petersen (CPP) Incorporated; 1415 Blue Spruce Drive, Fort Collins, Colorado, 80524. Contract for the American Petroleum Institute (API); Report CPP 98-0417, 1989.

Plate E J(ed): Engineering Meteorology: Fundamentals of Meteorology and Their Application to Problems in Environmental and Civil Engineering; Studies in Wind Engineering and Industrial Aerodynamics, 1; Elsevier Scientific Publishing Company, Amsterdam, 1982.

Post, L., Validation of the AEROPLUME model for the simulation of pressurized releases of vapour or two-phase mixtures, Shell Research Limited, Thornton Research Centre, TNER.94.014, Non-Confidential, 1994.

Puttock J S: Gravity-dominated Dispersion of Dense Gas Clouds; Institute of Mathematics and its Applications (IMA), Conference on Stably Stratified Flow and Dense Gas Dispersion, Chester, Cheshire, England; 3rd-5th April 1986; Oxford University Press, 1988.

Raj P K, and Morris J A: 'Source Characterization and Heavy Gas Dispersion Models for Reactive Chemicals', Technology & Management Systems Inc., Burlington, Massachusetts 01803-5128, AFGL-TR-88-0003(I), December 1987.

Ricou F P and Spalding D B: Measurement of Entrainment by axisymmetrical turbulent jets, J. Fluid Mech. **11**(1961), 21-32.

Rouse H, Yih C S, and Humphreys H W: Gravitational convection from a Boundary Source, Tellus **4**(1952), 201-210.

Scales L. E.: NAESOL - A software toolkit for the solution of nonlinear algebraic equations, User Guide - version 1.5, Shell Research Limited, Thornton Research Centre, TRCP.3661R, September 1994, Non-Confidential.

Schatzmann M: The Integral Equations for Round Buoyant Jets in Stratified FLows, J Applied Mathematics and Physics (ZAMP) **29**(1978), 608-630.

Schatzmann M: An Integral Model of Plume Rise, Atmospheric Environment **13**(1979), 721-731.

Schatzmann M and Policastro A J: An Advanced Integral Model for Cooling Tower Plume Dispersion; Atmospheric Environment **18**(1984), 663-674.

Schatzmann M and Policastro A J: Effects of the Boussinesq Approximation on the Results of Strongly-buoyant Plume Calculations; Journal of Climate and Applied Meteorology **23**(1984), 117-123.

Schotte W: Fog Formation of Hydrogen Fluoride in Air, Ind. Eng. Chem. Res. **26**(1987), 300-306.

Schotte W: Thermodynamic Model for HF Fog Formation; letter to Soczek C A dated 31 August 1988; E I du Pont de Nemours & Company, du Pont Experimental Station, Engineering Department, Wilmington, Delaware 19898, Private Communication**.**

Spillane K T: Observations of Plume Trajectories in the Initial Momentum influenced Phase and Parameterization of Entrainment; Atmospheric Environment **17**(1983), 1207-1214.

Stern A C, Boubel R W, Turner D B, and Fox D L: Fundamentals of Air Pollution, (second edition), Academic Press, London 1984. Chapter 17, pp 277-287.

Strohmeier von W and Briegleb G: Uber den Assoziationzustand de HF in Gaszustand. 1 (Neue experimentelle Messungen), Zeitschrift fur Elektrochemie **57**(1953), 662-667.

van de Sande E and Smith J M: Jet Break-Up and Air Entrainment by Low Velocity Turbulent Water Jets; Chemical Engineering Scient **31**(1976), 219-224.

van Ulden A P: On the spreading of a heavy gas released near the ground; Proceedings International Symposium on Loss Prevention in the Process Industries, Delft, Netherlands, 1974.

Van Ulden A P; A new bulk model for dense gas dispersion: two-dimensional spread in still air; Atmospheric Dispersion of Heavy Gas and Small Particles; editors Ooms G and Tennekes H; Springer Verlag, Berlin, 1984; pp 419-440.

Vierweg R: Betrachtungen zum System Fluorwasserstoff-Wasser; Chem. Tech. **12**(1963), 734-740.

Wheatley C J: A Theoretical Study of $NH^3$ Concentrations in Moist Air arising from Accidental Releases of Liquified $NH^3$ using the Computer Code TRAUMA, Safety and Reliability Directorate (SRD), United Kingdom Atomic Energy Authority (UKAEA), Wigshaw Lane, Culcheth, Warrington, Cheshire, England, WA3 4NE, SRD/HSE/R 393, February 1987.

Wheatley C J: Discharge of Liquid Ammonia to Moist Atmospheres - Survey of Experimental Data and Model for estimating initial conditions for dispersion calculations, Safety and Reliability Directorate (SRD), United Kingdom Atomic Energy Authority (UKAEA), Wigshaw Lane, Culcheth, Warrington, Cheshire, England, WA3 4NE, SRD/HSE/R 410, April 1987.

Wheatley C J: Theory of heterogeneous equilibrium between vapour and liquid phases of binary systems and formulae for the partial pressures of HF and $H_20$ vapour, Safety and Reliability Directorate (SRD), United Kingdom Atomic Energy Authority (UKAEA), Wigshaw Lane, Culcheth, Warrington, Cheshire, England, WA3 4NE, SRD R 357, April 1986.

Witlox H W M: Validation and Improved Formulation of the Entrainment Relation and Concentration Profile in the Heavy Gas Dispersion Program HEGADAS; January 1988, Private Communication**.**

Wieringa J: 'A Re-evaluation of the Kansas Mast Influence on Measurements of Stress and Cup Anemometer Overspeeding', Boundary Layer Meteorology **18**(1980) 411-430.

Zemansky M W: Heat and Thermodynamics; (5th edition); McGraw Hill Book Company 1968; Chapter 16, §16.1, pp 557-558.

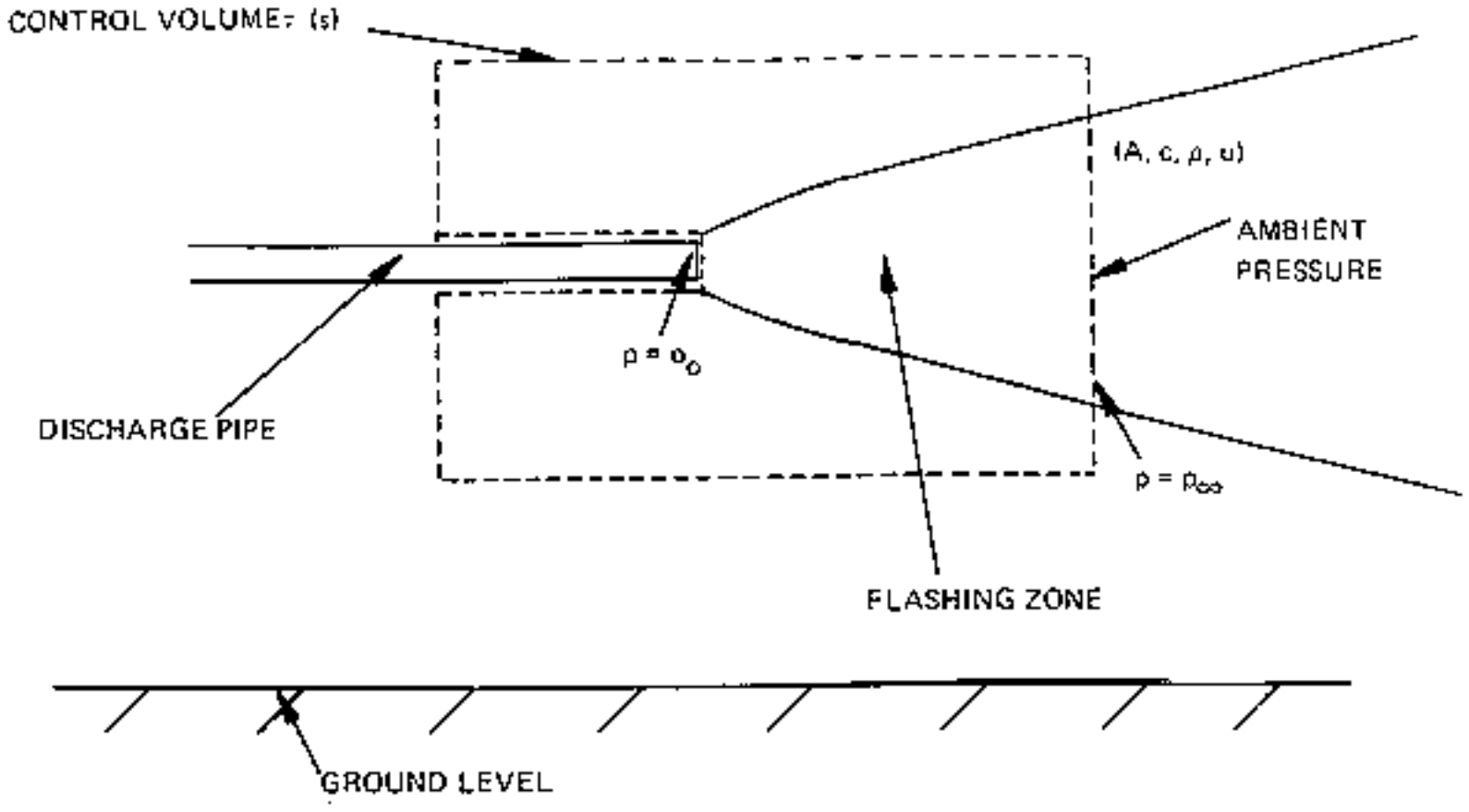


FIG. 5.1 — The zone of external flashing. On release, fluid expands to ambient pressure. Thermal equilibrium assumed. Entrainment and interphase slip taken to be negligible.

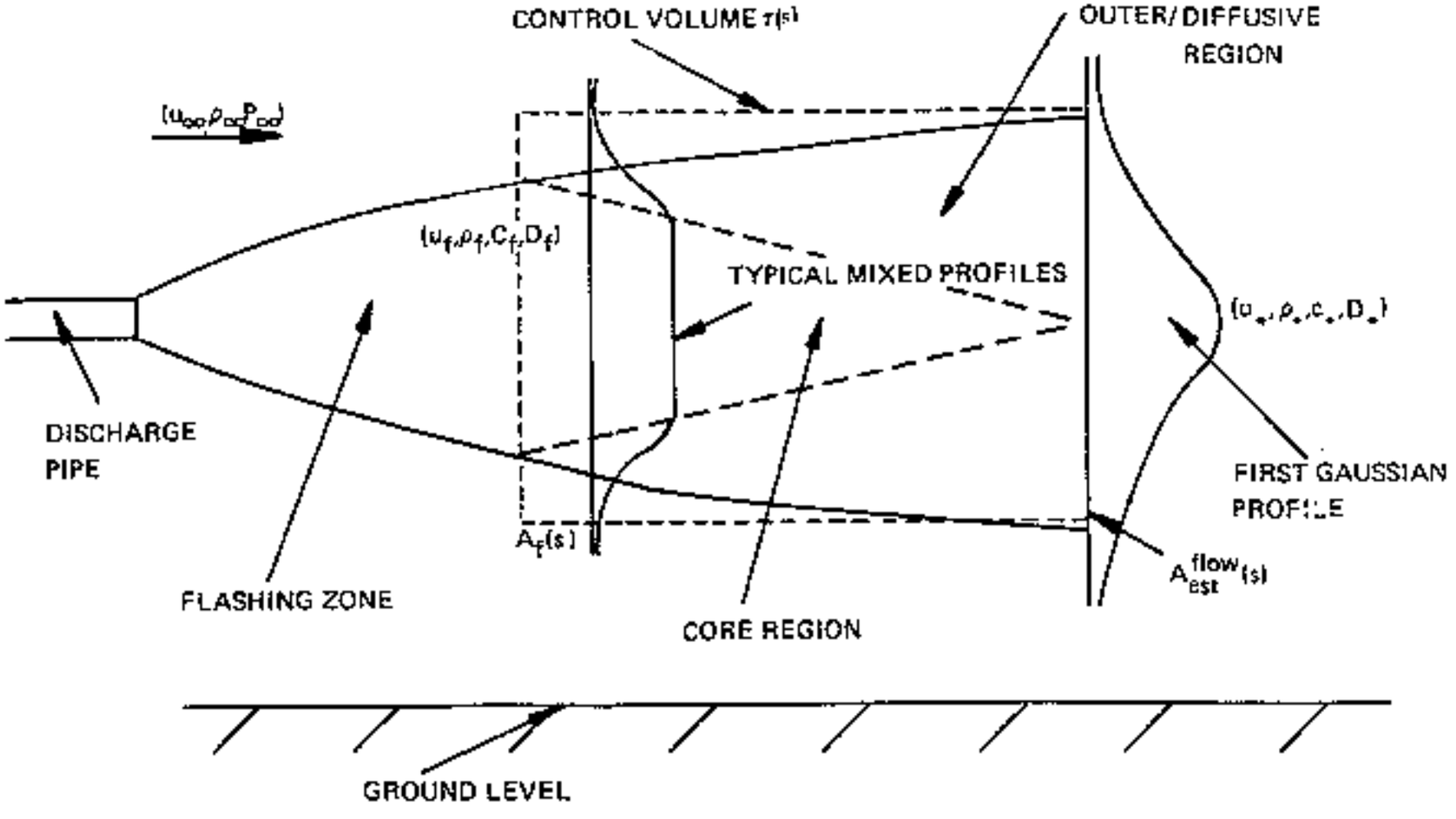


FIG. 5.2 – The zone of flow establishment. Transition region in which initially "top-hat" profiles are eroded by entrainment into outer region. Zone ends when undisturbed inner core region disappears to leave Gaussian profiles and self-similar flow.

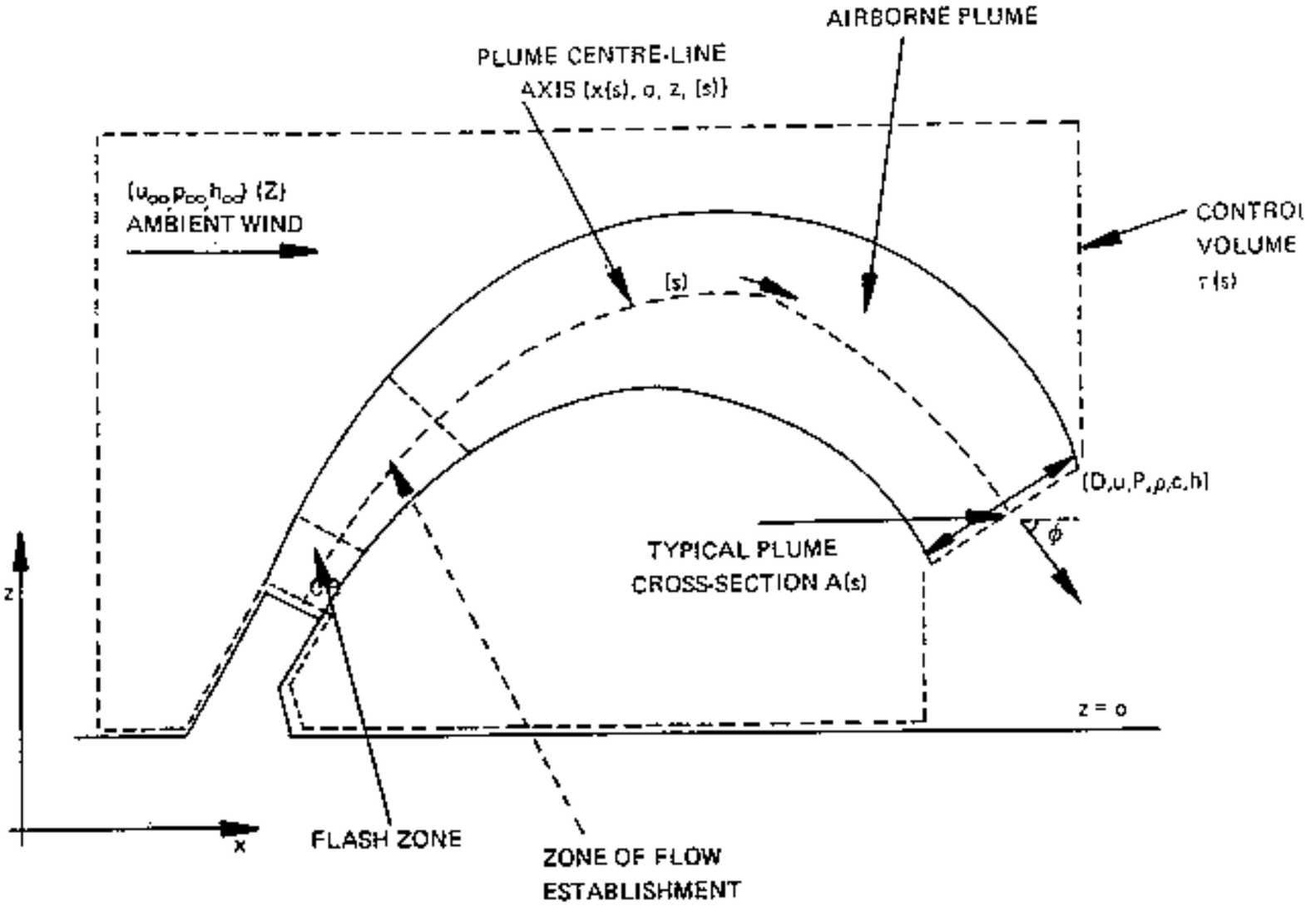


FIG. 5.3. — The airborne (established) plume. Negligible ground effect. Radial symmetry about plume centre-line.

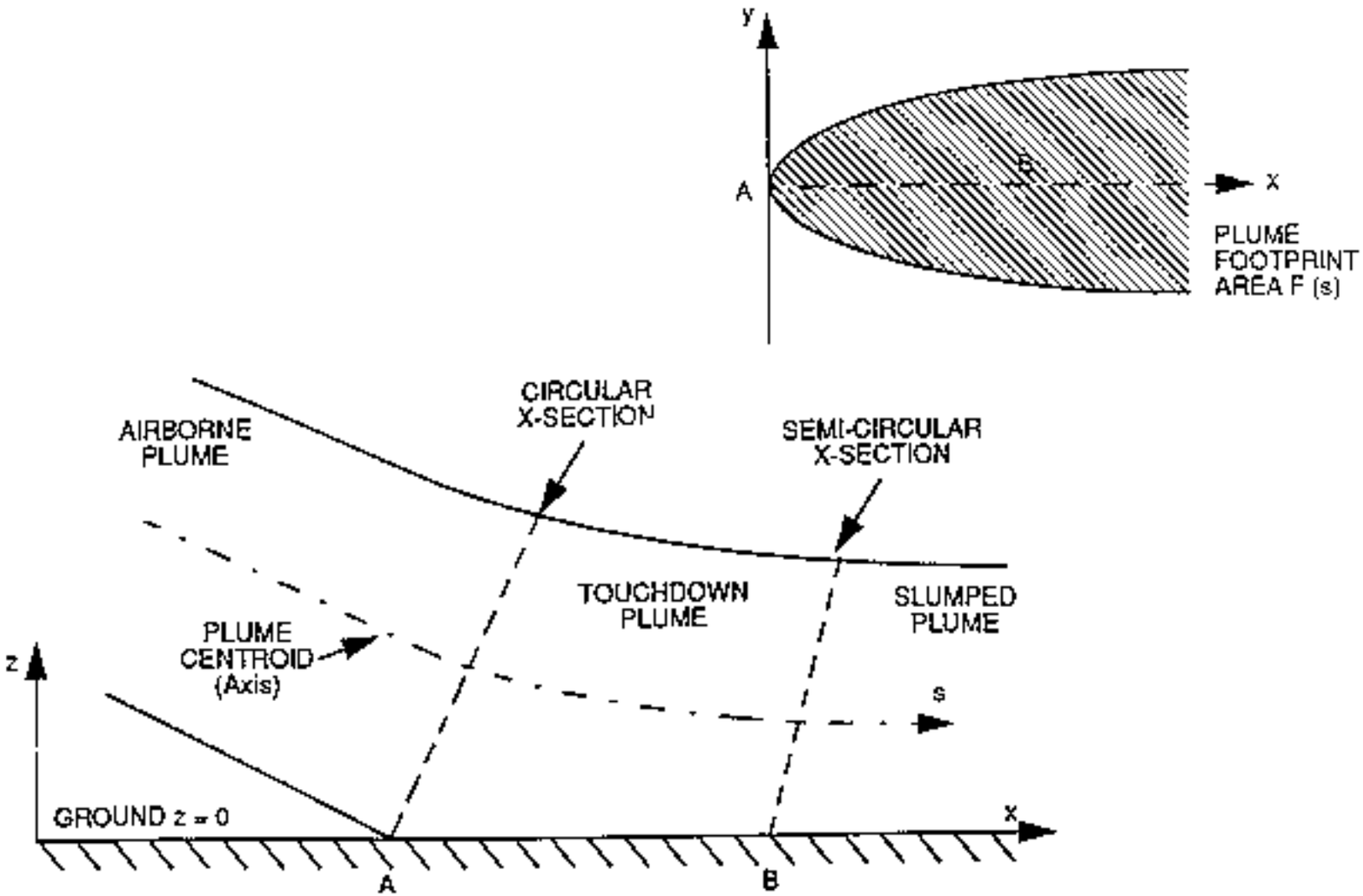


FIG. 5.4 - The touchdown plume. Transition of plume from circular X-section to semi-circular X-section in the touchdown region

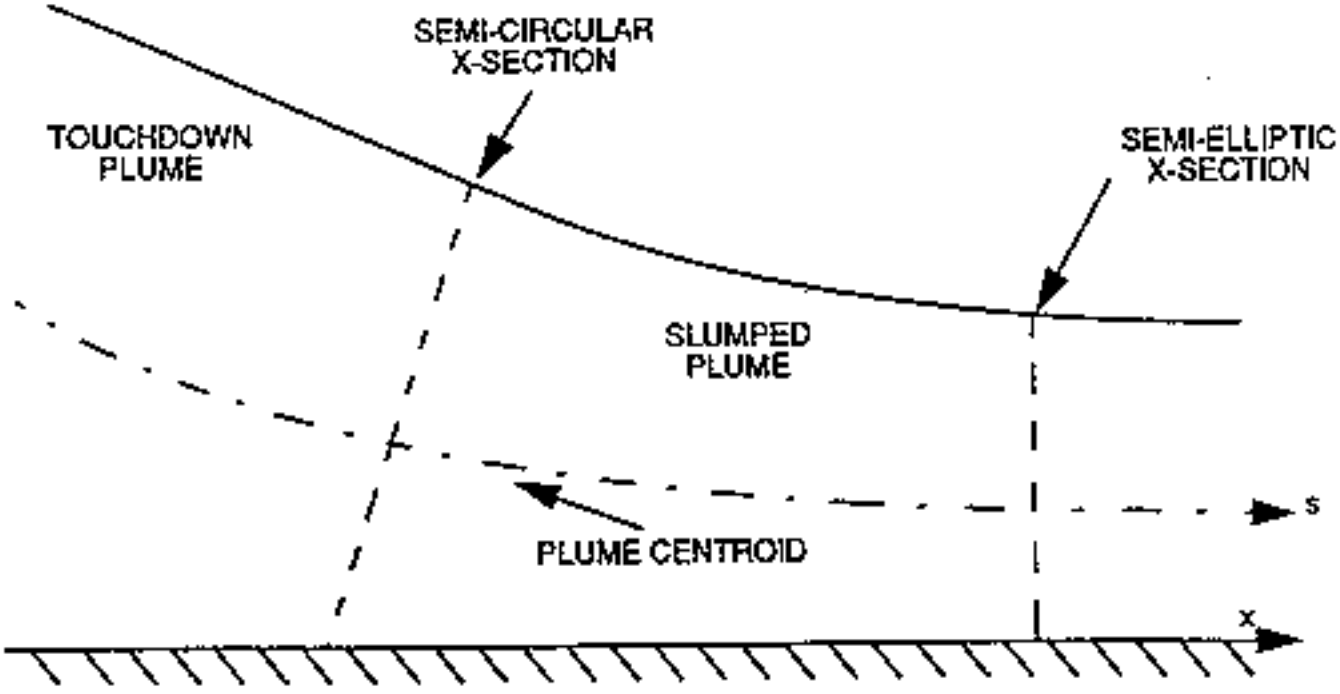


FIG. 5.5 - The slumped plume. Semi-elliptic X-section due to lateral gravity spreading

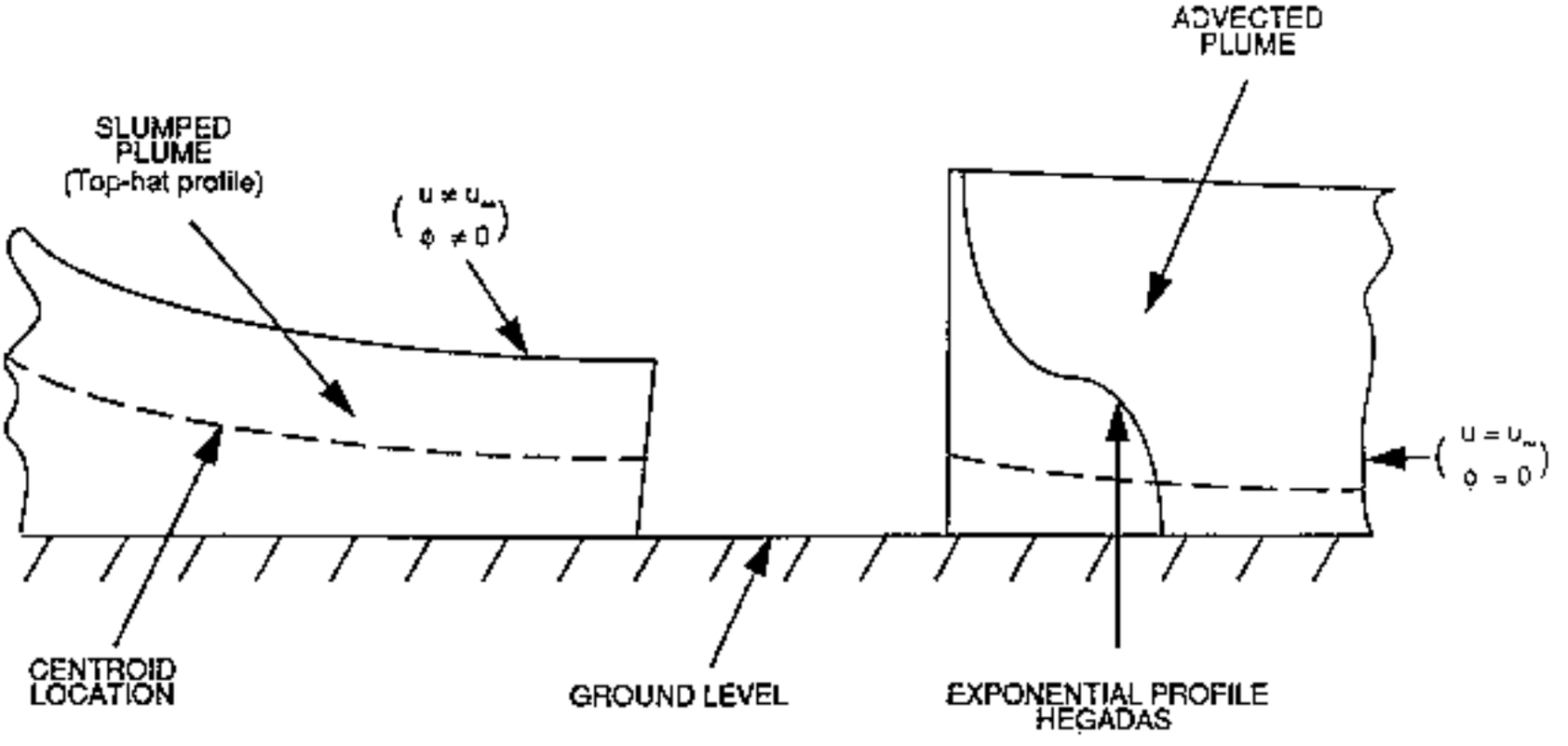


FIG. 5.6 - . Transition to advected dense gas plume (HEGADAS). Criteria for transition are small plume excess velocity over ambient, and small jet entrainment

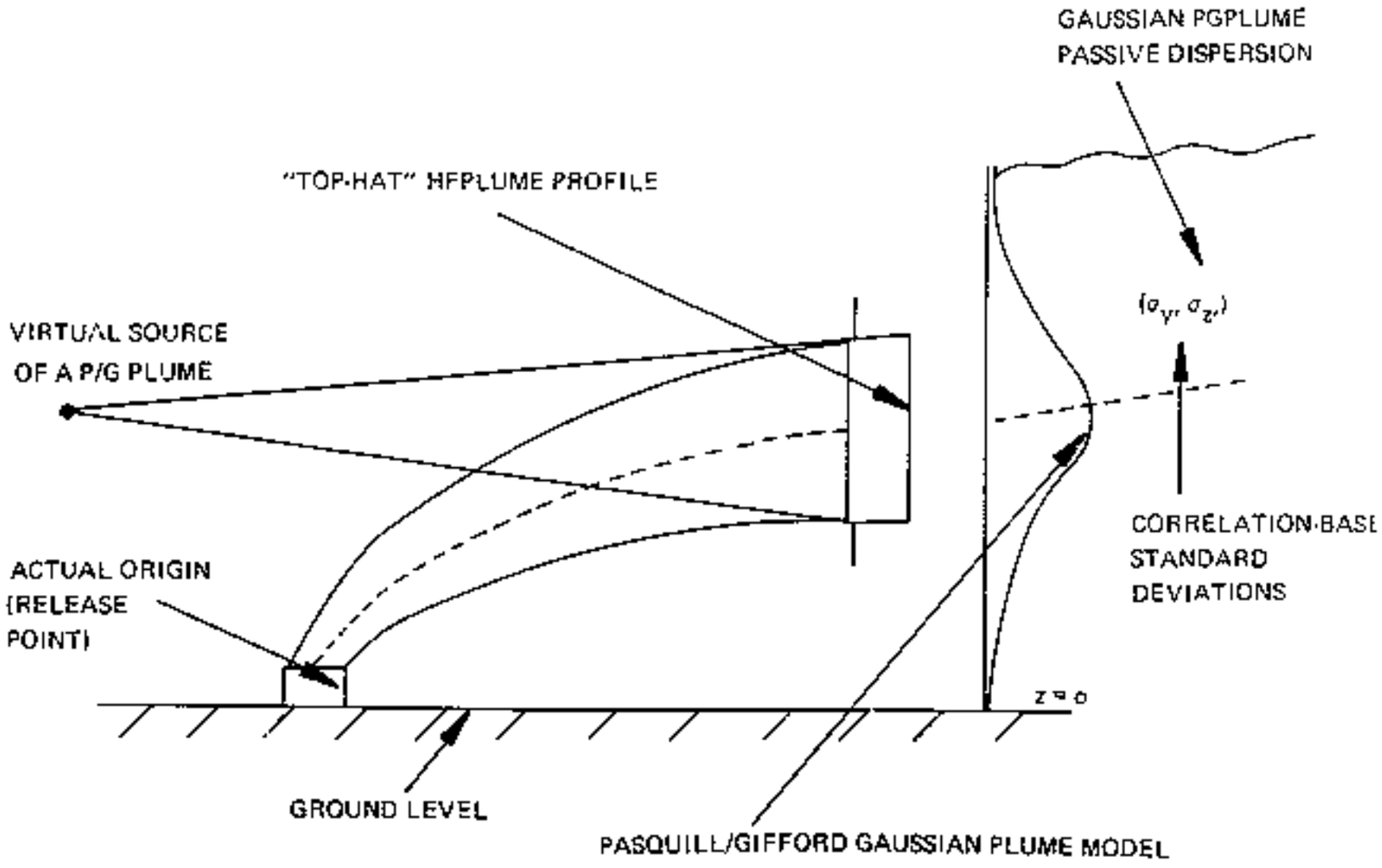


FIG. 5.7. — Transition to passive dispersion as an elevated Gaussian plume, when velocity excess over ambient is small and buoyancy/shear entrainment weak compared with passive entrainment.

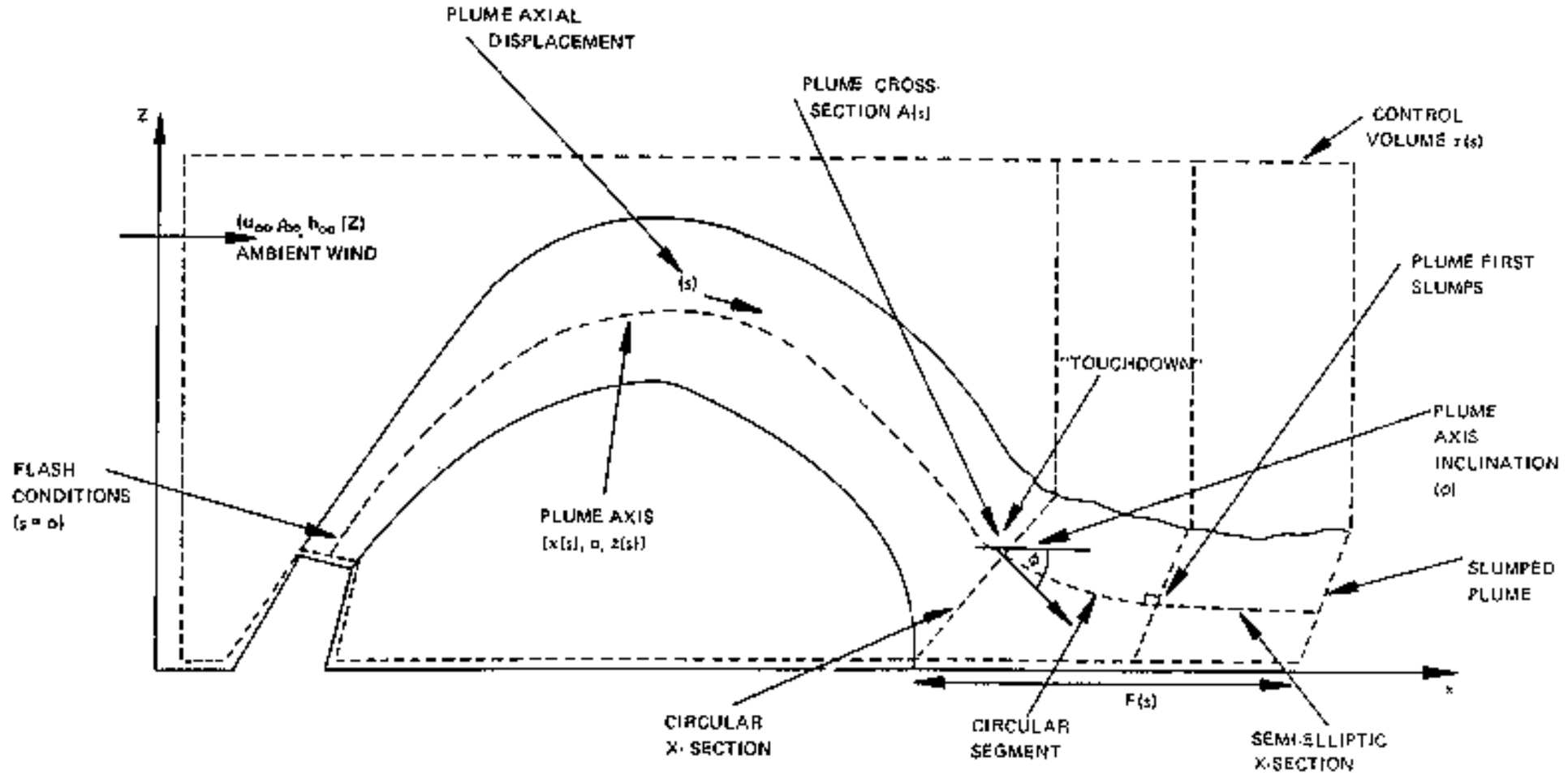


FIG. 5.8. — Illustration of the control volume $\tau(s)$, the plume coordinate system $(s,r,\Theta)$, and the cross-sectional geometry in the stages of plume development.

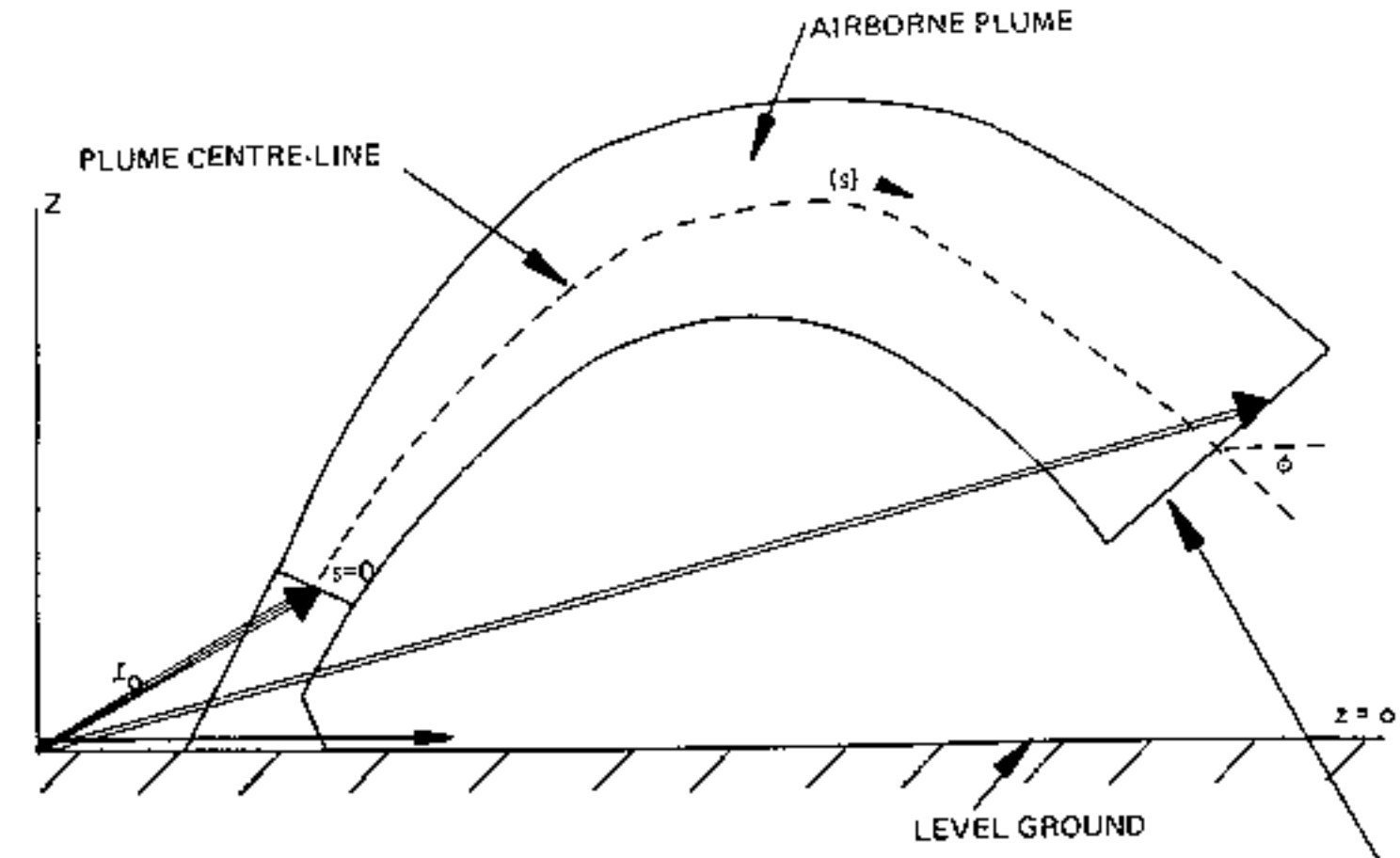


$$\underline{r} - \underline{r}_o = \begin{bmatrix} \int_o^s \cos\phi\,(s)\,ds \\ 0 \\ \int_o^s \sin\phi\,(s)\,ds \end{bmatrix} + r \begin{bmatrix} -\sin\phi\sin\theta \\ \cos\theta \\ \cos\phi\sin\theta \end{bmatrix}$$

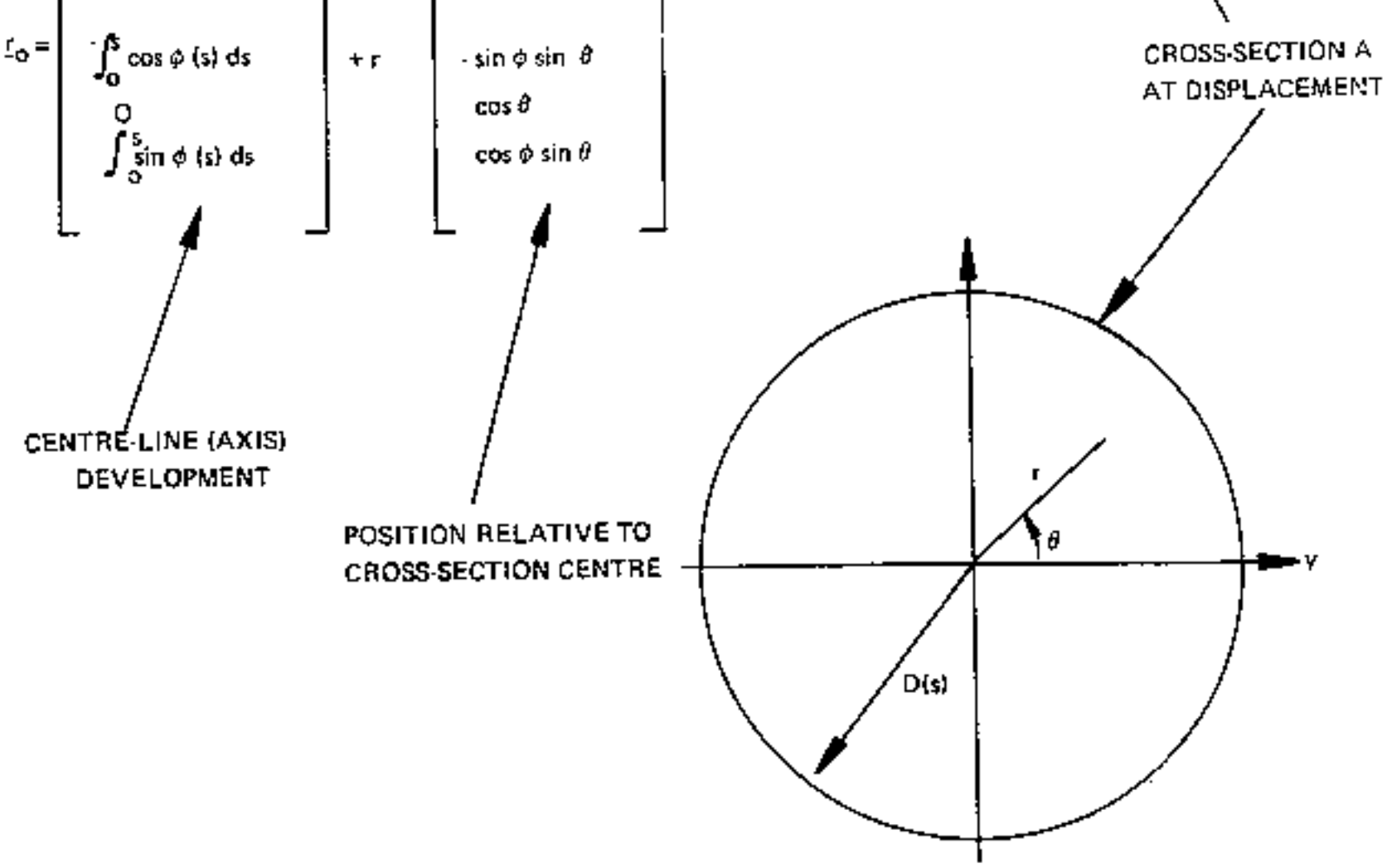


FIG. 5.9. — The plume coordinate system.

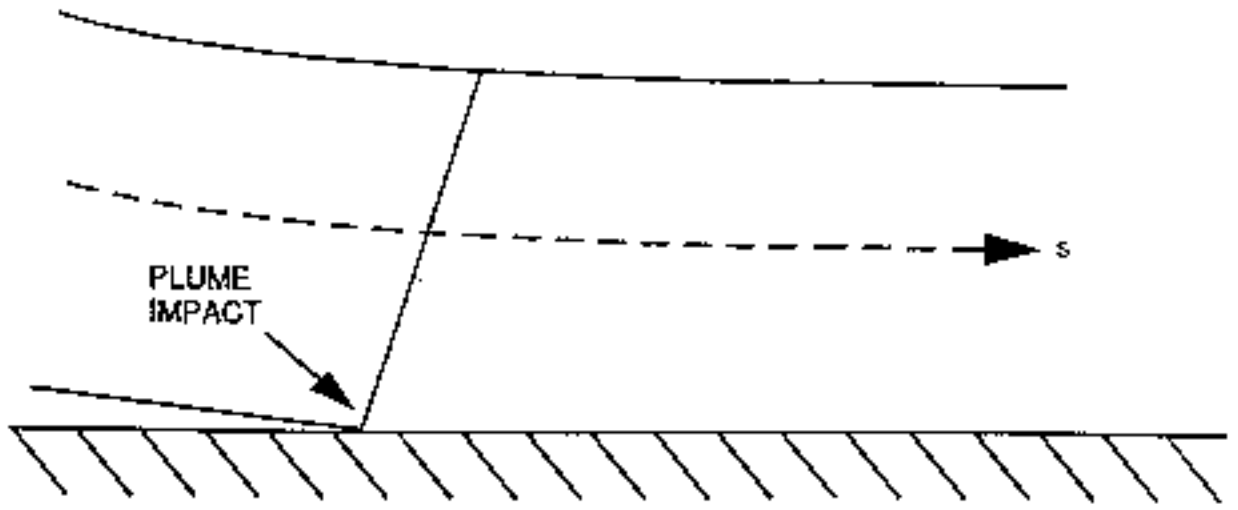


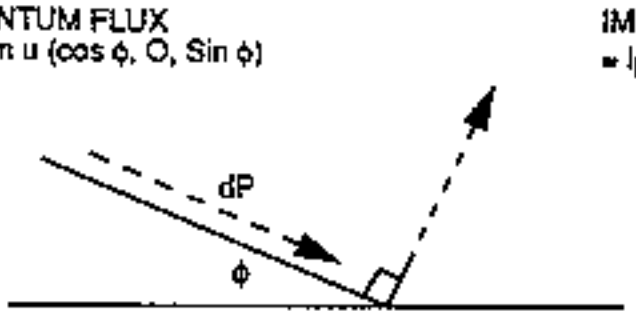


FIG. 5.10 - Plume Impact Pressure Forces. Fluid momentum impacting the ground is destroyed, exterting force per unit axis length of l u² |tanϕ|. Kinetic energy conserved in elastic impact

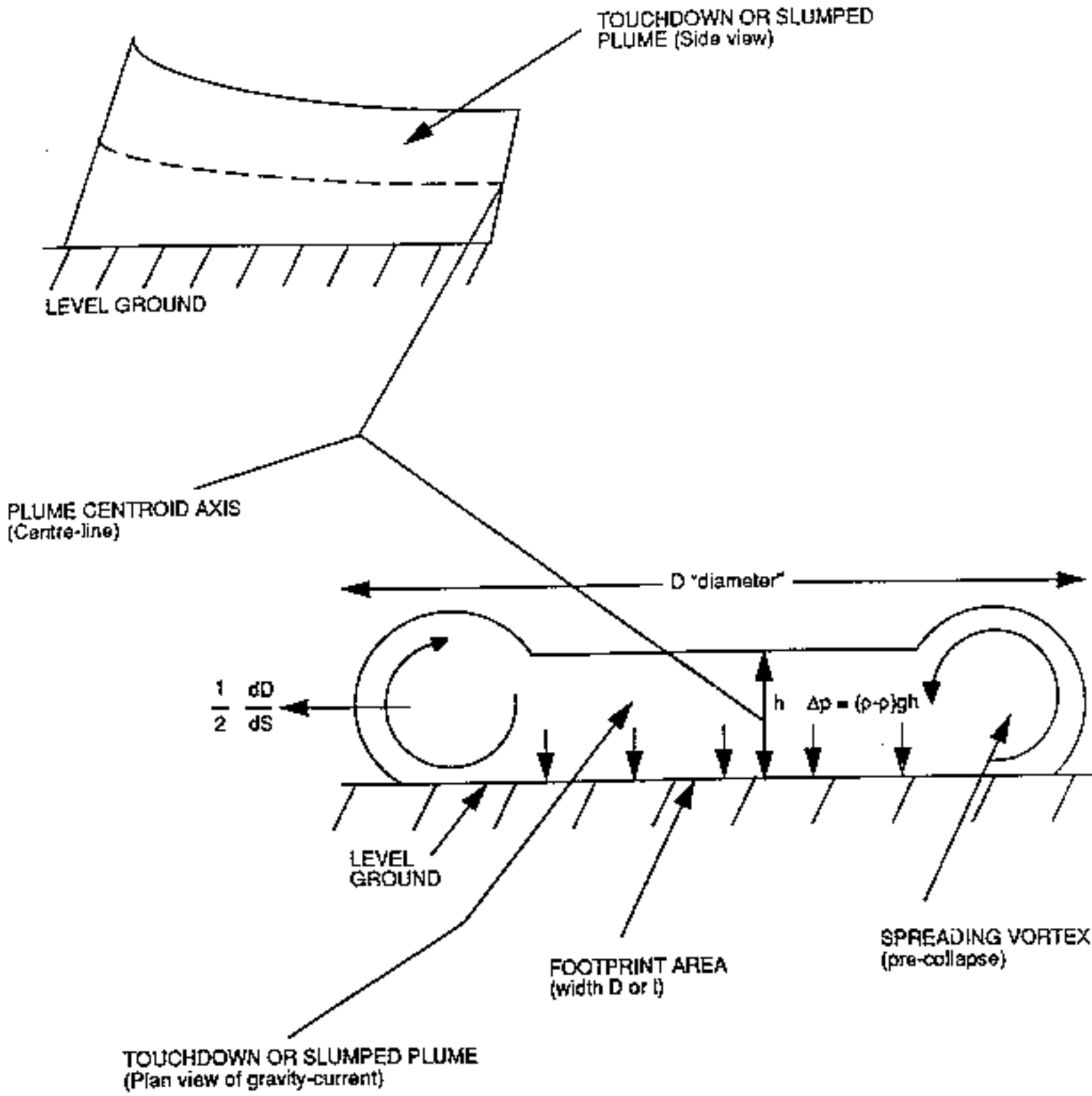


FIG. 5.11 - Gravity slumping and footprint area pressure forces. Lateral gravity spreading of heavy gas dominates slumping of plume

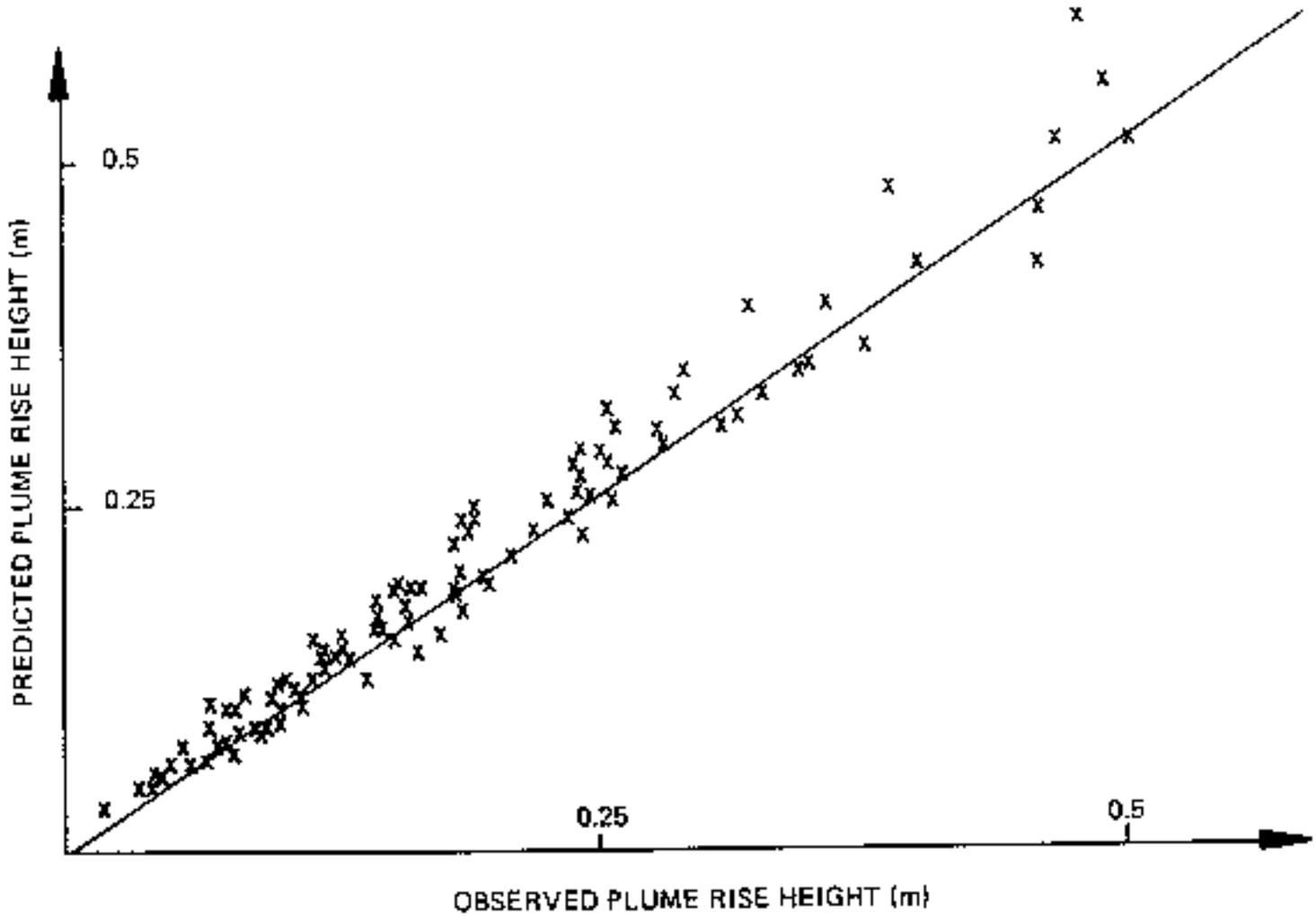


FIG. 5.12. – Comparison of the predicted plume rise height of buoyant plumes with the experimental data of Petersen (1978).

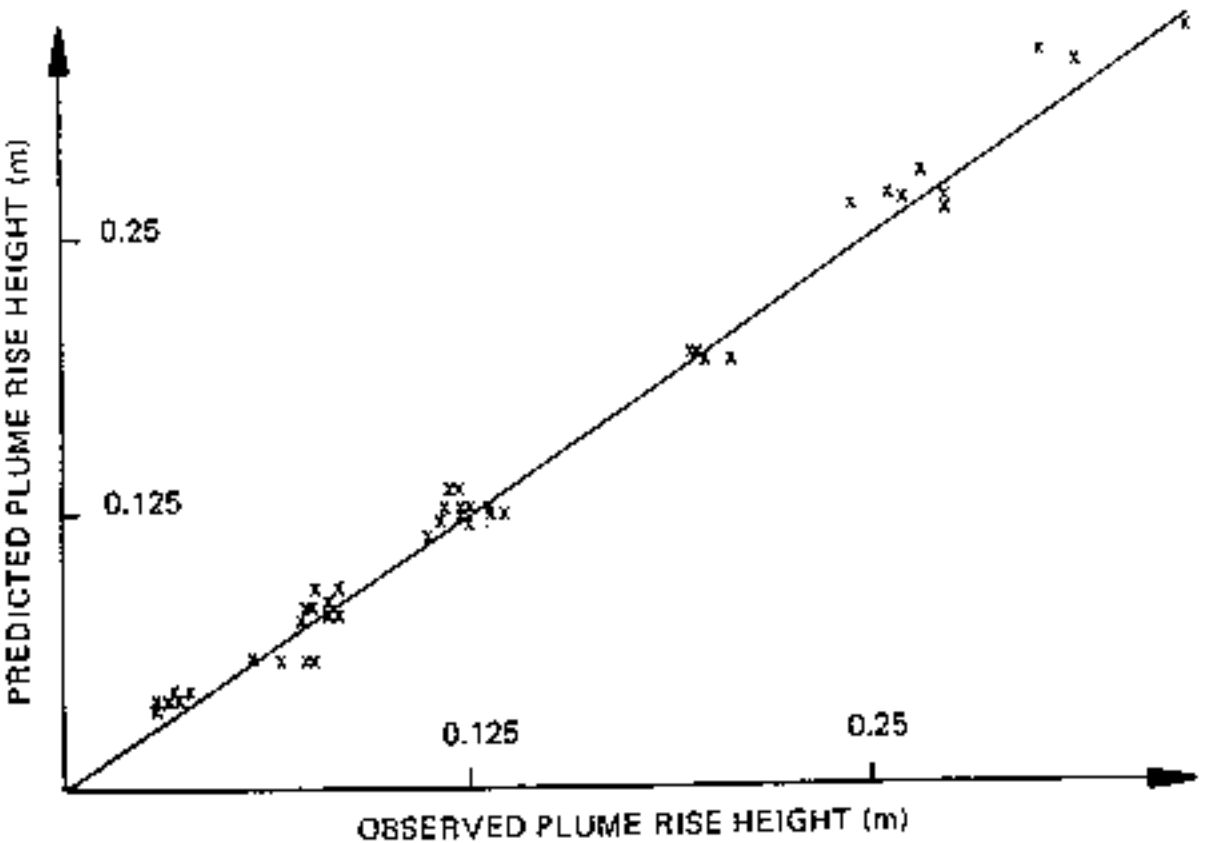


FIG. 5.13. — Comparison of the predicted plume rise height with experimental dense gas wind-tunnel data of Hoot, Meroney and Peterka (1973).

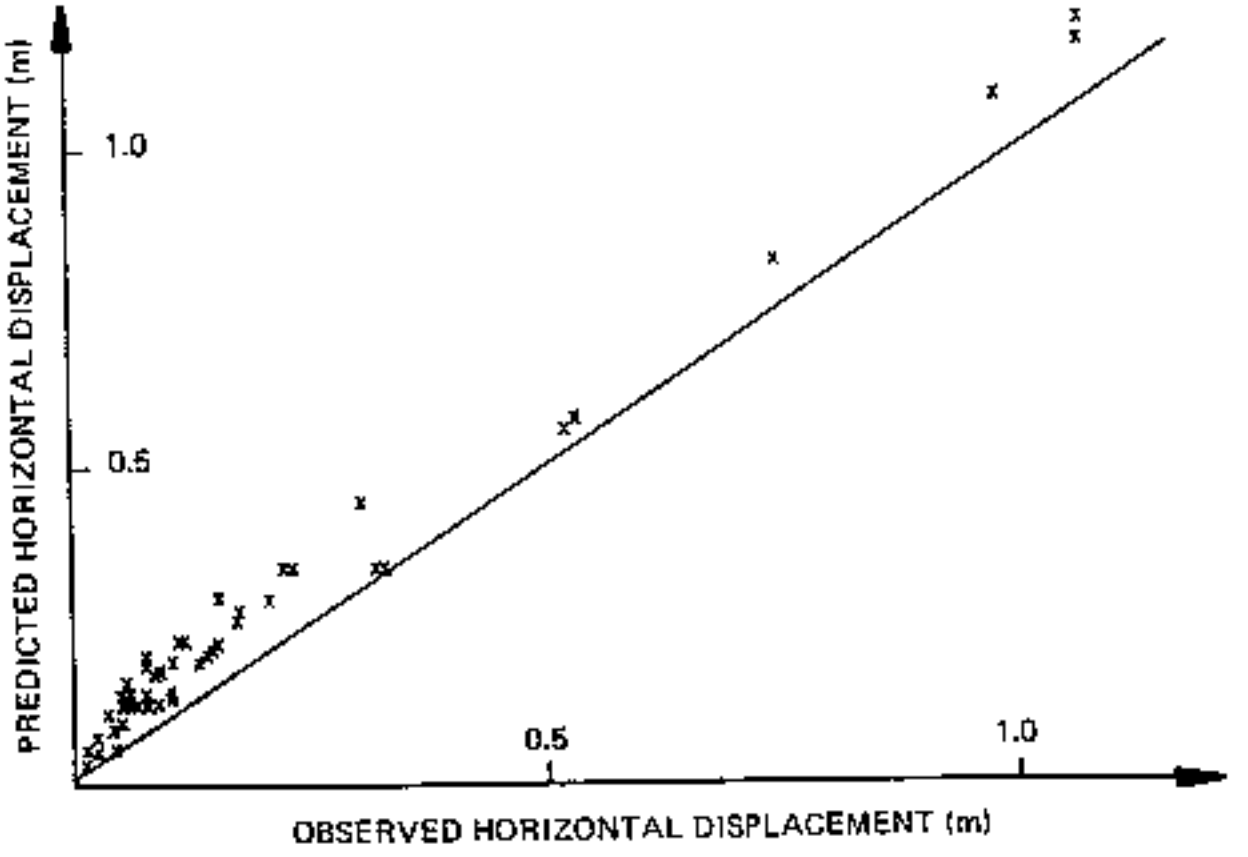


FIG. 5.14. — Comparison of the predicted location of maximum plume rise with experimental dense gas wind-tunnel data of Hoot, Meroney and Peterka (1973).

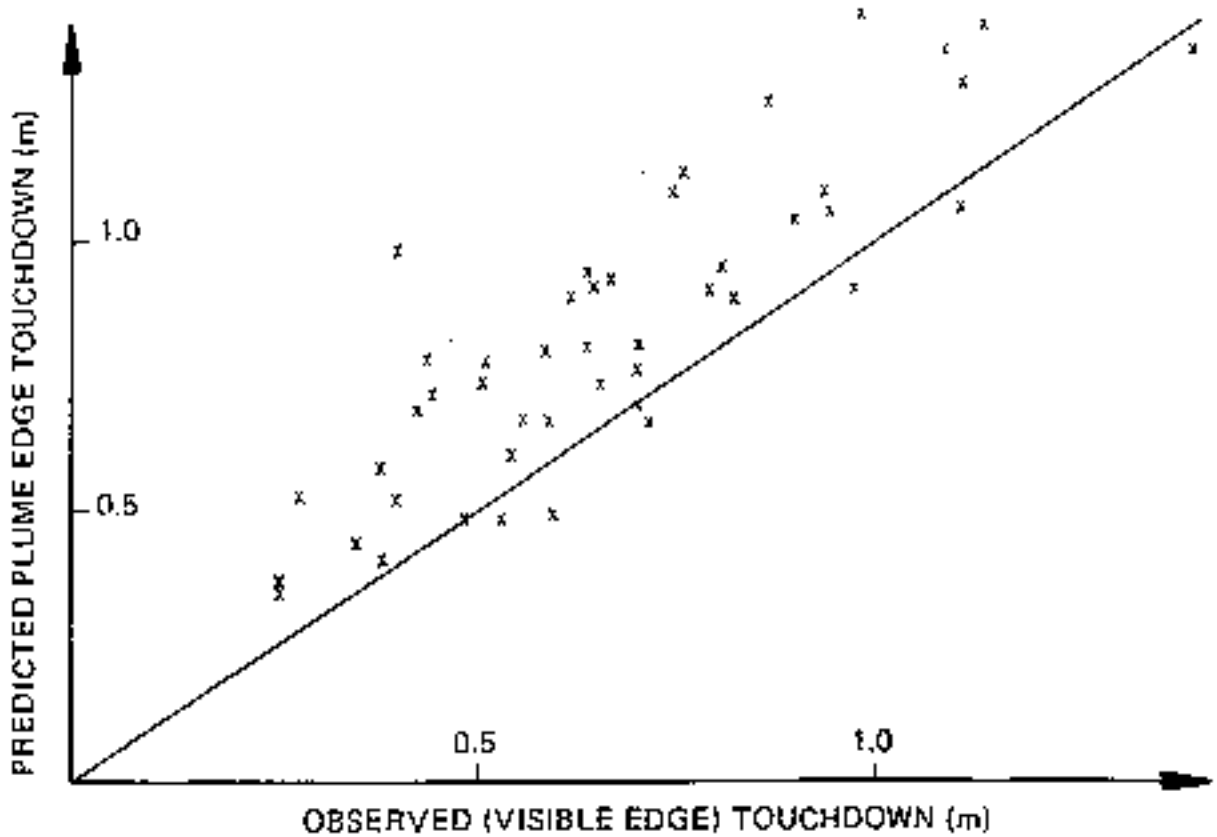


FIG. 5.15. — Comparison of the predicted point of plume touchdown with experimental (visible edge) touchdown of Hoot, Meroney and Peterka (1973).

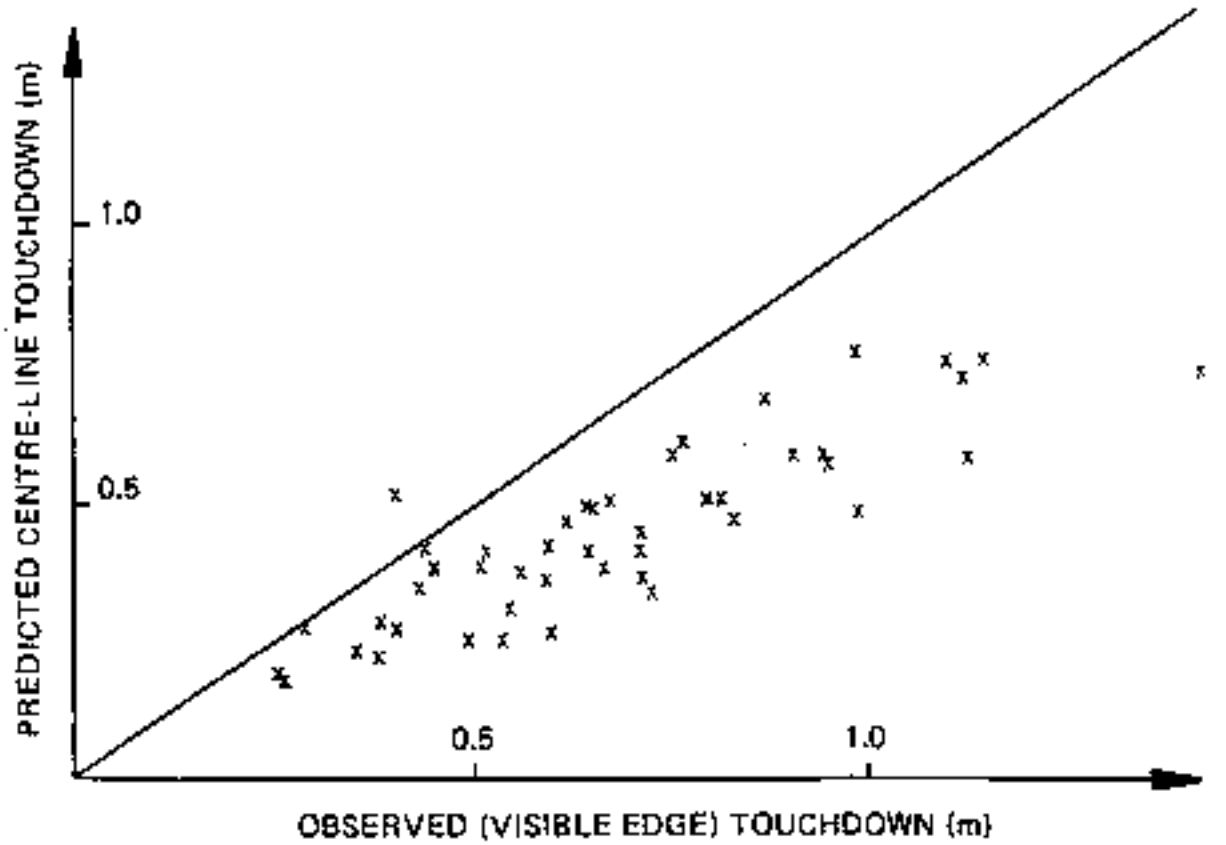


FIG. 5.16. — Comparison of predicted Centre-line touchdown with experimental Visible Edge touchdown data of Hoot, Meroney and Peterka (1973).

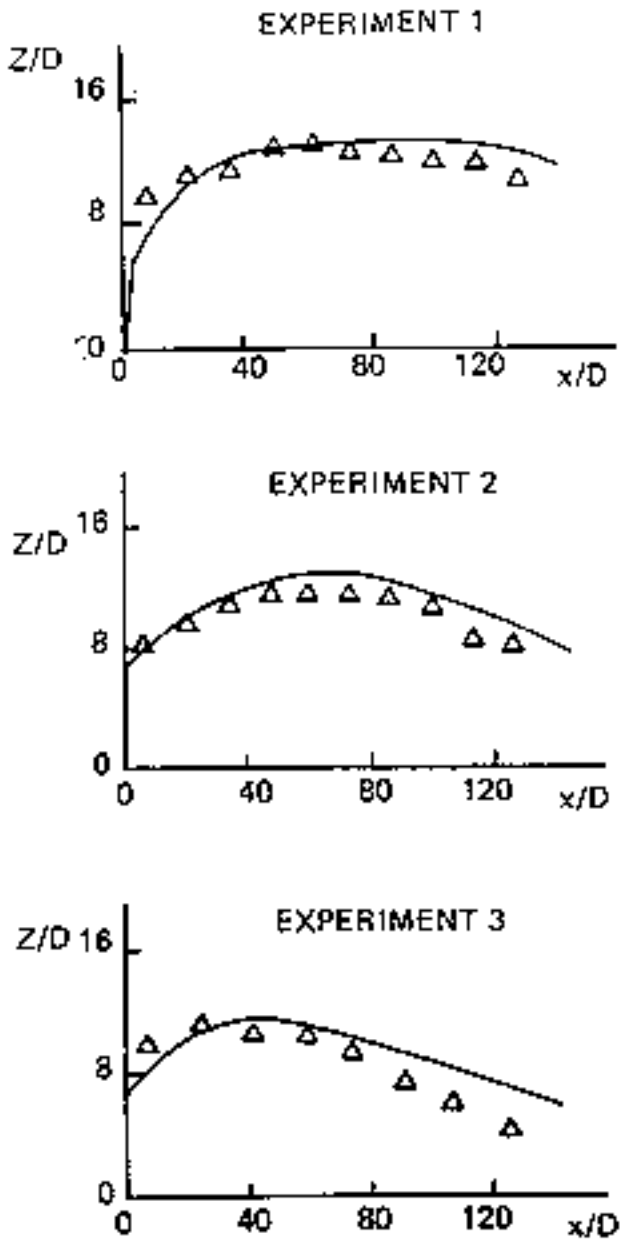


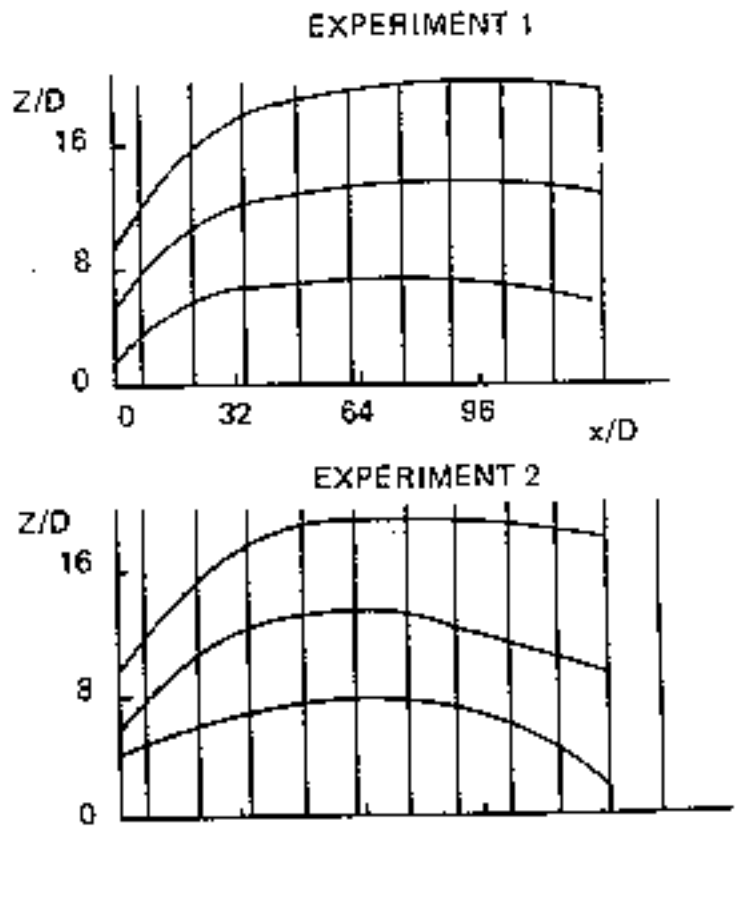


Measured and predicted plume paths
(Δ: experiments; — :prediction).

Experimental conditions ($T_a$: tunnel temperature; $T_c$ stack plume exit temperature)

| | D (m) | $U_a$ (m $s^{-1}$) | $U_c$ (m $s^{-1}$) | $T_a$ (K) | $T_c$ (K) | Re | Fr |
|---|---|---|---|---|---|---|---|
| Experiment 1 | 0.025 | 0.92 | 5.16 | 293 | 353 | 8600 | 3.45 |
| Experiment 2 | 0.025 | 0.97 | 5.75 | 292 | 393 | 9580 | 3.84 |
| Experiment 3 | 0.020 | 0.85 | 3.68 | 291 | 393 | 4900 | 3.68 |

D orifice diameter
$U_a$ ambient wind speed
$U_c$ centre-line speed
x horiz. distance
z (downward) vertical distance

FIG. 5.17. — Comparison of predicted centre-line plume trajectory and plume width with data from experiments 1, 2 and 3 of Li Leijdens and Ooms (1986).